DNA MISMATCH REPAIR AT AN ONCOGENIC HOTSPOT CORRELATED WITH PHASE OF THE CELL CYCLE AND ENVIRONMENTALLY RELEVANT CONCENTRATIONS OF THE ARCTIC POLLUTANT p,p'-DDE.

By

Josephine Simonetti

RECOMMENDED:

Advisory Committee Chair

Department Head

APPROVED:

Dean of the College of Science, Engineering and Mathematics

Dean of the Graduate School

5-1-01

Date

DNA MISMATCH REPAIR AT AN ONCOGENIC HOTSPOT CORRELATED WITH PHASE OF THE CELL CYCLE AND ENVIRONMENTALLY RELEVANT CONCENTRATIONS OF THE ARCTIC POLLUTANT p,p'-DDE.

A

THESIS

Presented to the Faculty

Of the University of Alaska Fairbanks

In Partial Fulfillment of the Requirements

For the Degree of

DOCTOR OF PHILOSOPHY

By

Josephine Simonetti B.S.

Fairbanks, Alaska

May 2001

ABSTRACT

PART I: Mismatch repair in G_1 synchronized mammalian cells

Deficiencies in DNA mismatch repair have been found in hereditary nonpolyposis colon cancer (HNPCC), as well as in sporadic cancers, illustrating the importance of this single repair system in maintaining genomic integrity. In bacteria, this repair system functions primarily, after DNA replication, in the correction of polymerase base insertion errors and in mammalian cells it was also assumed that the mismatch repair system functioned within a similar timeframe. However, DNA mismatches occur ubiquitously and their repair before DNA replication is of paramount importance for faithful genome copying. We investigated the activity of the mismatch repair system, in G_1 synchronized NIH 3T3 cells, in the repair of four mismatches at an oncogenic hotspot in the H-*ras* gene. Our results clearly show that the mismatch repair system is active and accurate during the pre-replicative G_1 phase of the mammalian cell cycle.

PART II: Effects of p,p'-DDE on cell toxicity and DNA mismatch repair ability

Umbilical cord blood, from Inupiat infants in Barrow Alaska, was examined for the presence of several environmental contaminants. All 24 blood samples analyzed contained measurable levels of p,p'-DDE (1,1-dichloro-2,2-bis(p-chlorophenyl)ethylene) with an average concentration of 0.33 μg/l. We examined whether this low concentration of p,p'-DDE had detectable effects on NIH 3T3 (mouse embryonic) and WS1 (human fetal) cells in culture. Initial experiments indicated that exposure to p,p'-DDE resulted in a decrease in the cell number of both cell types. Subsequent analysis revealed that this

decrease was due to cell death in NIH 3T3 cells and to cell cycle arrest in WS1 cells. We also examined the effect of p,p'-DDE on the ability of both cell types to repair mismatches at an oncogenic hotspot in H-*ras*. Preliminary results indicate that p,p'-DDE does not have a discernable effect on the ability of either cell type to correctly repair the G:T mismatch. However, p,p'-DDE exposure results in an *increased* rate of correct repair of the G:A mismatch by both cell types. Overall, this study demonstrates that p,p'-DDE, at concentrations relevant to the Alaskan environment has significant but different effects on two immature cell types in culture.

TABLE OF CONTENTS page

LIST OF FIGURES Page

LIST OF TABLES page

ACKNOWLEDGEMENTS

Thanks to everyone who have helped me get through this long process; Dr. Kandace Williams, Dr. Larry Duffy, Dr. Kelly Drew, Dr. Lynne Lucher, Dr. Nancy Matton and Ileana Bembeneck.

And you John who made it all possible, thanks for sticking with me, without your love and support I would not have gotten this far.

I. INTRODUCTION

PART I: Mismatch repair at an oncogenic hotspot in G_1 synchronized mammalian cells

A. Sources and implications of DNA damage

The primary function of DNA is the passage of unaltered genetic information from one generation to the next and it has been primarily for this reason that DNA has traditionally been assumed to be a very stable and static molecule. However, as we now know, DNA is subject to a constant barrage of damaging insults originating from many endogenous and exogenous sources (Reviewed in 1, 2). Furthermore any damage left unrepaired will be fixed permanently in the genome as a mutation following DNA replication. Because specific mutations are the primary cause of genetic disease, it follows that understanding the origin of mutations is essential to understanding the etiology of cancer and heritable human diseases.

Exogenous damage can arise from both physical and chemical origins. An important source of physical damage is UV radiation, which causes adjacent pyrimidines to become covalently linked to form helix distorting cyclobutane pyrimidine dimers and 6-4 photoproducts (2). Similarly, exposure to ionizing radiation produces modified bases such as thymine glycol as well as causing DNA single and double strand breaks (3).

Chemical sources of DNA damage are numerous but can be grouped into several categories, including the alkylating agents, the cross-linking agents, such as cisplatin and finally, the largest group which consists of those compounds requiring metabolic activation e.g. aflatoxin. These chemicals interact with DNA in various ways and cause

numerous types of lesions including abasic sites, DNA interstrand linkages and base modifications (4, 5, 6).

However, on a daily basis, it is normal cellular processes that cause the majority of damage to DNA. Nucleotide bonding rearrangements or tautomeric shifts can cause base misincorporation during DNA replication. Deamination of cytosine, adenine, guanine and 5-methlycytosine occurs in the normal cellular environment and the resulting products are miscoding lesions, for example, cytosine deaminates to uracil, which if not repaired will result in a G:C $\rightarrow$ A:T transition during replication. In addition, DNA undergoes spontaneous depurination and depyrimidination events culuminating in the appearance of abasic, or apurinic/apyrimidinic (AP) sites, with miscoding potential (7). In fact, AP sites originate from so many sources that they are reported to be the most abundant DNA lesion in living cells (8).

Oxidative damage to DNA, by reactive oxygen species, is considered to be another major source of endogenous damage. The primary sources of reactive oxygen species are the mitochondria, which leak oxygen radicals during aerobic metabolism (9, 10). DNA lesions, which result from oxidative damage, include fragmentation, base loss, strand breaks and nucleotide modifications such as thymine glycol and 8-hydroxyguanine (9, 10, 11).

Misincorporation of non-complementary bases during DNA replication is another major source of pro-mutagenic base pairing errors. The human genome is composed of 3 x 10^9 base pairs and undergoes one cycle of replication per day in a typical proliferating cell (12). The polymerases responsible for DNA replication have variable rates of base

misincorporation (13). For example, DNA polymerase β, the enzyme responsible for the synthesis of short segments of DNA during repair has an error rate of 1 in 5000, while the DNA polymerases δ and ε, both of which have an intrinsic 3' – 5' exonucleolytic activity, have an error rate of 1 in 10,000,000 (Reviewed in 14, 15, 16).

It is estimated that the total number of potentially mutagenic DNA damaging events resulting from spontaneous depurination, oxidative modification, non-oxidative base alterations and replication errors is on the order of 100,000 DNA damaging events per day per cell (17). Thankfully, before any of that DNA damage can be fixed in the genome as a mutation it will most likely be repaired by one of the following repair systems (i) damage reversal, (ii) Base excision repair, (iii) Nucleotide excision repair, and (iv) Mismatch repair (Reviewed in 18). In fact, the combined repair systems are so efficient that the estimated occurrence of mutations within a normal proliferating cell has been reported to be as low as 1.4×10^{-10} mutations/nucleotide/cell generation (19).

One of the hallmarks of cancer is the presence of multiple mutations within the same cell, even thousands in highly transformed cells (16). However, due to the efficiency of the various DNA repair systems, the normal cellular mutation rate is much too low to account for this amount of mutation accumulation and has led to the hypothesis that genetic instability or a "mutator phenotype" is an early event in cancer development (19, 20). The mutator phenotype hypothesis proposes that genes involved in maintaining chromosomal stability (e.g. tumor suppressor genes, DNA repair genes) are mutated early in tumor progression, thus permitting an enhanced rate of mutation that eventually leads to the development of cancer (21).

The greatest evidence for the existence of a mutator phenotype came with the discovery that DNA from the tumors of patients with hereditary non-polyposis colon cancer (HNPCC) exhibited microsatellite instability (Reviewed in 22). Microsatellites are repetitive nucleotide sequences whose lengths are relatively constant in normal cells but vary in tumor cells. It was discovered that this microsatellite instability in HNPCC occurred in tandem with defects in the mismatch repair pathway (23, 24). When human homologs of the bacterial and yeast mismatch repair genes were identified, genetic linkage analysis revealed that the location of each gene correlated with the location of the genes mutated in HNPCC cells (25, 26). For the first time a direct link was discovered between the development of cancer and inactivation of some of the genes responsible for maintaining genomic integrity. Microsatellite instability and the corresponding inactivation of one or more mismatch repair genes has since been discovered in a large number of tumors not associated with HNPCC and is proposed to be an important factor in the development of several sporadic cancers (16, 27, 28, 29).

Carcinogenesis, or malignant transformation, is a stepwise process characterized by the accumulation of multiple genetic alterations in critical genes such as proto-oncogenes and tumor suppressor genes and culminates in the appearance of a population of cells that can evade the normal cellular restraints on proliferation, differentiation, mobility and death (16). During the 1960's it was discovered that mutations induced in the DNA of bacteriophages were not randomly distributed but rather were focused at specific sites along the genome (30) and more recently in human cells, an examination of the mutational spectra induced by MNNG (N-methyl-N'-nitro-N-nitrosoguanidine) in the

HPRT gene found that only a small percentage of the potential number of damaged base sites were actually mutated (31). A site at which the frequency or rate of mutation exceeds that at other sites is called a "hotspot of mutation" and in fact current consensus is that the majority of human gene mutations are found at hotspots (32).

Prime examples of "mutational hotspots" are found in the genes of the *ras* family. Mutations in N, K and H-*ras* have been observed in various naturally occurring human tumors as well as carcinogen-induced animal tumors. As well, the transforming *ras* genes have been shown to be mutant alleles of cellular *ras* genes that are transformed by a single point mutation within their coding regions. Direct sequence analysis has demonstrated that there are activating mutations in the ras oncogene family in nearly 30% of human tumors. Furthermore, these mutations have been localized most frequently to codons 12, 13 and 61 (34, 35, 36, 37, 38, 39).

H-*ras* belongs to a family of genes that encode small GTP binding proteins. These proteins function as molecular switches and are active in their GTP-bound form and inactive in their GDP-bound form. The Ras proteins are part of a complex cellular transduction pathway that transmits external control signals for proliferation, differentiation and apoptosis from the plasma membrane to the nucleus via multiple effector proteins (33, 36, 37, 38, 40). Moreover, protein products of the mutated genes remain activated regardless of up-stream regulators (41).

Currently, there is not a definitive explanation as to why particular gene locations are "mutational hotspots" but several hypotheses have been put forward to explain them (42). The first hypothesis is that activating mutations are selected for due to the increased

survival rates that they confer. Although this explanation may seem plausible it does not explain why only some activation sites are found mutated in human tumors. For example, in H-*ras* there are several sites, in addition to codons 12, 13 and 61, which have been found to be activating mutations *in vitro* but have never been found in human tumors or animal model studies (36, 37, 38, 39). It follows, that since all activating mutations confer a similar survival advantage they should all be found with equal probability in tumors, but since this is not the case this hypothesis does not sufficiently explain mutational hotspots.

The second hypothesis proposes that certain DNA sequences are more susceptible than others to mutation. A number of studies both *in vivo* and *in vitro* have found that precise mutagen targeting does occur and numerous animal studies have demonstrated correlations between type of mutagen, location and resulting activating *ras* mutation (35, 36, 37, 43). In addition several studies have shown preferential carcinogen binding at mutational hotspots in the p53 tumor suppressor gene (44, 45). It is clear from this evidence that chemically induced mutations are targeted to specific DNA sequences.

The third hypothesis, proposed to explain mutational hotspots, states that there is decreased fidelity of repair or inefficient repair at particular DNA sequences. For example, nucleotide excision repair of pyrimidine dimers and benzopyrene adducts has been shown to occur correctly but more slowly at mutational hotspots in the p53 tumor suppressor gene (46, 47, 48).

As well, results, from studies examining the repair of inserted guanine adducts at different positions in H-*ras* (49, 50, 51) and the repair of UV induced lesions in the *SupF*

gene of an SV40 vector in Hela cells (52) have found that repair rates vary at different locations. In addition, previous work in this laboratory has shown that, depending on the specific base:base mispair, there is decreased fidelity of mismatch repair at the middle base pair position of codon 12 of H-*ras* (53). Moreover, further studies have shown that the same mismatches at codon 10, (which has the same sequence as codon 12 but is not a hotspot of mutation), have an improved rate of repair as compared to codon 12 (54). These studies demonstrate that specific DNA locations containing specific DNA lesions have decreased efficiency of repair and likely contribute to the occurrence of "mutational hotspots". Of course, the above hypotheses are not mutually exclusive and hotspots may occur due to a combination of these factors and/or other contributing events, which have not yet been determined.

B. Mechanisms of DNA repair

(i) Damage reversal

The simplest repair of DNA damage is to remove or reverse the lesion in a one-step reaction thus restoring the genome to its normal structure. The simplest direct reversal process is carried out by DNA Ligase I and involves rejoining the ends of a single strand break (55). However, this type of repair occurs only when the process that caused the break has not modified the strand ends (2).

Photo-reactivation is an additional repair mechanism that reverses DNA damage and is found primarily in yeast and bacteria. This system functions to remove UV lesions from cellular DNA. Photolyase, the enzyme involved in this process reverses cyclobutane

pyrimidine dimers to their parental monomers using visible light as an energy source (Reviewed in 56). The enzyme activity has been detected in a wide variety of organisms ranging from bacteria to non-placental mammals (57). However, the evidence for photo-reactivation in placental mammals is still hotly debated with no clear consensus as to the presence, absence or activity of this DNA repair mechanism (57, 58, 59, 60, 61, 62, 63).

In contrast, homologs of the direct repair "suicidal" alkylating enzymes have been found in many prokaryotic and eukaryotic organisms including humans. The alkyltransferase enzymes function to remove alkylation damage that results from exposure to either exogenous alkylating agents or cellular catabolites acting as monofuntional alkylating agents (2, 64, 65). For example, the O^6-methylguanine lesion miscodes for the incorporation of thymine instead of cytosine during replication and results in a G:C to A:T transition mutation. The alkyltransferase enzyme O^6-methlyguanine DNA methyltransferase, or MGMT, removes the methyl group from the O^6 lesion and transfers it to one of its own cysteine residues returning the base to its unmodified state and methylating the enzyme (Reviewed in 56, 66). Finally, since the methylated enzyme cannot be recycled it is degraded by the ubiquitin proteolytic pathway (67). This repair mechanism appears extremely inefficient since it removes only one lesion at the expense of an entire protein molecule when other, less costly multifunctional repair mechanisms are present in the cell . However, these one-step enzymes may have been retained because their repair of the DNA lesion occurs rapidly and efficiently relative to the other DNA repair mechanisms and are error free (63).

(ii) Base excision repair

Base excision repair (BER) is the major mechanism that replaces damaged bases with relatively minor modifications such as deoxyuracil, thymine glycol and 8-oxo-guanine (8). BER is performed in two stages: an initial damage recognition and removal stage carried out by individual DNA glycosylases targeted to specific base lesions and a general repair stage that restores the correct DNA base sequence (68).

DNA glycosylases are grouped into two distinct categories (i) monofunctional DNA glycosylases that remove the altered base 5' to the damage without cleaving the sugar-phosphate backbone and, (ii) bifunctional DNA glycosylases which remove the damaged base but also have an additional intrinsic AP lyase activity that cleaves at the 3' side of the damaged base leaving behind an incised AP site. Table 1 contains examples of human DNA glycosylases and the DNA damage that they repair (Reviewed in 2 and references indicated).

Table 1:Human DNA glycosylases and the damage they repair

NAME	Example of damaged removed	Mono- or Bifunctional	Reference
Uracil DNA glycosylase	Uracil due to cytosine deamination or base mis-incorporation	mono	69, 70, 71, 72
Thymine DNA glycosylase	Thymine from G:T, uracil from G:U mismatches	mono	73, 74, 75, 76
Mut Y adenine glycosylase	Removes adenine from A:C or G:A mismatches	Reported as both	68, 77, 78, 79
hNTHI DNA glycosylase,	Thymine glycol, (removes oxidized pyrimidines)	bi	71, 80
hOGG1	^{8}-OG:C	mono	81

Both types of glycosylase recognize and remove base damage by the same nucleotide flipping mechanism. Using this method the enzyme flips out the damaged base from the DNA helix into the enzyme's active site where breakage of the N-glycosyl bond linking the damaged base to the sugar-phosphate backbone occurs, creating an apurinic/apyrimidinic (AP) site (68). If the glycosylase is monofunctional a physically distinct AP endonuclease incises the sugar-phosphate backbone. On the other hand if the glycosylase is bifunctional its intrinsic AP lyase activity performs the incision step. Repair of the resulting AP sites can proceed by two pathways – a DNA polymerase β-dependent pathway (Short-patch BER) and a proliferating cell nuclear antigen (PCNA)-dependent pathway (Long-patch BER) (71, 82, 83, 84).

Short-patch BER involves the removal of a single damaged base followed by its replacement via a series of enzymatic steps. This process has been reconstituted in vitro with the purified human proteins; uracil DNA glycosylase, AP endonuclease (HAP 1/APE), DNA polymerase β, and either DNA Ligase I or DNA ligaseIII + XRCC1, (85, 86). For example, uracil, which occurs in DNA as a result of cytosine deamination or uracil mis-incorporation during DNA replication, is excised by uracil DNA glycosylase to create an AP site. The human AP endonuclease HAP 1/APE then hydrolyzes the DNA backbone generating 3'-hydroxyl and 5'-deoxyribose phosphate (dRP) ends. The dRP group is excised by the dRP lyase component of DNA polymerase β, producing a single nucleotide gap with 3'-hydroxyl and 5'-phosphate ends. DNA polymerase β fills in the gap, a DNA ligase seals the nick and the normal sequence of the DNA is restored (87) (Figure 1A). The exact role of XRCC1 is uncertain but it may act as a scaffolding protein and recruit and position other components of the repair process (86). Short-patch BER by the bifunctional glycosylases e.g. human 8-oxoguanine DNA glycosylase (hOGG1) occurs via the same mechanism except that the incised AP site requires additional processing by the HAP1/APE endonuclease before repair can proceed (80).

Long-patch BER involves the gap filling of several nucleotides. Recently, purified HAP1/APE, PCNA (proliferating cell nuclear antigen), RF-C (Protein replication factor C), FEN1, DNA polymerase δ or ε and DNA ligase I were shown to be required for efficient long patch BER at an in vitro AP site (8, 88) (Figure 1B). However, it is still unclear as to the exact role of each of these proteins in the repair pathway. PCNA appears to act as a molecular adaptor that brings together the protein units necessary to repair the

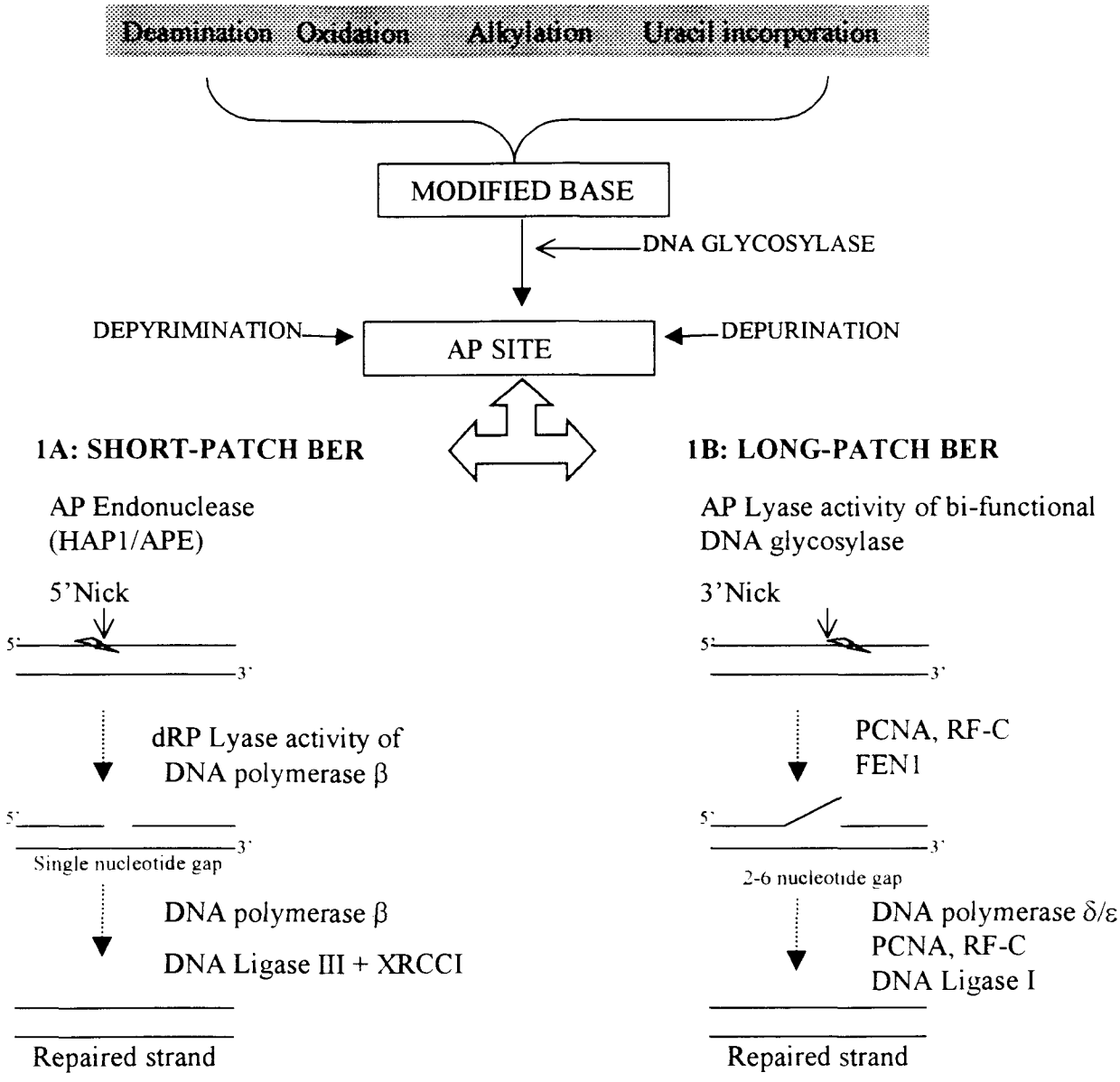

Figure 1:Human Base Excision Repair.
A: Short-patch BER, B: Long-patch BER
See text for description of processes.
Figure adapted from Krokan et al 1997 (71).

(iii) Nucleotide Excision Repair (NER)

A direct correlation between unrepaired DNA damage and carcinogenesis in humans was first established when it was discovered that the cancer prone hereditary disease xeroderma pigmentosum (XP) involved a defect in the repair of DNA lesions produced by UV light (90). In humans the primary mechanism for the repair of DNA produced by UV light is nucleotide excision repair (NER) (56, 91, 92, 93).

XP is clinically characterized by extreme photosensitivity, pigmentation abnormalities in sun exposed skin, mental retardation and other neurological abnormalities (Reviewed in 94). XP patients have a greater than 1000-fold increased risk of developing sun-exposed skin cancers, particularly basal cell carcinomas and melanoma and a 10- to 20- fold increased risk of developing several types of internal cancers under the age of 20 years. Seven complementation groups have been identified in XP patients and are designated XPA through XPG. Each group designation represents a defect in a specific NER gene that essentially inactivates the repair process. In addition, an eighth XP complementation group was identified and designated XPV, or variant form, and was found not to be defective in NER, but instead lacks a mechanism to bypass DNA damage during replication.

Nucleotide excision repair (NER) has the capacity to repair many different types of DNA lesions. However, in order for a lesion to be a substrate for NER it must cause both a distortion of the helix as well as chemically modifying the DNA. Pyrimidine dimers, such as those induced by UV light and the bulky adduct damage caused by

chemicals such as cisplatin, benzpyrene and aflatoxin are typical of the types of damage repaired by the nucleotide excision repair system (Reviewed in 93).

Nucleotide excision repair has been reconstituted in vitro with purified human proteins and involves approximately 20 – 30 polypeptides and occurs in four sequential steps (Figure 2) (96).

(1) Damage recognition: Sugasawa et al have established that, in NER, a protein complex consisting of XPC and hHR23B is responsible for initial damage recognition and subsequent recruitment of the remaining repair proteins to the damage site (95). However, it has been found that a complex consisting of XPA and RPA also performs a damage recognition function (93). Although the debate continues, recent evidence suggests that the damage type and the helix distortion it causes may determine the protein complex that recognizes it (97).

(2) Dual incision: In order for dual incision to occur on either side of the lesion, a complex consisting of XPC/hHR23B, XPA, RPA and TFIIH first binds to the damage site and causes an area of the helix to unwind. Full unwinding of the helix around the lesion requires ATP, which is provided by the XPB and XPD protein subunits of TFIIH, and results in the creation of cutting sites for the endonucleases XPG and ERCC1/XPF. XPG cuts at the 3' side of the open complex and the ERCC1/XPF complex cuts at the single-strand to double-strand transition 5' to the damage. Their combined actions cumulate in the excision of a single-stranded oligonucleotide 24-32 nucleotides in length containing the damage.

(3 – 4) DNA resynthesis and ligation: Finally, re-synthesis and ligation of the excised patch is carried out by RPA, RF-C, PCNA, DNA polymerase δ or ε and DNA Ligase I, thus restoring the DNA to its normal structure.

As is the case with base excision repair there are also two types of nucleotide excision repair. The process described above is designated global genome nucleotide excision repair (GG-NER) and as the name suggests, removes DNA damage from any place in the genome. In addition, a specific type of NER exists for active genes, in which the transcribed strand is repaired 5 to 10 times faster than the non-transcribed strand, and is referred to as transcription-coupled nucleotide excision repair (TC-NER) (98, 99, 100, 101). The mechanism of TC-NER is essentially the same as that for GG-NER except that during transcription the arrest of RNA polymerase II at the site of a lesion is thought to serve as an alternate recognition signal that then recruits the remaining repair proteins to the damage site (Reviewed in 102, 93).

Two diseases, Cockayne's syndrome (CS) (characterized by skeletal abnormalities, mental retardation, photosensitivity and shortened lifespan) and trichothiodystophy (TTD) (characterized by photosensitivity, short stature, brittle hair and shortened lifespan) are caused by defects in transcription-coupled NER (91, 94). Interestingly, a concomitant increase in cancer development is not associated with either disease and may be due to the retained capacity to carry out global genome NER (99). However, it must also be noted that both of these diseases are associated with a significantly shortenened lifespan, which in and of itself may explain the absence of an increased incidence of cancer, a long-term complication in these patients.

Although, the precise roles of each of the proteins participating in NER is not yet understood, recent studies have begun to elucidate some possible functions. For example, in addition to its role in the re-synthesis of the excised DNA tract, the single stranded binding protein RPA may serve to orientate the XPG and XPF/ERCC1 exonucleases to their respective 3' and 5' incision sites, (103). In fact, the plethora of proteins involved in this repair process has made it apparent to researchers that NER is an extremely complex and important repair pathway and that much more research is needed to fully understand it.

(a) DNA with bulky damage

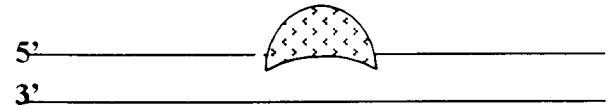

(b) Damage recognition

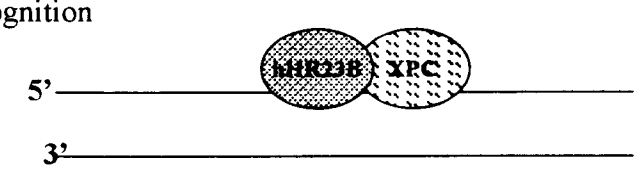

(c) Helix unwinding and dual incision

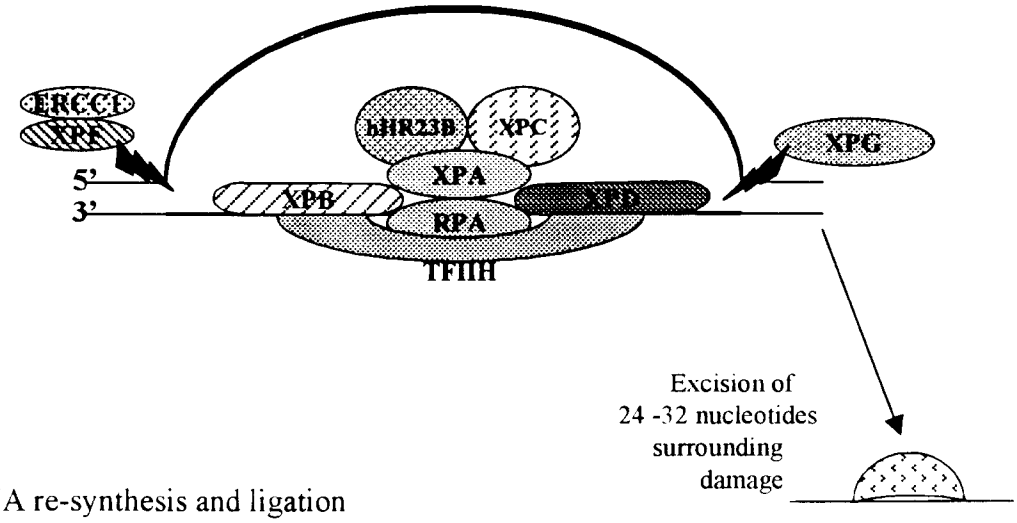

(d) DNA re-synthesis and ligation

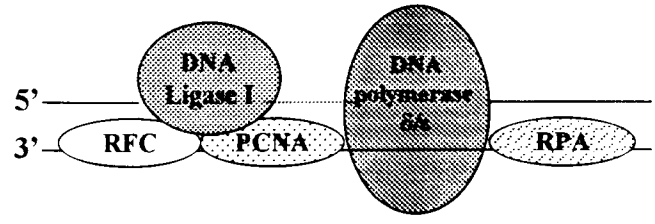

Figure 2: Human Nucleotide Excision Repair
Adapted from Mol *et al* 1999 (68)
See text for description of process

(iv) Mismatch repair

Since the discovery that hereditary non-polyposis colorectal cancer (HNPCC) is caused by inherited mutations in genes involved in mismatch repair there has been extensive study towards understanding how this human DNA repair mechanism functions. In general two types of base mis-pairing occur in DNA. The first occurs when non-complementary bases are mistakenly paired together and are not removed by proof-reading mechanisms during DNA replication. The second type of pairing error arises as a consequence of misalignment of the two DNA strands and, depending on the extent of misalignment, results in the formation of single-stranded loops of one or more bases in the DNA duplex which are termed insertion/deletion loops (IDLs). Base-base mismatches and IDLs can arise by a number of processes including, and perhaps most importantly, nucleotide misincorporation errors during DNA replication (17).

(a) Mismatch repair in E.coli.

In bacteria mismatch repair is a post-replicative DNA repair mechanism, which relies on the hemi-methylation state of newly replicated DNA to target repair to the nascent strand (2, 105, 107, 109, 141). Current knowledge of bacterial mismatch repair is that it involves ten components that can be separated into two groups. Group 1 is comprised of proteins that function primarily in DNA repair: MutS, MutL and MutH. Group 2 contains proteins that also function in other pathways of DNA metabolism: MutU (HelicaseII/UvrD), SSB (single stranded binding protein), DNA Ligase, DNA polymerase III holoenzyme and the DNA endonucleases (RecJ, Exo VII, Exo I and Exo X).

(b) Mechanism of bacterial mismatch repair:

Step1: The ATPase MutS binds to the mismatch as a homodimer (110). *Step 2*: MutS recruits MutL and MutH to the repair site where the DNA is manipulated into a loop structure termed an α-loop (111). *Step 3:* The MutS, L and H proteins attach to the base of the α-loop and proceed to translocate along the DNA. This movement is dependent on ATP hydrolysis and is presumed to function as a searching mechanism for the strand discrimination signal, which in bacteria is the brief post-replication hemi-methylation state of the DNA (parent strand methylated, daughter strand containing incorrect base remains unmethylated for a short period following replication). MutS is primarily responsible for ATP hydrolysis but MutL has recently been shown to also be necessary for that activity (112, 113). *Step 4*: MutH is activated by MutL to cleave the daughter strand at the nearest unmethylated GATC site to the damage. *Step 5*: MutL loads MutU (Helicase II/UvrD) onto the DNA in the correct orientation at the MutH nicked site where it proceeds to unwind the duplex DNA towards the mismatch (114, 115). *Step 6*: The displaced single-stranded DNA containing the mismatch is degraded by any one of the four endonucleases (RecJ, Exo VII, Exo I or Exo X) (107, 116), the resulting single stranded gap is stabilized by SSB protein filled in by DNA polymerase III holoenzyme and finally sealed by DNA ligase (107) (Figure 3).

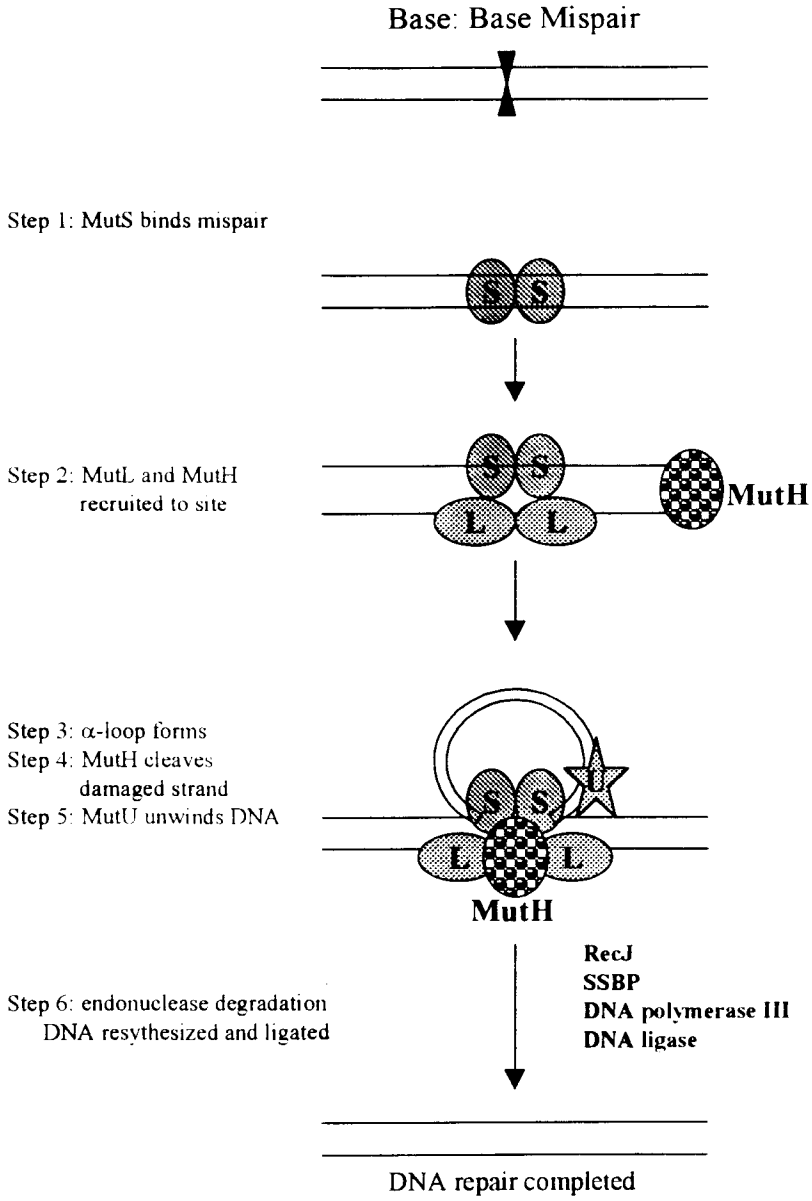

Figure 3: Model for mismatch repair in *E.coli*
see text for description of mechanism
Adapted from Dao and Modrich 1998 (106)

(c) Eukaryotic mismatch repair

The importance of mismatch repair is reflected by its conservation in organisms as diverse as bacteria and humans. In fact, homologues of the bacterial MutS and MutL proteins have been found in nearly all organisms examined (107). However, two important differences exist between bacterial and eukaryotic mismatch repair. The first is that in bacteria the strand discrimination signal is provided by the hemi-methylation state of the newly replicated DNA but in eukaryotic cells this signal does not exist. Secondly, in bacteria the proteins involved in the individual steps function as homodimers but in eukaryotes they function primarily as heterodimers.

Thus far six MutS homologs have been identified in eukaryotes (MSH 1-6) of which five have been identified in humans (hMSH2-6) (Table 2). Msh1 is required for normal mitochondrial function in yeast but as yet no mammalian homologs have been reported (117, 118). The most recently identified human MutS homologs are hMSH4 and hMSH5. Both of these proteins are expressed only in tissue actively engaged in meiosis where they are found as a heterodimer (119). However, their protein complex does not appear to participate in mismatch repair but may play a role in meiotic recombination (120). In contrast, the remaining human MutS homologs; hMSH2, hMSH3 and hMSH6, have all been shown to participate in mismatch repair and are discussed below.

Table 2: Mut homologs in yeast and humans (from 118)

E.coli	*S.cerevisiae*	*H.sapiens*
MutS	Msh2, Msh6, Msh3	hMSH2, hMSH3, hMSH6
	Msh1	Not identified
	Msh4, Msh5	hMSH4, hMSH5
MutL	Mlh1	hMLH1
	Pms1	hPMS2
	Mlh2, Mlh3	hPMS1, hMLH3
MutH	Not identified	Not identified
MutU (HelicaseII/UvrD)	Not identified	Not identified

Both hMSH2 and hMSH6 contain a conserved "Walker Type A" nucleotide-binding fold (121) and together form the hMutSα heterodimer. hMutSα restores DNA mismatch repair to tumor cells, binds to and initiates repair of base-base mispairs (122) and, although it has been reported to repair IDL's containing up to 12 unpaired bases, functions primarily in the repair of IDL's containing one inserted base (123, 124). The hMutSα heterodimer possesses an intrinsic ATPase activity, which is consistent with the presence of the "Walker Type A" nucleotide-binding fold (125). The ATPase is stimulated by the presence of mismatched DNA and has been found to be dispensable for mismatch binding but necessary for mismatch repair *in vitro* (125). There now appears to be a general consensus in the literature that mismatched DNA stimulates ATP hydrolysis in mismatch repair (126, 127). However, there is substantial dissent regarding the role of

ATP hydrolysis in mismatch repair (128, 129, 130). Two models have been proposed to explain the purpose of the interaction between hMutSα and ATP. The first proposes that upon binding the mismatched DNA, hMutSα undergoes an ATP-hydrolysis dependent translocation along the DNA backbone. The translocation then functions as a signal to the other components of mismatch repair as well as exposing the site of mismatch to them (130).

The second ATP interaction model proposes that hMutSα exists primarily in an ADP bound form. Binding of mismatched DNA provokes an ADP → ATP exchange and results in the formation of an ATP-bound sliding clamp that can diffuse along the DNA backbone and signal to the other components of mismatch repair (128, 129). In this Molecular Switch model hMutSα is "on" in the ADP bound form and "off" in the ATP-bound form. This model proposes that ATP hydrolysis is not necessary for translocation but plays a role in the recycling of the ADP-bound hMutSα complex (126). Further evidence in support of this model is that the rate limiting step in the initiation of hMutSα mediated mismatch repair is the ability of particular mispaired bases to invoke the ADP → ATP exchange reaction and has been linked to the efficiency of repair *in vitro* (131). Although, the debate continues as to the exact consequences of ATP and hMutSα interaction it is clear that ATP binding results in a conformational change in the protein complex that affects subsequent steps in the repair process.

The remaining MutS homolog, hMSH3 also possesses a "Walker Type A" nucleotide-binding fold (121) and together with hMSH2 forms the hMutSβ heterodimer.

hMutSβ supports the repair of IDL's having 2 or more unpaired bases but does not participate in the repair of single base-base mispairs or IDL's with less than two mispaired bases (120). In addition hMutSβ is reported to function as an ADP → ATP molecular switch in a manner similar to hMutSα (132).

It has recently been established that the hMSH6 subunit is responsible for mismatch recognition, binding and the ATPase activity of hMutSα (134). Furthermore, a mutation in the hMSH6 ATPase site disables the hMutSα sliding clamp and prevents translocation along the DNA (133). These findings highlight the importance of the hMSH6 subunit and also imply similar functions for the hMSH3 subunit of hMutSβ. However, the importance of hMSH6 and hMSH3 in the repair activity of hMutSα and hMutSβ is not reflected in the number of HNPCC kindred presenting with mutations in either gene. In fact mutations in either gene are rare in HNPCC (108, 135). This genetic evidence may be explained by a functional redundancy of these proteins whereby lack of either hMSH6 or hMSH3 is compensated for by the overlapping function of the remaining protein when it is complexed to hMSH2 (136).

Multiple MutL homologs have been identified in eukaryotic cells. As with MutS the human MutL homologs hMLH1, hPMS2 and hPMS1 interact to form the heterodimers hMutLα (hMLH1 and hPMS2) and hMutLβ (hMLH1 and hPMS1) (137, 138, 139). Recently, a third human MutL homolog named hMLH3 has been identified (140). hMLH3 is a homolog of the yeast Mlh3 protein. Mlh3 forms a heterodimer with Mlh1 and participates in the repair of IDL's and it has been suggested that hMLH3 may play a similar role in human mismatch repair (141). Genetic and protein-protein

interaction experiments have led to the proposal of a model for eukaryotic mismatch repair in which a heterodimeric complex of either hMutLα or β interacts with either hMutSα or β during their ATP dependent/independent translocation along the DNA backbone from either a mispaired base or an insertion deletion loop (Figure 4). At this time little more is known about these interactions except that they involve ATP and the recruitment of other repair proteins.

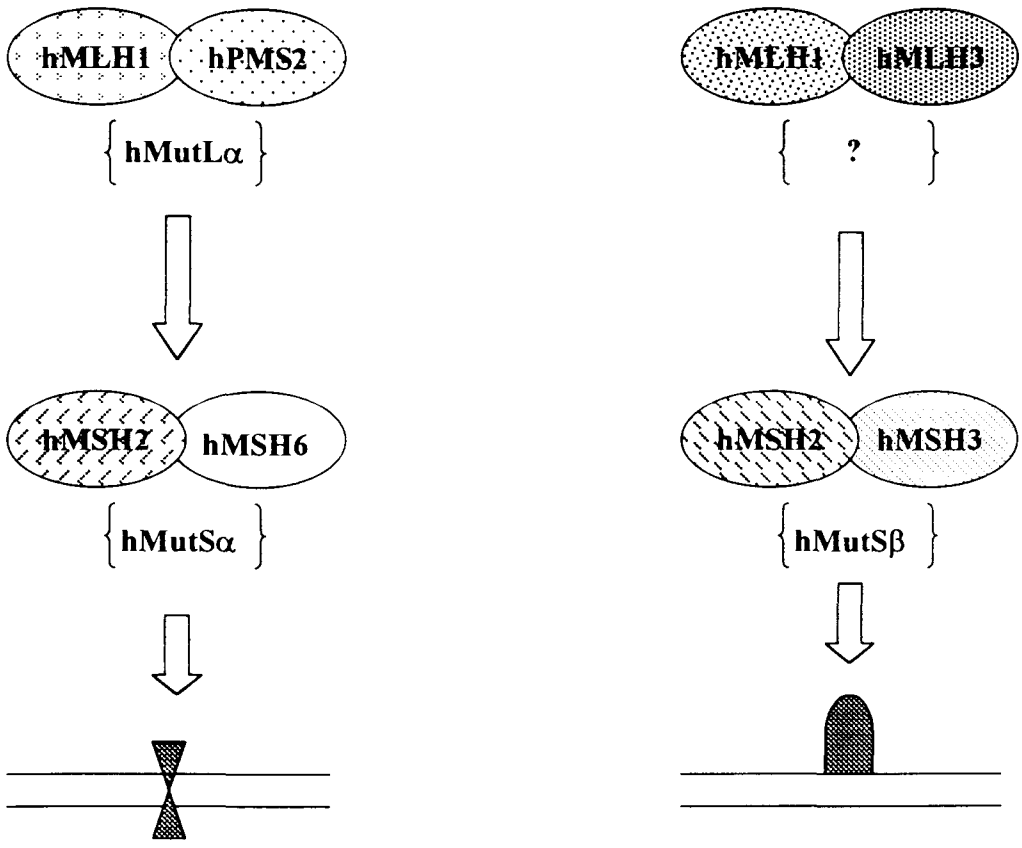

Base: Base Mispair
(a)

Insertion/Deletion Mispair
(b)

Figure 4: Human mismatch repair
Proposed interaction of human mismatch repair proteins
(a) hMutSα recognizes and binds to mispaired bases and recruits hMutLα to the repair site
(b) hMutSβ recognizes and binds to insertion/deletion mispairs and recruits the hMLH1/hMLH3 heterodimer to the repair site
Adapted from Jirincy 1998 (108)

(d) Other proteins implicated in mismatch repair

PCNA (proliferating cell nuclear antigen) has been shown to be required at an early step in mismatch repair that precedes excision of the mismatch (142) as well as for the DNA resynthesis step that follows mismatch excision (143). In addition PCNA can be co-immunoprecipitated with hMSH2, hMSH6, hMLH1 and hPMS2 (144, unpublished results from Williams laboratory 2001). A recent study has identified PCNA binding motifs in Msh3 and Msh6 and has shown that PCNA interacts with these proteins but not Msh2. As well, elevated mutation rates have been found in yeast when the PCNA binding motifs of these proteins are mutated and the authors suggest that the inability to bind PCNA may reflect reduced repair of mismatches recognized by the Msh2: Msh3 and Msh2: Msh6 heterodimers (145).

As yet no mechanism for strand discrimination has been identified in eukaryotic cells and no MutH homologs have been found. *In vitro* experiments have found that mismatch repair is directed to the DNA strand which contains a strand-specific and site-specific introduced nick and has raised the possibility that strand discontinuities flag the nascent DNA strand for mismatch repair (146, 147). As well, the involvement of PCNA in mismatch repair together with its functions in DNA replication has lead some researchers to conclude that PCNA acts to link the mismatch repair complex to DNA polymerase at the replication fork and in so doing facilitates recognition and repair of the nascent strand (142). However, this does not explain how mismatch repair functions in nonreplicating cells (139)

Genetic studies in yeast have found three endonuclease activities in mismatch repair: *ExoI* and the proofreading exonucleases of DNA polymerases δ and ε (148). *Exonuclease I* is a 5' → 3' exonuclease that has a preference for degrading double-stranded DNA and it is proposed that, in eukaryotes, its presence may eliminate the need for a DNA helicase in the 5' → 3' degradation step (149). In yeast *ExoI* interacts with Msh2 and its disruption leads to a weak mutator phenotype (150). Recently a human *ExoI* homolog (*hEXO1/HEX1*) has been identified and it has also been found to interact with hMSH2 (150, 151).

The exonuclease FEN1 (RAD27 in yeast) has been implicated in mismatch repair due, in part, to its interaction with PCNA and because its mutation in yeast causes a small increase in frameshift mutations similar to those seen in mismatch defective mutants (153). However it remains to be determined why so many, seemingly redundant, exonucleases are functional in mismatch repair. As well it has been shown that DNA polymerase δ (158) and the single stranded DNA binding protein RPA are required in eukaryotic mismatch repair (159). Although considerable progress has been made in identifying and understanding the proteins that function in mismatch repair it is apparent that many questions, ranging from the identification of the strand discrimination signal to the precise interactions of the proteins with the DNA and each other remain to be answered. Perhaps soon all of the proteins necessary for this process will be identified and it will be possible to reconstitute this repair mechanism *in vitro* and determine the precise role that each protein plays in the mismatch repair pathway.

(e) Mismatch repair and HNPCC

To date 70% of HNPCC cases have been reported to carry inherited germline mutations in hMSH2 and hMLH1 (154, 155, 156, 157). Few germline mutations in hMSH3, hMSH6, hPMS1 or hPMS2 have been reported, indicating that inherited mutations in these mismatch repair genes do not play a major role in HNPCC. It remains to be elucidated which, if any, mismatch repair genes are involved in the remainder of the HNPCC kindreds (22, 25, 160, 161, 162, 163). However, a recent study has found that functional deficiencies in the interaction of hMLH1 and hPMS2 were associated with HNPCC (164). This finding suggests that inactivation of mismatch repair can occur not only due to lack of protein expression, but also due to lack of interaction between expressed proteins. In addition promoter hypermethylation of hMLH1, rather than mutation within the gene sequences, also results in lack of protein expression and has been postulated to play a role in HNPCC (165, 166, 167). Although further studies are necessary, this finding may provide an explanation for the remaining HNPCC cases in which inactivating mutations in mismatch repair genes have not yet been found.

(f) Mismatch proteins participate in processes other than mismatch repair

It is apparent that mismatch repair is a complex process and so it comes as no surprise to learn that some of its components have been implicated in several other cellular processes. For example, hMutSα has been shown to bind DNA containing a variety of covalent adducts, including those caused by O^6-methylguanine, the anti-tumor drug cisplatin and UV light (168, 169, 170, 171). Furthermore, loss of mismatch repair activity

is associated with cellular resistance to these agents (172, 173). Recent studies have found that hMutSα binding of O^6-methylguanine stimulated the ADP → ATP exchange and activated the molecular switch function of hMutSα (174). In addition a similar study found that in cells lacking MGMT (O^6-methylguanine DNA methyltransferase), treatment with O^6-methylguainine inducing agents resulted in an accumulation of hMutSα in the nucleus in response to the damage (175).

However, evidence suggests that the involvement of hMutSα in the binding of these DNA lesions does not occur as a prelude to repair but rather flags a cytotoxic event that may eventually signal apoptosis (179). Mismatch repair proteins have been associated with apoptosis induced by numerous alkylating agents in both p53 dependent and independent pathways (176, 177, 178, 179, 180, 181). As well, apoptosis can be induced in both repair deficient and proficient cell lines by the overexpression of hMSH2 or hMLH1 indicating that these proteins may be part of a pathway that influences cell death (182). Several models have been proposed to explain the association of mismatch repair proteins and the initiation of apoptosis and two are discussed below (Reviewed in 174).

One model proposes that, since replication past an O^6-methylguanine lesion would result in nucleotide mis-incorporation (183, 184), the resultant mismatched pair would then become a substrate for the mismatch repair system. However, since the O^6-methylguanine lesion persists in the older DNA strand and is not repaired, this would lead to repeated cycles of futile repair resulting in strand breaks, cell cycle arrest and ultimately apoptosis. Furthermore, in mismatch repair deficient cells this "futile cycle" of

DNA repair cannot occur, apoptosis is not initiated and results in the development of a damage tolerant phenotype (185, 186, 187). Another model suggests that specific types of DNA damage are recognized by the mismatch repair system, activate the hMutSα molecular switch and result in the formation of a sliding clamp in close proximity to the DNA lesion. However, in this scenario DNA repair is not initiated and the resulting accumulation of DNA-bound sliding clamps is proposed to ultimately signal apoptosis (188).

Mismatch repair is also associated with transcription-coupled repair (TCR). The first evidence for this came from studies in *E.coli* where mutations in MutS and MutL eliminated TCR repair of UV photoproducts (189). Soon after it was found that human cell lines deficient in mismatch repair were also deficient in TCR of UV damage although NER was active in these cells (190). Follow-up studies have since found that mutation in either hMSH2 or hMLH1 resulted in reduced TCR of damage induced by UV radiation whereas mutation in hMSH2 alone was associated with an inability to carry out TCR of damage induced by ionizing radiation (191). Furthermore, the yeast Msh2 protein has been found in a complex with NER proteins further linking mismatch repair to nucleotide excision repair (192) and a recent study has found that hMSH2, hMSH5 and hMLH1 are components of the BASC (BRCA1 associated genome surveillance complex) protein complex (193). This type of evidence has lead researchers to suggest that, in addition to their roles in mismatch DNA repair, mismatch repair proteins may perform a general surveillance function in which they monitor the genome for many other types of damage.

Mitotic recombination between homologous genes is one of the mechanisms responsible for cells becoming homozygous for a particular recessive gene (Reviewed in 199). Spontaneous and carcinogen-induced homologous recombination occurs most frequently between identical DNA sequences and has been implicated in specific genetic alterations required for malignant transformation, such as chromosomal rearrangements, translocations, deletions and gene amplifications (200). Recombination between two similar but non-identical sequences will form a heteroduplex intermediate containing mispaired DNA, which is corrected by the mismatch repair system (194). However, in mismatch repair defective cell lines the frequency of recombination is often dramatically elevated (194, 195, 196). Consequently mismatch repair activity has been found to play a role in removing non-homologous DNA during gene conversions and single strand annealing events in yeast (197, 198).

(g) Mismatch repair and the cell cycle

In proliferating mammalian cells, DNA synthesis and cell division are performed at specific intervals within the cell cycle (Reviewed in 201, 202). The cell cycle is a highly ordered process that in mammalian cells is composed of four phases: $G_1 \rightarrow$ pause or resting phase prior to DNA replication; S $\rightarrow$ DNA synthesis phase; $G_2 \rightarrow$ pause after DNA synthesis and M $\rightarrow$ mitosis. Along with the machinery that promotes cell cycle progression cells are also equipped with cell cycle checkpoints that ensure correct ordering of events in the cell cycle. Cell cycle checkpoints are regulatory pathways that control the order and timing of cell cycle transitions and ensure that critical events such

as DNA replication are completed with accuracy (203). Cell cycle arrest at a particular checkpoint is also induced in response to DNA damage. For example, cells containing damaged DNA arrest at G_1-S and G_2-M, so as to gain time for repair and to avoid fixing mutations during DNA replication and cell division (204).

In addition to controlling cell-cycle arrest the proteins involved in the DNA damage checkpoints have also been shown to be involved in the activation of DNA repair pathways (206, 207). Moreover, the reverse is also true, as it has been shown that DNA repair pathways are involved in the activation of DNA damage checkpoints. For example, G_2 arrest, induced by treatment with 6-TG or MNNG, was not observed in hMLH1-defective cells until active mismatch repair had been restored by chromosome transfer (205, 208). In addition, G_2 arrest induced by O^6-methylguanine generating drugs occurred only in mismatch repair proficient cells and not in their mismatch repair defective counterparts (209).

As we know, mismatch repair in bacteria is a post-replication DNA repair mechanism, which functions primarily in the removal of base mismatch errors introduced during DNA replication. Due to the similarities between the repair systems it was assumed that eukaryotic mismatch repair was also a post-replication DNA repair mechanism. It follows, that if this were also the case in mammalian cells, then mismatch repair would function primarily if not exclusively in the G_2 phase of the cell cycle. Although, there is no concrete evidence to support the theory that mismatch repair is active in the G_2 phase of the mammalian cell cycle, the finding that the mismatch repair

system is involved in a G_2 cell cycle arrest provides indirect evidence for the activity of this repair system in that phase of the cell cycle.

As discussed above, nucleotide mispairs occur by a variety of processes. In addition, it has been shown that mismatch repair proteins recognize many types of DNA damage that occur throughout the cell cycle. We therefore speculated that the mismatch repair system functions in phases of the cell cycle other than G_2. Previous investigations have found that levels of the mismatch repair proteins hMSH2, hMLH1 and hPMS2 do not change appreciably throughout the cell cycle (210, 211) and that expression of mismatch repair proteins occurs in tissues that no longer replicate (212). However, the presence of these proteins is not necessarily an indicator of activity and may be due to their putative roles in damage recognition or damage surveillance. One of the goals of this research has been to determine if the mismatch repair system is active in the repair of several base:base mismatches at the codon 12 H-*ras* hotspot of mutation during the G_1 phase of the mammalian cell cycle.

PART II: Effects of p,p'-DDE on cell toxicity and mismatch repair ability at an oncogenic hotspot

The Inupiat residents of Alaska along the Arctic Ocean coast are concerned that traditional food sources containing environmental pollutants, such as pesticide residues and heavy metals, may contribute to their unique childhood and adult disease profile (213).

In 1996 the community health department of the Alaska Area Native Health Service began a preliminary study of maternal blood plasma and newborn umbilical cord blood from residents of the northern coastal town of Barrow. Blood samples thus far collected have been analyzed for the presence of various environmental contaminants. In addition to other chemicals, measurable levels of p,p'-DDE (1,1 dichloro-2,2-bis(p-chlorophenyl)ethylene), (hereafter DDE) were found in 100% of the samples studied. In maternal plasma the concentration of DDE ranged from 0.353–3.505 μg/l (20 samples) with an average concentration of 1.263μg/l. Newborn umbilical cord blood concentrations of DDE ranged from 0.118–0.840 μg/l (24 samples) with an average concentration of 0.331 μg/l (214).

DDE is the major metabolic breakdown product of the pesticide DDT (1,1,1 trichloro-2,2-bis-(p-chlorophenyl)ethane). The use of DDT was banned in the United States and in many other countries in the early 1970's when environmentalists determined that there were links between DDT and various ecological disturbances, including the decline of selected bird populations and numerous instances of fish kills

(215). Insecticidal use of DDT still persists today in many countries including southern Asia, Central and South America and Africa (216).

Due to the complex ring structure of DDT, slow biotransformation occurs in mammals resulting in the accumulation of DDT and its metabolites in body tissues (217). Analysis of human tissues exposed directly to DDT yields a ratio of approximately 5 PPM DDT to 15 PPM DDT metabolites (primarily DDE) (215). As well, serum from rats exposed to dietary DDT contains a mixture composed of a greater amount of the parent compound than its metabolites (218). However, no measurable amounts of DDT were found in any of the blood samples tested indicating that the Alaskan Inupiat population is not exposed directly to the parent compound. Rather, the presence of only DDE indicates that exposure occurs primarily through the biomagnification of this persistent metabolite through the worldwide food chain.

DDE is extremely lipophilic and accumulates in adipose tissue (219, 220). As well, it has been reported that species with long life spans can accumulate high tissue levels of the compound (221). The Alaskan Inupiat, maintaining a subsistence lifestyle, preferentially consumes the adipose tissue of animals at the higher trophic levels of the food chain, (e.g. whales, seals and walruses). A diet consisting of foods from these sources is thought to be the primary exposure route of this human population to DDE. Although some environmental monitoring for DDE and other chemicals is currently ongoing, there is, as yet, no reliable estimate of the amount of DDE that the Alaska Inupiat, depending on lifestyle and dietary habits, may be exposed to.

The EPA has listed DDE as a probable human carcinogen (222). The chemical has been found to induce liver tumors in mice (223), to cause DNA strand breaks in Chinese hamster cells (224) and to inhibit platelet aggregation (225). DDE exposure *in utero* results in the demasculinization of male rats, which is manifested by reduced angogenital distance and retained thoracic nipples (226). Both *in vivo* and *in vitro* studies have identified DDE as an androgen receptor antagonist and an inhibitor of androgen-induced transcriptional activity (227, 228). Furthermore, it has been demonstrated that DDE is an inducer of the phenobarbital (PB) -type cytochrome P-450 (CYP) mixed-function monoxygenases (229). It has been proposed that the demasculinizing effects of DDE may be due to both the chemical's anti-androgenic effects and induced expression of the CYP-enzymes (230). However, the DDE concentrations used in all of the aforementioned studies are several orders of magnitude greater than the concentrations measured in the Alaskan blood samples.

Current evidence indicates that fetuses and infants are more susceptible than adults to a variety of environmental toxicants. A recent report demonstrated that several of the CYP enzymes, such as those involved in testosterone metabolism, were induced in rats exposed to low levels of DDE, although the sexual and developmental defects observed at the higher doses were absent (230). These inappropriate enzyme inductions may have serious consequences for the developing embryo at a time when it is physiologically immature and most sensitive to hormone fluctuations (231). Therefore, in this study we investigated the effects of DDE exposure on two different cell types. NIH 3T3 is an immortal aneuploid murine embryonic fibroblast cell line. WS1 cells are non-

transformed human embryonic fibroblasts with a normal chromosome number. Inclusion of these two distinct cell types enabled us to identify the common cellular effects of DDE on immature mammalian cells as well as those effects unique to the WS1 human fetal cells.

The aim of these studies was to determine whether concentrations of DDE, relevant to the Alaskan environment, had any measurable toxic effect on immature mammalian cells in culture including site-specific DNA mismatch repair as discussed previously. Initial experiments were performed to determine if exposure to DDE had any effect on the overall cell quantity per exposed plate of either cell type. Based on these initial positive results, subsequent short-term and long-term exposure assays were performed to determine possible mechanisms for these observed fluctuations in cell number. Decreases in cell number could be due to cell death, either by necrosis or apoptosis, or cell cycle arrest. As discussed in part I, a delay or arrest in the progression of a proliferating cell through the cell cycle can occur in response to DNA damage. DNA damage can trigger cell cycle arrest at virtually any point in the cell cycle so as to provide additional time both for the transcription of DNA repair genes and the repair of DNA damage (232, 233).

In an attempt to elucidate the genotoxic potential of DDE, we included assays which examined the direct DNA damaging potential of DDE as well as the chemical's effect on the ability of both cell types to repair specific types of DNA damage. The Comet assay was used to examine the genotoxicity of DDE and a modification of an *in vivo* DNA repair assay was used to investigate the effect of DDE on DNA repair.

Briefly, two base:base mismatches were constructed at the oncogenic codon 12 H-*ras* hotspot using a method similar to that employed in previous studies (see materials and methods). The DNA was then introduced into both embryonic cell types in the presence of DDE and the mismatch repair rates at this oncogenic hotspot were subsequently determined. Although preliminary, the results of this study show that relatively small concentrations of persistant organic pollutants, such as DDE, exert effects on several different processes in immature cells in culture.

II. MATERIALS AND METHODS

A. Reagents: 2,2-bis(4-chlorophenyl)-1,1-dichloroethylene (DDE) was purchased from Aldrich-Sigma chemical company. Dulbecco's modified Eagle medium (DMEM), minimum essential medium (MEM), OptiMem, Lipofectamine transfection reagent and Trypsin-EDTA were purchased from Gibco BRL Life Technologies Inc. Clonfectin liposome reagent was purchased from Clontech Inc. Fetal bovine serum (FBS) and bovine calf serum (CS) were purchased from Hyclone Laboratories. Hygromycin was purchased from Calbiochem-Novabiochem Corporation. Streptavidin-horseradish peroxidase, anti-mouse immunoglobulin antibody, Thermosequenase sequencing and ECL Western blotting detection kits were purchased from Amersham Pharmacia Biotech. SeaKem GTG and Nusieve 3:1 agarose were purchased from FMC Bioproducts. Qiaquick Gel Extraction and Qiaquick PCR purification kits were purchased from Qiagen Inc. The Prime-a-gene nick translation kit was purchased from Promega. The Quantum Prep plasmid miniprep kit was purchased from Biorad Laboratories Inc. Sephadex G50, G100, Proteinase K, phenol: chloroform: isoamyl alcohol (25: 24: 1), PMSF (phenyl methyl sulfonyl fluride), DTT (dithiothreitol), DMSO, 10X Denhardt's reagent, Sigma-Fluor scintillation cocktail, denatured salmon sperm, carbenicillin, kanamycin and all other chemicals and reagents were purchased from Sigma Chemical company unless otherwise stated.

B. Cell lines and bacteria: NIH 3T3 and WS1 cell lines were purchased from American Type Culture Collection (ATCC). NIH 3T3 cells were grown in DMEM/10% CS. WS1

cells were grown in MEM/10% FBS. Both cell cultures were maintained at 37°C in 5% CO_2. Competent DH5α *E.coli* bacteria were purchased from Life Technologies Inc. NR9374 (Mut L- and Mut Y-) *E.coli* bacteria were a kind gift from Dr. Roel M. Schaaper, National Institute of Environmental Health Sciences.

C. DNA: Plasmids pbc-N1 and pT24-C3 were purchased from American Type Culture Collection (ATCC). Plasmid p220.2 was a kind gift from Dr. William Sugden, University of Wisconsin. M13mp18 and M13mp19 were purchased from Sigma Chemical Company. All synthetic oligonucleotides were purchased from Operon Technologies Inc. Radioactively labeled nucleotides were purchased from NEN Life Science Products, Inc.

D. Enzymes: *Afl*III, *Pvu*I, *Hind*III, *Dpn*I, *Dpn*II, *Ecor*V and *Bam*HI were purchased from New England Biolabs. *Bst*98I and Turbo *Nae*I were purchased from Promega Corporation. *Xho*I, *Kpn*I and T4 ligase were purchased from Boehringer Mannheim Corporation. Shrimp alkaline phospatase (SAP), Exonuclease I and T4 polynucleotide kinase were purchased from USB Corporation. Amplitherm PCR enzyme was purchased from Epicenter technologies.

E. Plasmid and M13 constructs

Previously this laboratory had taken the following steps to produce the plasmids and M13 bacteriophage constructs used in the preparation of mismatched plasmids (234). First, a shuttle vector containing human H-*ras* genomic DNA was constructed by inserting the wild-type (wt) human H-*ras* genomic sequence (*Bam*HI 6.4 kb segment from pbc-N1)

into the *Bam*HI site in the polylinker region of the Epstein-Barr Virus (EBV) shuttle vector p220.2. Removal of the original *Hind*III site in the polylinker region of p220.pbc was then accomplished by DNA polymerase I (Klenow fragment) 5' → 3' exonucleolytic digestion and subsequent blunt-end ligation by standard procedure to produce p220.pbc-H/B plasmid.

A 2 kb *Bam*HI – *Kpn*I segment of p220.pbc-H/B containing exon 1 was ligated into the polylinker region of bacteriophage M13mp 19 and subjected to oligo-directed mutagenesis to create two new restriction enzyme recognition sites, *Hind*III and *Bst*98I, 30 base-pairs apart flanking H-*ras* codon 12 in exon 1. Three separate rounds of oligonucleotide-directed mutagenesis were performed with the M13-*ras* plasmid to change a total of four bases: codon 6 : G → T (no amino acid change but creates a unique *Hind*III site) and codon 15: GGC → CTT (Gly → Leu, both neutral non-polar amino acids, to create a unique *Bst*98I site). Restriction digestion and dideoxy sequencing were used to select M13+*ras* clones that contained only the above-indicated base changes. The *Bam*HI – *Kpn*I segment, containing the new sites, was excised from the double-stranded M13+*ras* DNA and inserted into p220.pbc-H/B in place of the original 2 kb H-*ras* segment thus producing the modified plasmid renamed p220.pbc+H/B.

Next, the 2 kb *Bam*HI - *Kpn*I segment of the H-*ras* gene, containing codon 12,was isolated from the p220.pbc+H/B plasmid and ligated into the polylinker region of pUC 19, M13mp 18 and M13mp 19 to produce p*ras*BK2.0, M13*ras* 18.9 (+ strand contains non-coding sequence from H-*ras*) and M13*ras* 19.1 (+ strand contains coding sequence from H-*ras*) respectively.

PART I: Mismatch repair at an oncogenic hotspot in G_1 synchronized mammalian cells

Section I: Method of G_1 synchronization, fluorescent activated cell sorting analysis, plasmid replication kinetics and mismatch repair protein expression in G_1 nuclear extracts

A. G_1 synchronization and fluorescent activated cell sorting analysis

G_1 synchrony was achieved using the serum starvation method as described by Rabinovitch *et al* 1990 (235). NIH 3T3 cells were seeded in duplicate at 4.9×10^5 cells per 10 cm dish in media containing either 0.25% CS or 10% CS (controls) and incubated for 3 days at 37°C in 5% CO_2. At designated time-points (see Table 3) on days 2 and 3 duplicate samples were harvested as follows. At each time-point media was removed and each plate rinsed with 5 mls of 1X PBS. 3 mls of 0.025% Trypsin-EDTA was then added and plates were returned to the 37°C incubator for 3 minutes. The Trypsin- EDTA/cell solution was then removed to a pre-chilled disposable conical vial containing 3 mls of DMEM/10% CS/10% DMSO, and pelleted by centrifugation at 200 x g at 4°C for 5 minutes. Finally, all but 20-50µl of the liquid was aspirated off and the pellets were frozen at -70°C.

On day 4 at 0 hrs the media on all remaining plates was replaced with fresh media (DMEM + serum) containing 10% CS and the plates were returned to the incubator. At 2 hr intervals between 0 and 24 hr, after the addition of fresh media, duplicate plates were harvested, (as described above). The completed experiment was then shipped frozen on

dry ice to the laboratory of Dr. Peter Rabinovitch at the University of Washington (Seattle, WA) where flow cytometric analysis was performed. The number of cells in the G_1, S, G_2/M phases of the cell cycle were quantified using the 4,6-diamidino-2-phenylindole reagent for DNA quantification (236).

B. Plasmid replication kinetics

Replication of the p220.pbc plasmid within synchronized NIH 3T3 cells was studied to determine if the plasmid continued to replicate synchronously with the cell cycle following G_1 arrest.

(i) Transfection of G_1 synchronized cells

NIH 3T3 cells were plated at 1.1 X 10^6 cells in a 15 cm dish in media containing either 0.25% or 10% CS (controls) and incubated for 3 days at 37°C in 5% CO_2. On day 4, 1 hour prior to the start of transfection, all plates were re-fed with fresh DMEM containing 10% CS.

A 3 μg aliquot of p220.pbc-**H/B** and 300 μg of Lipofectamine were added to 200 μl of OptiMem and incubated for 30 minutes at room temperature. Each plate was rinsed with 10 mls of 1X PBS and then 5 mls of OptiMEM was added followed by the plasmid transfection mixture. The plates were then placed at 37°C with gentle rotation for 30 minutes followed by a further 5 ½ hour incubation without agitation at 37°C in 5% CO_2. At the end of this period the transfection mixture was removed and replaced with media containing 10% CS and the plates were returned to the incubator. At various time-points

(see Figure 8) duplicate control and synchronized plates were harvested as follows. Each plate was rinsed with 10 mls 1 X PBS and incubated for 5 minutes at 37°C with 5 mls of 0.025% Trypsin-EDTA. The contents of each plate were then removed to a conical vial, containing 5 mls of DMEM/10% CS, centrifuged for 5 minutes at 200 x g and frozen at -20°C.

(ii) Plasmid recovery and digestion

Plasmid DNA from each of the frozen cell pellets was recovered using the Quantum Prep Plasmid Miniprep kit as described by the manufacturer (Biorad Laboratories Inc.). Each sample was then digested with 10 units of *Dpn*II. Digestion of DNA by *DpnII* enzyme is blocked by prokaryotic adenine methylation and therefore only that DNA which has replicated 2 or more times in mammalian cells will be digested. As a control, included with each set of samples were control reactions containing p220.pbc –H/B DNA treated with either *Dpn*I or *Dpn*II. *DpnI* digests DNA at the same restriction sites as *DpnII* but only when that DNA has been methylated at adenine residues. The completed digest reactions were then electrophoresed on a 1% Seachem GTG agarose gel.

(iii) DNA transfer and immobilization (Southern Blot)

The agarose gel from step (ii) was then immersed in, 0.25 N HCL for 30 minutes, then denaturing buffer (3M NaCl, 0.4M NaOH) for 30 minutes and finally washed in alkaline transfer buffer (3M NaCl, 8mM NaOH) for 15 minutes. The DNA was then transferred under alkaline conditions to an S+S Nytran positively charged nylon membrane using the

alkaline capillary transfer method as described by the manufacturer (Schleicher and Schuell, Inc.). Following transfer, the membrane was neutralized in 0.2 M sodium phosphate pH 6.8 for 3 minutes and the DNA immobilized on the membrane by UV cross-linking. Briefly, the damp membrane was exposed in an UV Stratalinker (Stratagene) to UV at 254 nm for 5 minutes at a distance of approximately 15 cm from the light source. The total UV exposure of the membrane was 120 mJ/cm^2.

(iv) Radioactive probe preparation

The p220.pbc-**H/B** plasmid, at a final concentration of 100 ng/µl, was digested with each of the enzymes *EcoR*V and *Bam*H1 (2 units per µg DNA). The digestion products were then separated by electrophoresis on a 1% SeaKem GTG agarose gel. The 613 bp *EcoR*V/*Bam*H1 fragment was excised from the gel and recovered using the Qiaquick Gel Extraction Kit as described by the manufacturer and quantified.

The 613-bp *EcoR*V/*Bam*H1 fragment (hereafter referred to as the DNA probe) was then radioactively labeled with [α]-32p CTP (6000 Ci/mMol, NEN Life science products, Inc.) using the Prime-a-Gene Nick Translation Kit as described by the manufacturer (Promega Corporation Inc.). The reaction was then passed through a G100 sephadex column in order to remove all unincorporated radioactive nucleotide. The specific activity of each labeled probe preparation was assessed by liquid scintillation counting in 5 mls of Sigma-Fluor liquid scintillation cocktail. Only those radioactively labeled probes whose activity was 10^9 cpm/µg of DNA or greater were used in subsequent hybridization steps.

(v) Hybridization

The UV crosslinked membrane from (ii) was incubated at 42°C for 2 hours with agitation in pre-hybridization buffer (50% formamide, 6X SSPE, 5X Denhardt's reagent, 1% SDS, 100 μg/ml denatured salmon sperm DNA). The radioactively labeled DNA probe from step (iv) was denatured at 95°C for 5 minutes and placed on ice. The membrane was immersed in hybridization buffer (50% formamide, 6X SSPE, 5X Denhardt's reagent, 0.5% SDS, 100 μg/ml denatured salmon sperm DNA), at a volume of 1 ml of hybridization buffer per $1x10^5$ cpms of radioactive probe, then the denatured probe was added and the membrane was incubated at 42°C overnight in a shaking water-bath. The membrane was then washed as follows: 3 times in 7X SSPE + 0.5% SDS for 15 minutes; twice in 1X SSPE + 1%SDS for 15 minutes at 37°C: and finally for 1 hour at 42°C in 0.1X SSPE + 1% SDS. The moist membrane was then wrapped in saran wrap and exposed to Biomax X-ray film (Eastman Kodak Corporation) at −70°C with an intensifying screen.

C. Mismatch repair protein expression in G_1 nuclear extracts

This assay was performed to determine if the mismatch repair protein MSH2 could be detected in nuclear extracts prepared from G_1 synchronized NIH 3T3 cells.

(i) G_1 nuclear extract preparation

NIH 3T3 cells were plated at 1 x 10^6 cells per 15 cm plate in DMEM/10% CS. Twenty-four hours later the media was replaced with DMEM / 0.25% CS and the cells incubated for a further 3 days to achieve G_1 synchrony (see Table 3).

Nuclear and cytoplasmic extracts were prepared by the method of Dignam et al with some changes as described below (237). On day 4 the cells were harvested by trypsinization and centrifuged at 450 x g at 4°C for 3 minutes. The pelleted cells were re-suspended in isotonic buffer (20 mM Hepes pH 7.9, 20% glycerol, 0.1 M KCL, 0.2 mM EDTA, 0.5 mM PMSF [phenylmethylsulfonyl fluoride], 0.5 mM DTT [dithiothreitol], and centrifuged at 450 x g at 4°C for 3 minutes. The cell pellet was then washed with 5 mls of hypotonic buffer, (20mM Hepes pH 7.9, 5mM KCL, 0.5 mM $MgCl_2$, 0.2 M sucrose), re-suspended at 2 X 10^7 cells/ml in the same buffer and placed on ice for 10 minutes. The cells were then lysed with 10 strokes of a Dounce homogenizer, observed microscopically for plasma membrane lysis and centrifuged at 300 x g at 4°C for 3 minutes to pellet the nuclei. The supernatant (cytoplasmic extract) was subsequently removed and stored frozen at -70°C.

The nuclei pellet was re-suspended at 2 X 10^8 cells/ml in Buffer A (hypotonic buffer plus 0.5 mM DTT and 0.1% PMSF). The nuclei solution was mixed by rotation

with the addition of 0.03875 volumes of 4M NaCl for 1 hour at 4°C followed by centrifugation for 20 minutes at 15,000 x g at 4°C. The supernatant (nuclear proteins) was removed and mixed by rotation for 30 minutes at 4°C with the addition of 0.42 g/ml of $(NH_4)_2SO_4$ and then centrifuged at 16,000 x g at 4°C for 30 minutes. The pellet was then re-suspended at 1.8 x 10^9 cells/ml in resuspension buffer (20 mM Hepes pH 7.9, 20% glycerol, 0.1 M KCL, 0.2 mM EDTA, 0.5 mM PMSF, 0.5 mM DTT) and dialyzed against 50 volumes of the same buffer for 90 minutes at 4°C and subsequently stored at -70°C. The nuclear and cytoplasmic protein extracts were quantified by the Bradford assay (238).

(ii) Western blotting

G_1 nuclear and cytoplasmic extracts (15 – 20 μg protein per lane) were mixed with an equal volume of 2X SDS sample buffer (1% Tris-HCL/SDS pH 6.8, 6% SDS, 20% glycerol, 2% 2-mercaptoethanol, 10 μg/ml bromophenol blue) The samples were heated for 5 minutes at 100°C with the caps open, placed on ice and loaded onto a 7.5% discontinuous SDS polyacrylamide gel (stacking gel 30% acrylamide/ 0.8% bisacrylamide, 4% Tris-HCL/SDS pH 6.8: separating gel 30% acrylamide/0.8% bisacrylamide, 4% Tris/HCL/SDS pH 8.8) and electophoresed at 10 mA for 2 hours. The resulting gel was then transferred overnight at 10 mA onto a pre-wetted nitrocellulose membrane (Schleicher and Schuell, Inc.) using a Trans-Blot apparatus (Bio-rad Laboratories, Inc.) in a transfer buffer consisting of 2.5 mM Tris and 19.2 mM glycine.

Next, the membrane was placed in blocking buffer (5% non-fat milk in Tris-buffered saline pH 7.6, 0.1% Tween 20) for 1 hour with agitation. The membrane was then washed by rinsing briefly twice in TBS-T (Tris buffered saline pH 7.8, 0.05% Tween 20), placing the membrane in fresh TBS-T with agitation for 15 minutes and then placing it again in fresh TBS-T twice more for 5 minutes with agitation. The membrane was next incubated with MSH2 primary antibody (Santa Cruz Biotechnology) at a 1:200 dilution with agitation for 1 hour. Excess primary antibody was washed from the membrane by rinsing twice briefly in TBS-T, placing the membrane in fresh TBS-T with agitation for 15 minutes and then placing it again in fresh TBS-T twice for 5 minutes with agitation. The membrane was then incubated in TBS-T with a horseradish peroxidase (HRP)- conjugated anti-mouse immunoglobulin antibody at a dilution of 1:1000. Excess secondary antibody was washed from the membrane again by rinsing briefly twice in TBS-T, placing the membrane in fresh TBS-T with agitation for 15 minutes and then placing it in fresh TBS-T twice more for 5 minutes with agitation. Bound antibodies were detected by ECL detection of the HRP enzyme as described by the manufacturer (Amersham Pharmacia Biotech).

Section II: Mismatch repair in the G_1 phase of the mammalian cell cycle

A. Mismatch construction at codon 12 of H-ras

(i) Fragment preparation

Mismatches at the middle base pair position of codon 12 of H-*ras* were prepared by the following method. The first step was to digest 100 μg of the p*ras*BK2.0 plasmid with both *Afl*III and *Pvu*I enzymes. The reaction mix contained 1 unit enzyme/μg plasmid DNA with a final concentration of 0.25 μg DNA/μl and released a 2.5 kb fragment containing the inserted H-*ras* segment. The products of this reaction were then digested with *Bst*98I in a final DNA concentration of 50 ng/μl using 10 units of enzyme/μg DNA. The products from the *Bst*98I digest were then digested with *Hind*III using 10 units enzyme/μg DNA. The four restriction enzyme digestions produce fragments of size 1.7 kb, 392 bp, 305 bp and selectively excise the 30 bp segment containing codon 12 of H-*ras* from the *ras* containing DNA (Figure 5, step 1).

(ii) Oligonucleotides

Oligonucleoides complementary to the 30 bp region comprising codon 6 → codon 15 but containing an incorrect nucleotide at the middle nucleotide position of codon 12 were obtained from Operon Technologies Inc. Coding strand oligonucleotides had the sequence 5' GGT GGG CGC CG**G** CGG TGT GGG CAA GAG TGC GC – 3', with the bolded **G** replaced with either a T to produce **T**:C mismatches or an A to produce **A**:C mismatches at H-*ras* codon 12 middle base position. Non-coding strand oligonucleotides had the sequence 5' GCG CAC TCT TGC CCA CAC CG**C** CGG CGC CCA CC – 3',

with the bolded **C** replaced either with a T to produce a G:**T** mismatch or with an A to produce a G:**A** mismatch at the middle base position of codon 12, H-*ras*.

Each of the four oligonucleotides were 5' phosphorylated using T4 polynucleotide kinase at a final DNA concentration of 0.125 µg/µl using 16 units enzyme/µg as described by the manufacturer. The reactions were incubated at 37°C for 60 minutes and then centrifuged through a dH_20 equilibrated Sephadex G-50 spin column at 300 x g for 3 minutes. The phosphorylated oligonucleotides were then stored frozen at -70°C in ddh_20 at a final concentration of 500 ng/µl.

(iii) Melt and reanneal for site- and strand- specific mismatch construction

Generation of heteroduplex DNA was made according to the choice of mismatched 30 bp oligonucleotide and single stranded M13*ras* complementary DNA. Use of single-stranded M13*ras* 18.9 (non-coding strand) and the appropriate mismatch-containing coding strand oligonucleotide produced **T**:C and **A**:C mismatches. Use of single-stranded M13*ras* 19.1 (coding strand) and the appropriate mismatch-containing non-coding strand oligonucleotide resulted in G:**T** or G:**A** mismatches.

Double-stranded mismatches were created by annealing the phosphorylated oligonucleotide with the complementary single stranded M13*ras* DNA and the DNA fragments produced in the *Afl*III, *Pvu*I, *Bst*98I and *Hind*III digests of p*ras*BK2.0 at a 50:1:1 molar ratio of oligonucleotide: M13*ras*: fragments. The fragments were heated for 10 minutes at 100°C and then cooled to 95°C over 2 minutes. During the cool down period the M13*ras*, 10X annealing buffer (400 nM Tris pH 7.5, 200 nM $MgCl_2$ and 500

nM NaCl) and mismatch oligonucleotides were added to a final concentration of 50 ng/μl DNA and 1X annealing buffer. The reaction was then allowed to cool to 22°C over 150 minutes (Figure 5, step 2).

(iv) Isolation of the site- and strand-specific mismatch containing 1.8 kb fragment

The melt and re-anneal reaction mix containing the partially double-stranded M13*ras* molecule was next cleaned using the Qiaquick PCR purification kit as described by the manufacturer (Qiagen Inc). The elutant was next digested with 20 units each of the enzymes *Xho*I and *Kpn*I per μg of DNA at a final concentration of 100 ng DNA/μl. The reaction contents were then separated by electrophoresis on a 0.8% SeaKem GTG agarose gel. The 1.8 kb mismatch containing fragment was then excised, purified using the Qiaquick Gel Extraction Kit as described by the manufacturer (Qiagen, Inc.) and quantified (Figure 5, step 3).

(*v) Assembly of the completed mismatched plasmid*

Vector preparation. The p220.pbc-**H/B** plasmid was digested with 20 units each of *Xho*I and *Kpn*I per μg DNA at a final concentration of 100 ng DNA/μl. The reaction products were subsequently separated by electrophoresis overnight at low voltage on a 0.7% SeaKem GTG agarose gel. The 13.5 kb band was excised, purified as above and quantified. This vector contained the remaining H-*ras* genomic sequence (minus the 1.8 kb fragment), Epstein-Barr Virus (EBV) origin of replication, eukaryotic hygromycin resistance, bacterial carbenicillin resistance and bacterial replication sequences (246).

Annealing and ligation: To ensure that the mismatch-containing oligonucleotide was indeed present, a greater excess of mismatch-containing oligonucleotide was again annealed to the fragment. Phosphorylated oligonucleotide and the 1.8 kb fragment were mixed together at a 200:1 molar ratio of oligonucleotide:1.8 kb fragment at a DNA concentration of 30 ng/µl in a buffer consisting of 50 mM Tris-HCL pH 7.6, 10 nM dithiothreitol and 500 µg/ml bovine serum albumin. The mixture was placed in a 2-liter beaker containing 85-90°C water and allowed to cool slowly to room temperature. The 1.8 kb fragment was then ligated to the 13.5 kb *XhoI* / *KpnI* vector at a 2:1 molar ratio of fragment to vector using 0.5 units T4 DNA Ligase per µg DNA as described by the manufacturer (Boehringer Mannheim). This final ligation step produced a p220.pbc+**H/B** plasmid containing a site- and strand-specific mismatch at H-*ras* codon 12, middle base pair position (Figure 5, step 4). In addition, this heteroduplex was easily distinguished from any undigested vector contamination (p220.pbc-**H/B**) by the presence of the *Hind*III and *Bst 98I* sites at codons 6 and 15 respectively.

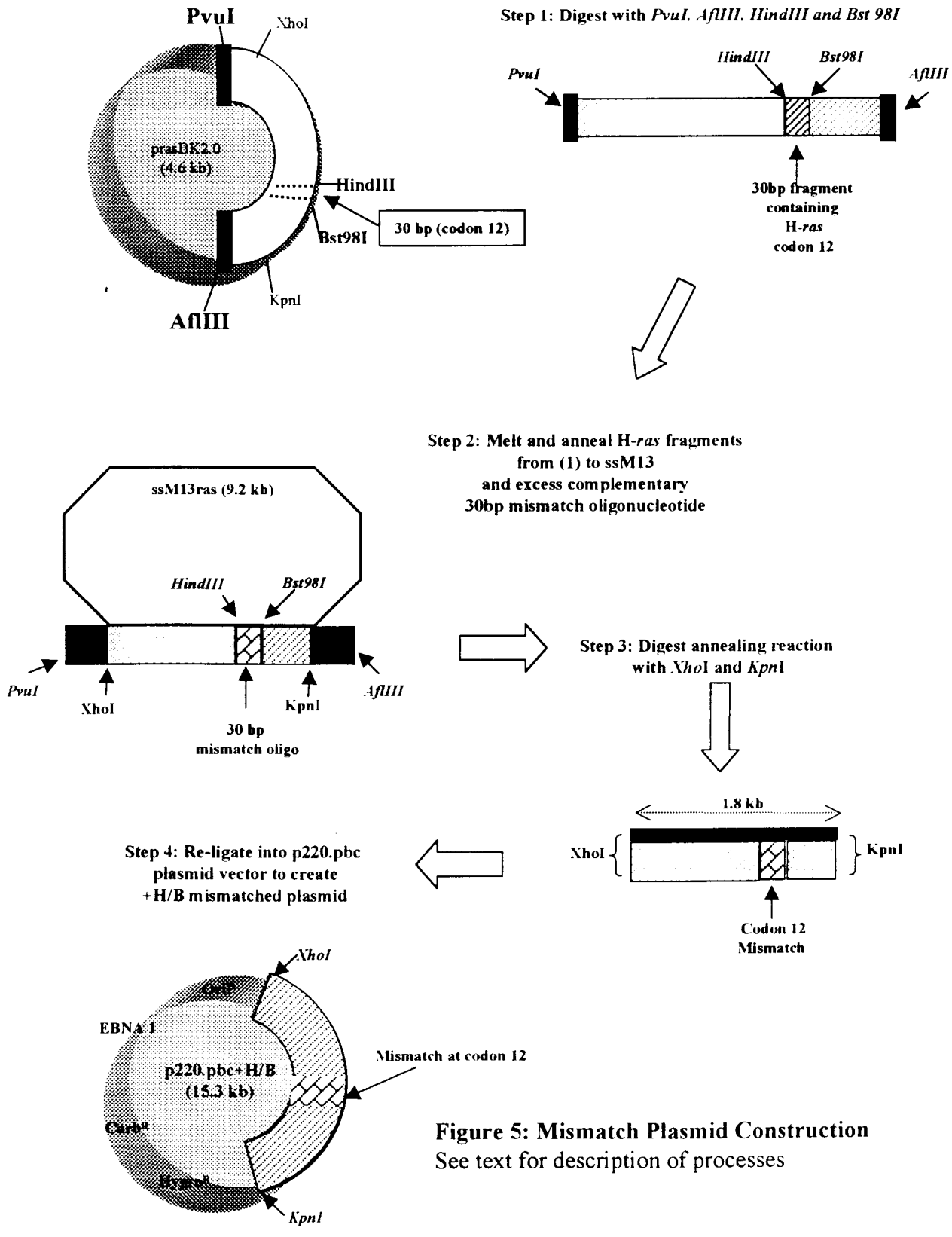

Figure 5: Mismatch Plasmid Construction
See text for description of processes

B. Transfection of G_1 synchronized NIH 3T3 cells and transformation DH5α E.coli with mismatched plasmid

(i) Bacterial transformation: Competent E.*coli* DH5α cells were transformed with 50 ng of mismatch containing plasmid as described by the manufacturer and were grown overnight at 37°C on LB agar containing 100 μg/ml carbenicillin.

(ii) *Transfection of G_1 synchronized NIH 3T3 cells*

For *in vivo* repair of mismatches in G_1 synchronized cells, NIH 3T3 cells were seeded at 4.9×10^5 cells per 10 cm plate in DMEM containing 0.25% CS and incubated for 3 days at 37°C in 5% CO_2. On day 4, 1 hour prior to the start of transfection, the media on each plate was replaced with fresh DMEM and 10% CS.

For each plate, 175 ng of mismatched plasmid and 17.5 μg of Clonfectin liposome reagent (prepared as described by the manufacturer, Clontech Inc.) were added to 200 μl of OptiMEM and incubated at room temperature for 30 minutes. Each plate was rinsed with 5 mls 1 X PBS, followed by the addition of 3 mls of OptiMEM and the plasmid mixture. The plates were then placed at 37°C with gentle rotation for 30 minutes followed by 3 ½ hours in 37°C, 5% CO_2 without agitation. At the end of this time the OptiMEM was removed and replaced with DMEM + 10% CS and the plates were returned to the incubator. NIH 3T3 hygromycin resistant cells were subsequently selected for by the addition of 125 units of hygromycin per ml of media, starting 48 hours after transfection. At the end of 3 weeks, hygromycin resistant colonies on each plate were

methanol fixed (97%) and stained with 1% crystal violet in 20% ethanol. Included with each transfection were positive (p220.pbc –H/B) and negative (no DNA) control plates.

C. Mismatch repair analysis

(i) DNA extraction

Bacteria: Plasmid DNA from carbenicillin resistant DH5α colonies was isolated by the following method. Individual bacterial colonies were removed from the plates with a sterile toothpick and placed in 0.5-ml microcentrifuge tubes. To each sample tube a 100 µl aliquot of lysis buffer (10 mM Tris-HCL pH 8.3, 50 mM KCL. 0.1 mg/ml gelatin, 0.45% NP-40, 0.45% Tween 20, 2.5 mM $MgCl_2$), containing 12 ug of Proteinase K (Sigma Chemical Company) was added (239). The tubes were incubated for 1 hour at 55°C followed by 10 minutes at 95°C. The samples were then extracted with 2 volumes of phenol: chloroform: isoamyl alcohol, and precipitated overnight at -20°C in 1/10 volume of 3 M sodium acetate and two volumes of 100% ethanol. The DNA was pelleted by centrifugation for 30 minutes at 12,000 x g, dried by vacuum centrifugation with heat for 20 minutes and finally resuspended in 10 µl of sterile ddH_20.

NIH 3T3 cells: To analyze repair of mismatches *in vivo* in G_1 synchronized NIH 3T3 cells, DNA was isolated from hygromycin resistant colonies by the following method. Cloning cylinders (Bellco Glass, Inc.) were placed over each previously fixed and stained colony and were adhered to the culture dish with sterile silicone vacuum grease. A 100 µl aliquot of lysis buffer (described above) containing 12 µg Proteinase K was added to the

cloning ring and incubated for 10 minutes at room temperature. The solution in each cloning ring was repeatedly aspirated to dislodge any remaining cells from the culture plate and subsequently transferred to a 0.5-ml centrifuge tube and incubated for 1 hour at 55°C followed by10 minutes at 95°C. The samples were then extracted and precipitated exactly as described above for *E.coli*. The DNA lysates were then re-suspended in 10 µl of sterile ddH_2O and used in the PCR amplification reaction described below.

(ii) PCR amplification

A 5-µl aliquot of each DNA lysate from each colony (*E.coli* and NIH 3T3) was PCR amplified with 2.5 units of Amplitherm enzyme (Epicenter Technologies) in the supplied buffer plus 3.5 mM $MgCl_2$, 200 µM of each dNTP and 100 ng of each primer (described below) in a final volume of 100 µl, with the amplitherm enzyme separated from the other reactants by a wax layer (Chill-Out 14, MJ Research, Inc.). The reactions were heated to 95°C for 3 minutes followed by 35 cycles of 40 seconds at 96°C, 40 seconds at 61°C and 1 minute at 72°C. The samples were then incubated for an additional 7 minutes at 72°C to allow completion of extension reactions and finally cooled to 4°C.

The primers used for the PCR reaction were: 5' H-*ras* → 5'-TGA GGA GCG ATG ACG GAA TAT-3' and 3' H-*ras* →5' CAG GCT CAC CTC TAT AGT GGG GTC-3' (Operon Technologies Inc.). Amplification using these primers produces a DNA product of 129 bp containing exon 1 of human H-*ras* plus several base pairs of the intronic region surrounding exon 1, thus precluding amplification of mouse genomic H-*ras*. Several negative controls (no DNA added to PCR reaction) and positive controls

(0.01 ng p220.pbc-H/B added to PCR reaction) were included with each set of PCR amplification reactions. Amplification was determined by electrophoresis on a 2% SeaKem GTG agarose gel (Figure 6, A).

(iii) Contamination check of amplified H-ras segment

Each PCR amplified sample was tested to confirm that it did not result from transfection of undigested vector (p220.pbc –H/B). 20 µl of amplified product was purified with Qiagen's PCR Purification kit, as described by the manufacturer, and digested with 100 units of *Hind*III enzyme. The samples were examined by electophoresis on a 4% NuSieve 3:1 agarose gel. Only those samples which had been PCR amplified from the +H/B mismatched plasmid are cut by this enzyme to produce two fragments of which only the larger 107 bp fragment is clearly visible on the agarose gel (Figure 6, B).

(iv) Mismatch repair analysis

A 20 µl aliquot of each +H/B amplified PCR product was digested with 4 units of Turbo *Nae*I restriction enzyme in the supplied buffer for 4 hours. The products of this reaction were electophoresed on a 4% NuSieve 3:1 gel and analyzed. Only PCR amplified DNA containing the wild-type sequence at codon 12 of H-*ras* is cleaved by this enzyme giving rise to two distinctly smaller DNA fragments of size 88 and 41 bp (Figure 6, C). If the PCR amplified DNA in a particular sample indicated either incomplete or complete lack of cutting an aliquot of the sample was sequenced in order to determine the exact sequence at codon 12.

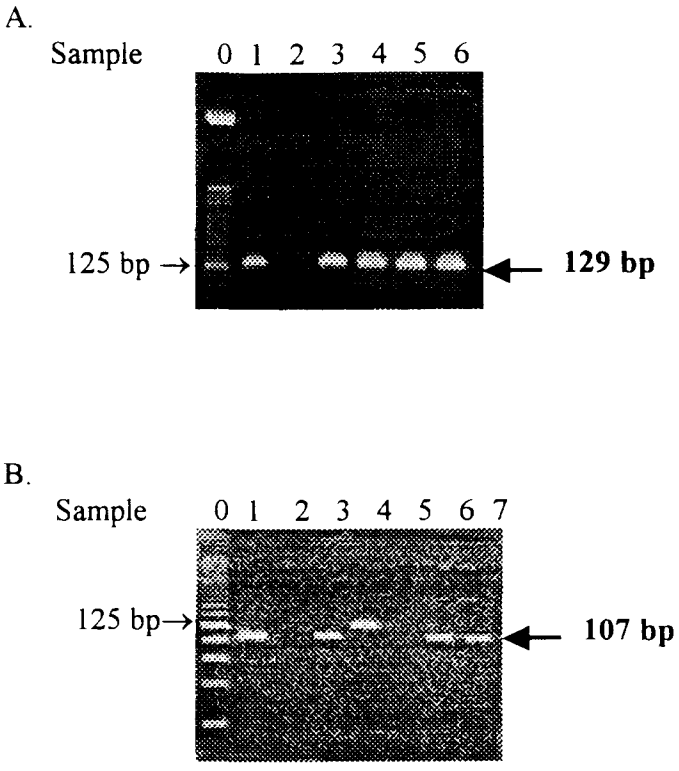

Figure 6 : Mismatch repair analysis

Examples of (A) PCR amplification, (B) *Hind*III verification, and (C) *NaeI* digest mismatch repair rate determination

Lane 0 in A + B + C contains 25 bp ladder with the → indicating the 125 bp band.

(A) PCR amplification: Lanes 1, 3-6 contain the amplified 129 bp fragment of H-*ras* Lane 2 represents a negative control sample into which no DNA has been added.

(B) *Hind*III digest of PCR product to test for –H/B plasmid contamination. Lanes 1,3,6,7 contain PCR product which has been cleaved by *Hind*III to produce a 107 bp band, thus indicating the presence of a +H/B mismatched plasmid. The sample in Lane 4 remains undigested by *Hind*III indicating that this sample resulted from –H/B plasmid contamination (see text for explanation)

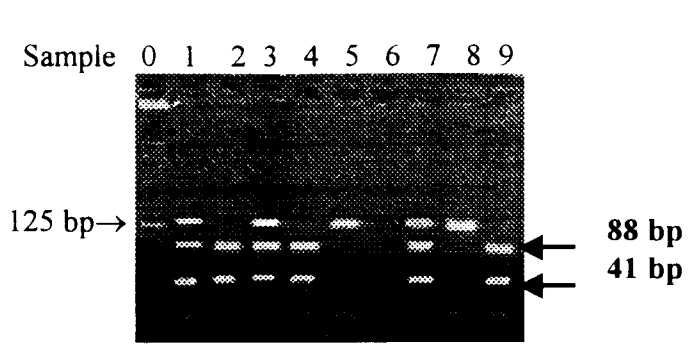

Figure 6 continued

(C) *Nae*I digests of +H/B PCR product. Lanes 1,3,7, show partial digests indicating that these samples contain a mixture of wildtype (88 bp + 41 bp)and mutated sequences (129 bp). Lanes 2,4,9 show complete cutting of the 129 bp band into 88 and 41 bp fragments indicating that the mismatch has been repaired back to wildtype. Lanes 5 + 8 contain samples which have remained undigested by *Nae*I indicating the presence of only a mutated sequence at codon 12 of H-*ras*.

(v) Sequencing

As determined by the *Nae*I digest, each sample to be sequenced was first prepared by treatment with the enzymes *SAP* (Shrimp Alkaline Phosphatase, USB Corporation) and *Exo*I (USB Corporation). A 20 µl aliquote of each PCR reaction was incubated with 10 units of each enzyme for 15 minutes at 37°C followed by 15 minutes at 80°C to inhibit further enzyme activity. The samples were subsequently cleaned using the Qiagen PCR Purification Kit as described by the manufacture. These procedures combined remove excess salt, unincorporated dNTP's and primer DNA from the PCR reaction mix and results in an improved sequencing reaction.

Cycle sequencing was performed using the radiolabeled primer cycle sequencing protocol from Amersham's Thermo Sequenase cycle sequencing kit (Amersham Pharmacia Biotech Inc.). For each reaction the same 3' H-*ras* primer used in the PCR reaction was 5'end labeled with [γ]-32p ATP (6000 Ci/mMol; NEN Life Sciences Inc.) using T4 polynucleotide kinase as described by the manufacturer. The sequencing reaction was set up according to manufacturers instructions but with the following amended cycling parameters: (a) 96°C for 2 minutes, (b) {96°C 1 minute, 68°C for 30 seconds, 72°C 1 minute} for 60 cycles. The sequencing products were loaded on a 12% polyacrylamide gel (19:1 acrylamide to bisacrylamide) and run for 3 hours at 2200 Volts. The gel was then fixed in 20% methanol: 20% acetic acid dried and exposed overnight at -70°C to X-ray film (Eastman Kodak Corporation). The exact sequence at codon 12 could then be read from the developed film (Figure 7).

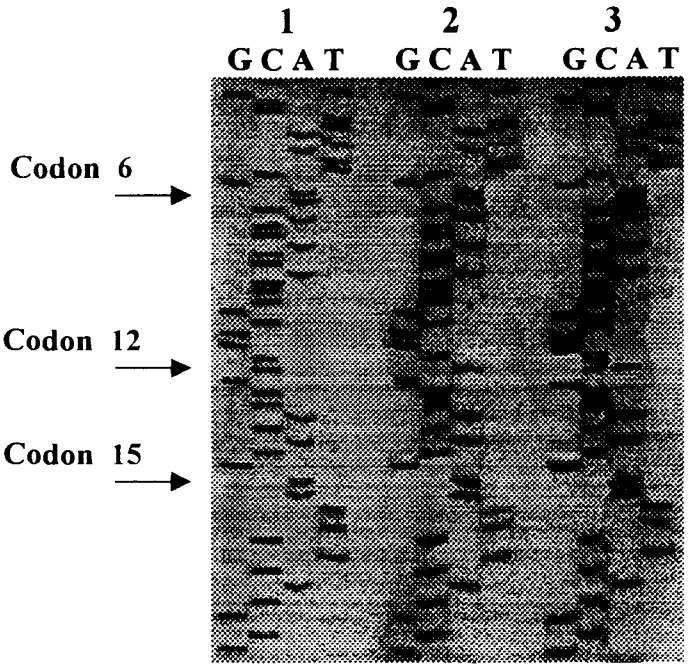

Figure 7

Mismatch repair analysis; example of a Polyacrylamide Sequencing gel autoradiograph.

All three samples contain +H/B samples as is indicated by the sequences at codon 6: (3' GAA) and codon 15: (3' GAA). Lane 1 shows a wild-type sequence at codon 12 (3' CCG).

Lane 2 shows a mutated sequence at codon 12(3' CAG), that resulted from the incorrect repair of a G/A mismatch. Lane 3 contains a mixture of wildtype and mutated sequences at codon 12 3'(C C/A G)

PART II: Effects of p,p'-DDE on cell toxicity and mismatch repair ability at an oncogenic hotspot

Section I: Preliminary experiments to investigate the toxicity of environmentally relevant concentrations of p,p'-DDE on two immature mammalian cell types

A. p,p'-DDE preparation

p,p'-DDE (hereafter DDE) stock solution was prepared by dissolving the chemical in acetone to a final concentration of 125 µg/µl. DDE working solution was then prepared by diluting the stock solution to a final concentration of 1.25×10^{-3} µg/µl with deionized water. For this study, the average cord blood concentration of DDE (0.35 µg/l) was designated the 1X DDE treatment. As well, concentrations corresponding to ten (10X) and one hundred times (100X) the average cord blood levels were included. Therefore, DDE working solution was added to the cell culture media to a final concentration of: 0.35 µg/l (1X), 3.5 µg/l (10X) or 35 µg/l (100X). Control cells were treated with the same final amount of acetone per liter of media as 1X treated cells (2.8×10^{-5} µl acetone per 10 ml media) and in the text are referred to as acetone alone or control samples.

B. Short-term assays of chemical toxicity

(i) Assay for changes in cell number

At specific time intervals, after the initiation of chemical exposure, the number of cells per sample was assayed to determine if DDE treatment resulted in any detectable changes in cell quantity. Both cell types were plated in duplicate at 5×10^5 cells per 10 cm dish. 12-15 hrs later the cells were fed with media supplemented with acetone alone (control),

or DDE at 1X (0.35μg/l) or 10X (3.5 μg/l) concentrations. At 2 hr intervals the media was removed and the plates immediately frozen at –20°C. The DNA quantity per sample was assessed by fluorescence using the diaminobenzoic acid (DABA) assay (240). The fluorescence of known numbers of cells was determined and subsequently used to convert DNA quantity per sample into number of cells per sample.

(ii) Cell viability (Trypan blue) assay

The trypan blue assay of cell viability was performed to elucidate if the decreases in cell number observed in the DABA assay were caused by cell death. Both cell types were plated in duplicate at 1.0×10^6 cells per 15 cm dish. 12-15 hrs later the cells were fed with media containing either acetone alone (control) or DDE at 1X or 10X concentrations. At 2, 4 or 6 hours duplicate plates of each cell type were trypsinized and re-suspended in Hank's buffered saline solution (HBSS) (an additional 12 hour time-point was included for NIH 3T3 cells). Non-viable cells were identified by their permeability and subsequent staining with 0.4% trypan blue solution (241). At least 1000 cells per treatment were microscopically examined and the number of dead cells (blue) expressed as a percentage of the total number of blue and unstained cells counted.

(iii) Assays for total glutathione (GSH + GSSG) and reduced glutathione (GSH)

Total glutathione levels (GSH + GSSG) were measured to determine if exposure to 1X or 10X DDE resulted in significant alterations in the overall concentration of this multifunctional cellular component. Reduced glutathione levels (GSH) were also measured to determine if the same DDE exposures resulted in significant changes in the oxidation state of glutathione.

(a) Assay for total glutathione {GSH + GSSG}

A modification of the Tietze assay (242, 243) was used to determine total glutathione levels in cells exposed to acetone alone (control), 1X or 10X DDE. In this assay, GSSG is reduced to GSH by glutathione reductase in the presence of NADPH. Reduced GSH is then oxidized by 5,5'- dithiobis (2-nitrobenzoic acid) (DTNB) to form GSSG and 5-thio-2-nitrobenzoic acid (TNB). The rate of TNB formation is proportional to the sum of GSH and GSSG present in the sample and is monitored spectrophotometrically at 412 nm.

(b) Assay for reduced glutathione {GSH}: Reduced glutathione was measured using the Bioxytech GSH 400 colorimetric assay as per the manufacturer's protocol (OXIS International Inc.).

For each assay, both cell types were plated in duplicate at 5 x 10^5 per 10 cm dish. 12-15 hrs later the cells were exposed to media supplemented with either acetone alone (control) or DDE at 1X or 10X concentrations for 2, 4 or 6 hours (an additional 12 hour

time-point was included for NIH 3T3 cells). At each time-point, duplicate plates for each assay were rinsed with phosphate buffered saline (PBS), trypsinized and pelleted by centrifugation for 5 minutes at 200 x g at 4°C. The amount of protein per plate was quantified by the Bradford assay (238). Total and reduced glutathione were assayed as described above. Standard curves were prepared for each assay and were used to determine the amount of total or reduced glutathione per milligram protein of each sample. Quantities of both total and reduced glutathione are expressed as a percentage of the control levels assayed at the same time-points.

(iv) DNA damage assay

The Comet assay (244), with minor alterations as described below, was used to assess if exposure to DDE resulted in DNA damage. Briefly, cells were plated in duplicate at 1.0 x 10^6 on 15 cm dishes each containing 3 sterile frosted slides (Erie Scientific Co.). 12-15 hrs later the cells were exposed to media supplemented with either acetone alone (control) or DDE at 1X or 10X concentrations. Four hours after the addition of DDE the plates were rinsed twice with PBS and the glass slides were prepared for use in the Comet assay.

75 µl of 0.5% 3:1 agarose (Ameresco) in physiological saline was spread onto each slide, covered with a coverslip and placed on ice in the dark for 10 minutes. Then 100 µl of agarose solution was layered on top of the first, covered with a coverslip and placed on ice for an additional 10 minutes. When the agarose had solidified, the coverslip was removed and the slides immersed overnight in ice-cold lysing solution (2.5 M NaCl,

1% N-lauroyl sarcosinate, 100 mM EDTA, 10 mM Tris (pH 10.0), 0.1 μg/ml Proteinase K and 1% Triton X-100). The slides were then incubated in alkaline electrophoresis buffer (300 mM NaOH, 0.1% 8-hydroxyquinoline and 10 mM EDTA) for 20 minutes at room temperature, after which time current was applied to the chamber at 22 V for 20 minutes. The slides were then rinsed in 1 M ammonium acetate in ethanol for 30 minutes, drained and covered in 100% ethanol for 2 hours and lastly rinsed with 70% ethanol for 5 minutes.

Pre-stain (5% DMSO, 30 mM NaH_2PO_4 and 5% sucrose) was added to each slide followed by 1 μM YOYO–1 fluorescent stain (Molecular Probes). The slides were examined and photographed with an Axiovert 35 microscope (Zeiss, West Germany) equipped with a 35 mm camera and an FITC filter with a wavelength combination of: excitation at 490 nm, dichromic at 500 nm and emission at 515 nm. The total DNA length (displacement from the leading edge of the nucleus to the end of the tail) of each nucleus from a minimum of 50 cells per treatment was measured using the developed film.

(v) Cell cycle kinetics assay

This assay was performed to determine if exposure of proliferating cells to DDE resulted in cell cycle fluctuations. Fluorescent activated cell sorting (FACS) cell cycle kinetic analysis was performed in the laboratory of Dr. Peter Rabinovitch, Dept. of Pathology, University of Washington, Seattle WA. Specifically, measurement of the G1, S and G2/M compartment distributions was performed by flow cytometric analysis of BrdU (5-bromo-deoxyuridine) quenched Hoescht dye fluorescence (236).

Each cell type was plated in triplicate at 5 x 10^5 per 10 cm dish. 12-15 hrs later the cells were treated with media containing 1.0 x 10^{-4} M BrdU and 50 μM deoxycytidine plus either acetone alone (control), 1X or 10X DDE concentrations. At intervals of two hours the plates were rinsed with PBS and trypsinized into media containing 10% DMSO for storage at –20°C. The samples were then shipped on dry ice to the University of Washington where FACS analysis was performed (as described previously).

C. Long-term assays of chemical toxicity

(i) Colony forming ability

This assay was performed to determine if exposure to DDE affected the long-term survival of NIH 3T3 and WS1 cells, and consequently their ability to form colonies. Survival of each treatment concentration is expressed as a percentage of the number of colonies formed on the control plates. 800 cells were plated for each WS1 experiment and 200 cells for each NIH 3T3 experiment in duplicate on 15 cm dishes. 12-15 hrs later the cells were fed with media containing either acetone alone (control) or DDE at 1X or 10X concentrations. The cells were allowed to grow for an additional 12-14 days in the DDE containing media without refeeding, at which time the colonies were visualized by staining with 0.5% crystal violet in 20% ethanol. Colonies containing 50 or more cells were counted and percent survival was calculated as the average number of colonies for each concentration of DDE relative to acetone alone (control) plates. Each colony forming experiment was repeated at least three times and the average of three independent experiments was determined for each cell type.

(ii) Transformation assay: This assay was performed to determine if exposure to DDE had an effect on the number of transformed foci formed by NIH 3T3 cells (245). NIH 3T3 cells were plated at 3 x 10^5 cells per 10 cm plate. 12 –15 hours later the cells were treated as described with media containing, either acetone alone (control), 1X, 10X or 100X DDE and subsequently refed biweekly for four weeks with fresh DDE containing media. The cells were then fixed with 97% methanol and stained with O.5% crystal violet in 20% ethanol. The number of darkly staining foci on each plate was counted and comparisons were made between the numbers of foci found on the control, 1X, 10X and 100X plates.

(iii) Statistical analysis: Data values are expressed as the mean ± SD where appropriate. Mean values were considered to be statistically different when the probability value P was less than 0.05 as calculated by one-way analysis of variance (ANOVA) and Scheffe's comparisons.

Section II: Effects of environmentally relevant concentrations of p,p'-DDE on mismatch repair at an oncogenic hot-spot

In order to study mismatch repair in WS1 cells it was necessary to devise a protocol that would discriminate between the site-specifically mismatched H-*ras* plasmid and the human chromosomal H-*ras* sequences from the human cells. All of the site-specific mismatch experimental preparation steps were carried out as described in Part I except that the final vector into which the 1.8 kb fragment was ligated was not capable of replicating in mammalian cells (pbc-N1; see below). After transfection the plasmid was extracted from the cells, transformed into mismatch deficient bacteria (NR9374) and the plasmid was subsequently isolated from individual colonies. Mismatch repair rates were determined in the same manner as in Part I and, because the bacteria are mismatch repair deficient and the mismatched plasmid is incapable of replication in the eukaryotic cells, the repair results obtained are a direct representation of the mammalian cells mismatch repair capability.

A. Plasmid and M13 constructs

The plasmid pbc-N1 (10.7-kb) was purchased from American Type Culture Collection (ATCC) and consists of 6.4-kb of human genomic H-*ras* inserted into the *Bam*H1 site of pBR322 (244). The resulting plasmid differs from the p220.pbc plasmid in a number of ways. Pbc-N1 lacks a viral origin of replication, making this plasmid incapable of replication in mammalian cells. However, pbc-N1 retains all of the other elements necessary to construct site- and strand-specific mismatches at codon 12 of H-*ras*. All

other vectors used in the construction of site- and strand-specific mismatched pbc-N1 were as described in materials and methods Part I.

B. Mismatch construction

(i) Fragment preparation; (ii) Oligonucleotides; (iii) Melt and reanneal; (iv) Isolation of the 1.8 kb fragment; As described in Part I except only G:**A** and G:**T** mismatches were constructed (see also Figure 5).

(v) Final assembly of the site- and strand–specific mismatched pbc–N1 plasmid

Vector preparation: The pbc-N1 plasmid was digested with 20 units each of *Xho*I and *Kpn*I per μg DNA at a final DNA concentration of 100 ng/μl. The reaction products were subsequently separated by electrophoresis at low voltage on a 0.8% SeaKem GTG (FMC Bioproducts) agarose gel. The 8.9 kb band was excised, recovered using the Qiaquick Gel Extraction Kit as described by the manufacturer (Qiagen Inc.) and quantified. This purified segment contained the remaining H-*ras* genomic sequence (minus the 1.8 kb fragment surrounding codon 12), bacterial carbenicillin resistance and bacterial replication sequences.

Annealing and ligation: To ensure that the mismatch-containing oligonucleotide was indeed present, excess mismatch-containing oligonucleotide was annealed to the 1.8 kb fragment as described. Phosphorylated oligonucleotide and the 1.8 kb fragment were mixed together at a 200:1 molar ratio of oligonucleotide: 1.8 kb fragment at a DNA concentration of 30 ng/μl in a buffer consisting of 50 mM Tris-HCL pH 7.6, 10 nM

dithiothreitol and 500 μg/ml bovine serum albumin. The mixture was placed in a 2-liter beaker containing 85-90°C water and allowed to cool slowly to room temperature. The 1.8 kb fragment was then ligated to the 8.9 kb *Xho*I/*Kpn*I pbc-N1 vector at a 2:1 molar ratio of fragment to vector using 0.5 units T4 DNA Ligase per μg DNA as described by the manufacturer (Boehringer Mannheim) This final ligation step produced a 10.7 kb pbc-N1 plasmid containing a site- and strand-specific mismatch at H-*ras* codon 12 middle base pair position. In addition the plasmid containing the mismatch could easily be distinguished from wildtype plasmid by the presence of the *Hind*III and *Bst* 98I sites as described in Part I..

C. Transfection of DDE treated NIH 3T3 and WS1 cells with mismatched plasmid

NIH 3T3 and WS1 cells were seeded at 5 x 10^5 cells per 10 cm plate. One hour prior to the start of transfection each plate was re-fed with fresh media containing 10X DDE (or media alone for all DDE negative plates) and returned to the incubator.

Both cell types were transfected with 300 ng of G/**A** or G/**T** mismatched pbc-N1+H/B plasmid. Transfection was carried out using Lipofectamine reagent at a 100:1 ratio of liposome to DNA as described by the manufacturer (Life Technologies). Each plate was rinsed with 5 mls of 1X PBS. To each plate 4 mls of OptiMem was added as well as 10X DDE to all DDE treated plates, followed by the addition of the liposome: DNA mixture. The plates were then placed on a rotator for 30 minutes at 37°C followed by a further 5 ½ hour incubation at 37°C in 5% CO_2 without agitation. At the end of this

transfection period each plate was fed with fresh media, containing 10X DDE where appropriate, and returned to the incubator for a further 24 hours.

D. Mismatch repair analysis

(i) Cell harvest and plasmid extraction

At the end of the 24-hour incubation period the cells on each plate were harvested by trypsinization (as described above) and pelleted by centrifugation at 200 x g for 5 minutes. The plasmid DNA was recovered from the cell pellet using the Quantum Prep Plasmid Miniprep kit as described by the manufacturer (Biorad Laboratories Inc.).

(ii) Transformation of NR9374 mismatch repair deficient bacteria

NR9374 competent bacteria were prepared by the following method. NR9374 bacteria from a glycerol stock were grown overnight at 37°C on a LB agar plate containing 30 μg per ml of kanamycin. NR9374 colonies were then transferred to SOB medium (2% Bacto-tryptone, 0.5% bacto yeast extract, 2.5 mM $MgCl_2$, 0.85 mM NaCl) and incubated with shaking at 37°C. After 3 hours the optical density at 550 nm was checked with an OD_{550} of 0.5 indicating a cell density of 5×10^7 cells/ml. Cells were grown until they reached a density of at least 1×10^7 cells/ml but were not permitted to exceed 1×10^8 cells/ml. The cultures were then cooled on ice for 10 minutes, followed by centrifugation at 2500 x g for 10 minutes. The cell pellets were then re-suspended in FSB solution (pH 6.4) (10 mM potassium acetate pH 7.5, 45 mM MnCl2, 10 mM $CaCl_2$, 100 mM KCL, 3 mM Hexamminecobalt chloride, 10% glycerol), placed on ice for 10 minutes and then

centrifuged at 2500 x g for 10 minutes. Finally, each cell pellet was re-suspended in 4 mls of FSB.

Purified plasmid extracted from each plate of mammalian cells was then added to 200 µl of freshly prepared NR9374 competent cells. Each solution was incubated on ice for 30 minutes, followed by 90 seconds at 42°C and a further 2 minutes on ice. 800 µl of SOC (SOB and 20 mM glucose) was added to each solution and placed in a 37°C shaking incubator for 60 minutes at 225 rpm. The bacterial solutions were then spread on LB agar/carbenicillin (100 µg/ml) plates and grown overnight at 37°C.

(iii) Mini-preparations and DNA extraction from individual NR9374 colonies

Individual NR9374 bacterial colonies from (ii) were plucked with a sterile toothpick and placed in 2-mls of LB broth and 100 ug/ml carbenicillin and grown overnight at 37°C in a shaking incubator. The pbc-N1 plasmid was then purified from the bacterial culture using the Wizard Plus SV Miniprep DNA Purification System as described by the manufacturer (Promega Corporation Inc.).

(iv) PCR amplification

A 10 µl aliquot from each DNA isolate was PCR amplified with 2.5 units of AmpliTaq Gold (Applied Biosystems) in the supplied buffer plus 3.5 mM $MgCl_2$, 200 µM of each dNTP and 100 ng of each primer in a final volume of 100 µl, with the enzyme separated from the other reactants by a wax layer (Chill-Out 14, MJ Research, Inc.). The reactions were heated to 95°C for 9 minutes followed by 30 seconds at 95°C and 1 minute at 61°C

for 30 cycles. Finally, the samples were incubated for 10 minutes at 61°C to allow completion of extension reactions and cooled to 4°C. The primers used for the PCR reaction were as described in Part I; Materials and methods.

(v) Contamination check of amplified H-ras segment

Each PCR amplified sample was tested to confirm that it did not result from transfection of undigested vector (pbc-N1-H/B) as described Part I; Materials and methods (Figure 6, B).

(vi) Mismatch repair analysis

A 20 µl aliquot of each +H/B amplified PCR product was digested with 4 units of Turbo *Nae*I as described in Part I; Materials and methods (Figure 6, C).

(vii) Sequencing

Sample cleanup and sequencing were carried out as described in Part I, Materials and methods.

III. RESULTS

PART I: Mismatch repair at an oncogenic hotspot in G_1 synchronized mammalian cells

Section I: G_1 synchronization, fluorescent activated cell-sorting analysis, plasmid replication kinetics and mismatch repair protein expression in G_1 nuclear extracts

A. G_1 synchronization and fluorescent activated cell-sorting analysis (FACS).

To examine the activity of the mismatch repair system in the G_1 phase of the cell cycle it was necessary to find a method of cell synchrony whose effects were fully reversible but which synchronized the majority of cells in the G_1 phase of the cell cycle. In previous investigations serum starvation has been found to be the most reliable method to achieve both of these goals with NIH 3T3 cells (Personal communication from Dr. Peter Rabinovitch, University of Washington).

FACS analysis was used to determine the percentage of NIH 3T3 cells in G_1 after 3 days of growth in 0.25% CS/DMEM and for the 24 hours following replacement with media containing 10%CS/DMEM on day 4 at 0 hours. Re-feeding with 10% CS reversed the effects of serum starvation and allowed the cells to re-enter the cell cycle (235).

As shown in Table 3 over 96% of the cells were in G_1 on day 4 at 0 hr when re-feeding took place (Published in 54). In addition, greater than 96% of the cells remained in G_1 for up to 12 hours after re-feeding. From 12 hours onwards the percentage of cells in G_1 decreased, indicating that the cells had successfully progressed to succeeding stages of the cell cycle. In fact, plates of re-fed G_1 synchronized cells regained normal growth rates and reached confluence, albeit at a later time than control plates (data not shown).

Table 3: Percentage of NIH 3T3 cells in the G_1 phase of the cell cycle with and without serum starvation

Day and Time harvested	Percentage of cells in G_1[a]	
	Serum Starved[b]	Control[c]
Day 2	85.2%	55.2%
Day 3	94.3%	63%
Day 4, 0 hr	96.8%	74.7%
Day 4, 2 hr	96.9%	nd[d]
Day 4, 4 hr	96.7%	nd
Day 4, 6 hr	97.8%	nd
Day 4, 8 hr	98%	nd
Day 4, 10 hr	97.9%	50.9%
Day 4, 12 hr	97.5%	45.3%
Day 4, 14 hr	78.8%	nd
Day 4, 16 hr	52.3%	nd
Day 4, 18 hr	8.4%	50.7%
Day 4, 20 hr	9.6%	nd
Day 4, 22 hr	22.7%	nd
Day 4, 24 hr	38.8%	68.7%

[a] Percentage of cells in G_1 was determined by fluorescence activated cell sorting (FACS). Plates for each time point were collected in duplicate.

[b] Cells were serum starved in 0.25% calf serum/DMEM beginning on Day 1. On Day 4 at 0 hr, this media was replaced with 10% calf serum/DMEM.

[c] Control cells were grown in 10% calf serum/DMEM. This media was replaced with fresh 10% calf serum/DMEM on Day 4 at 0 hour.

[d] nd = not determined. Published in Matton et al 1999 (54).

B. Plasmid replication kinetics

Plasmids derived from the Epstein Barr virus have been shown to replicate autonomously once per cell cycle in human and simian cells (247). However, it is unknown if this occurs in murine cells and whether cell cycle synchronization also affects plasmid replication. We examined the replication kinetics of the p220.pbc-H/B plasmid in NIH 3T3 cells in order to determine if and/or how G_1 synchrony affected plasmid replication. The restriction enzyme *Dpn*II was used to compare plasmid replication in G_1 synchronized and actively growing cells. Digestion of DNA by *Dpn*II is blocked by prokaryotic adenine methylation, therefore, only those plasmids that had replicated in mammalian cells were sensitive to digestion. Digestion reactions were southern blotted and hybridized with a 613 bp radioactive probe prepared from the p220.pbc –H/B plasmid.

The results of the plasmid replication kinetics study in NIH 3T3 cells are shown in Figure 8. Because unreplicated plasmid DNA within mammalian cells remains undigested by *Dpn*II, the radioactive probe hybridizes to the whole plasmid and results in the appearance of a radioactive band at 15.3 kb corresponding to the size of the uncut plasmid. In contrast, replicated plasmid DNA is digested by *Dpn*II to produce 45 smaller fragments of which the sequence corresponding to the radioactive probe is contained in a fragment also of size 613 bp. As a control p220.pbc-H/B plasmid was digested with *Dpn*I

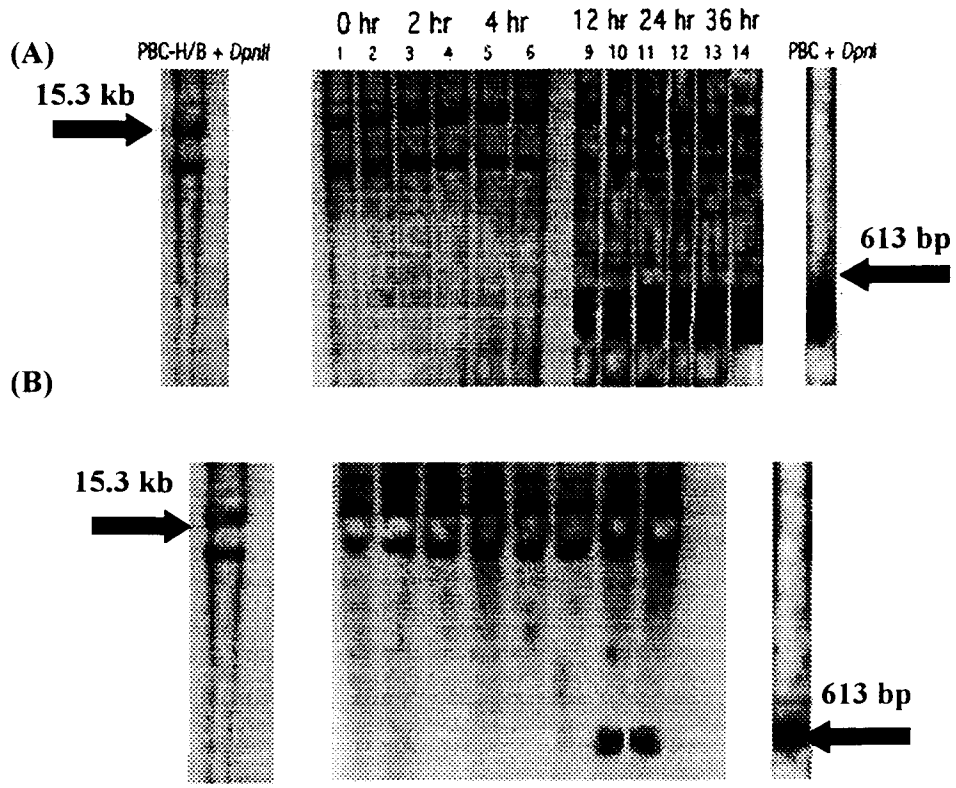

Figure 8: Plasmid replication kinetics

Actively proliferating (A) and G_1 synchronized (B) NIH 3T3 cells were transfected with plasmid DNA. At various time-points, the plasmid was recovered, digested with *Dpn*II to detect replicated plasmid DNA and hybridized with a radioactively labelled 613 bp fragment of p220.pbc plasmid (see materials and methods). Replication of the plasmid DNA in mammalian cells is visualized by the appearance of a 613 bp radioactive band on the autoradiogram.
(A): In actively proliferating cells, replicated plasmid is detected by 12 hours after transfection, lanes 9-14 (duplicate plates harvested at each timepoint). (B): In G_1 synchronized cells , replicated plasmid is not detected until 96 hours after transfection or 97 hours after refeeding with 10%CS/DMEM (lanes 34 + 35), illustrating that in cell cycle arrested cells there is a significant delay in the replication of the plasmid DNA.

enzyme. This enzyme cuts at the same restriction sites as *Dpn*II but cuts only DNA with adenine methylation produced by prokaryotic replication.

In actively proliferating control cells the 613-bp band, indicating plasmid replication, is clearly detected by 12 hours after transfection (Figure 8A, lanes 9 –14). In contrast, in G_1 synchronized cells the 613 bp band is seen for the first time in cellular extracts 96 hours after transfection or 97 hours after refeeding with 10% CS/DMEM took place (Figure 8B, lanes 34 +35). These results show that replication of the extrachromosomal p220.pbc-H/B plasmid is delayed for a substantial period in G_1 synchronized NIH 3T3 cells as compared to proliferating cells. Thus, this EBV plasmid does indeed appear to replicate synchronously with the murine cell cycle. Therefore, if mismatch repair is active in these cells during G_1 there should be sufficient time for repair to occur before replication of the plasmid DNA could take place.

C. Mismatch repair protein expression in G_1 nuclear extracts

As discussed in the introduction, the mismatch repair system is not the sole method of DNA repair available to mammalian cells. In addition mismatch repair has been historically designated a "post-replicative" DNA repair mechanism because of initial discoveries and studies using the *E.coli* system. This assay was performed to determine if a particular mismatch protein could be detected in nuclear extracts from G_1 synchronized mammalian cells. Although not necessarily an indicator of activity, the presence of the protein would provide additional evidence that mismatch repair is active in the G_1 phase of the mammalian cell cycle. At the time when these experiments were performed hMSH2 was the only commercially available antibody that could also be used with

mouse cellular extracts and it was for this reason that it was the only MMR protein probed for in NIH 3T3 G_1 extracts.

Nuclear and cytoplasmic extracts were prepared from G_1 synchronized populations of NIH 3T3 cells. The preparations, containing equal amounts of total protein, were subsequently Western blotted for the presence of the MSH2 mismatch repair protein and the results are shown in Figure 9. It is clearly shown that the full length 102-kDa MSH2 protein is present in both G_1 nuclear and cytoplasmic extracts (Figure 9, Lanes 1 and 3). In addition, the protein appears to be present in relatively similar amounts in both G_1 and non-synchronized cytoplasmic (lanes 1 + 2) and nuclear extracts (lanes 3 + 4).

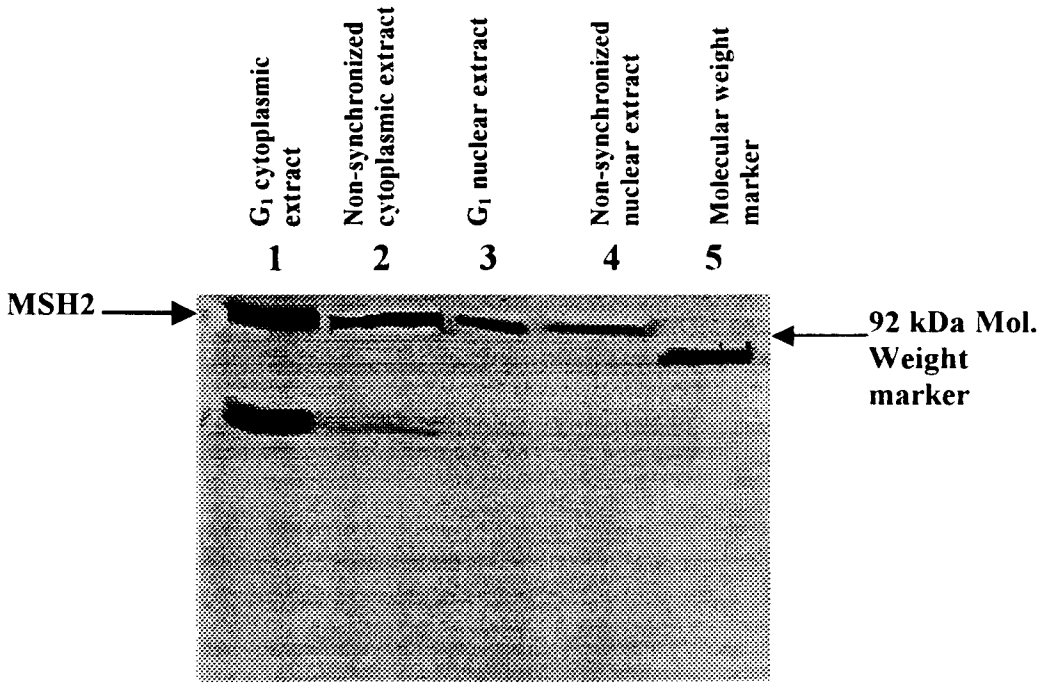

Figure 9: Western blot of NIH 3T3 G_1 nuclear and cytoplasmic extracts

G_1 synchronized NIH 3T3 nuclear and cytoplasmic extracts were subjected to a Western blot to detect the mismatch repair protein MSH2 (102 kDa indicated by arrow) (see materials and methods). MSH2 is present in relatively equal amounts in both G_1 nuclear and cytoplasmic extracts as compared to non-synchronized extracts prepared by the same method. **Lane 1**: 40 μg NIH 3T3 G_1 cytoplasmic extract. **Lane 2**: 40 μg NIH 3T3 non synchronized cytoplasmic extract; **Lane 3**: 40 μg G_1 nuclear extract; **Lane 4**: 40 μg non-synchronized nuclear extract; **Lane 5**: Molecular weight marker.

Section II: Mismatch repair in the G_1 phase of the mammalian cell cycle

A. Mismatch repair rates at codon 12 of H-ras in G_1 synchronized cells

The repair rates of four specific mismatches at the middle nucleotide position of H-*ras* codon 12 contained within the p220.pbc plasmid and transfected into NIH 3T3 G_1 synchronized cells are shown in Table 4. We observed almost complete correct repair of all four mismatches, (G:**T** = 92%, G:**A** = 100%, A:**C** = 100%, T:**C** = 100%). Intriguingly, G_1 synchronization was the only experimental situation in which we observed an instance of incorrect repair that resulted in a mutation at codon 12 (G:**T** → **A:T**) (see Table 4). As well, because of the extended time in G_1 none of the mismatches were replicated before mismatch repair occurred, which resulted in a lack of samples containing wild type and mutated sequence mixtures or unrepaired replicated mismatches. This is a dramatic difference from results obtained from non-synchronized cell experiments where mixtures were found; G:T = 0%, G:A = 65%, A:C = 42%, T:C = 20% (53).

Each mismatch preparation was prepared at least twice and also transformed into DH5α *E.coli* as a control. It has been previously demonstrated by this laboratory that codon 12 of H-*ras* is not a hotspot of mutation in these bacteria (53). Comparison of the G_1 results with DH5α mismatch repair results (Table 5) indicate that *E.coli* have a correct repair rate that is similarly high or higher than the G_1 synchronized NIH 3T3 cells (with the exception of G/A which is repaired more accurately in NIH 3T3 G_1 synchronized cells). These results further confirm that H-*ras* codon 12 is not a hotspot of mutation for DH5α *E.coli*.

Previously, this laboratory determined *in vivo* rates of repair for G:A, G:T, A:C and T:C mismatches at the middle nucleotide position of H-*ras* codon 12 in non-synchronized NIH 3T3 (53). Figure 10 shows a comparison between repair rates in our recent G_1 synchronized and previously determined non-synchronized NIH 3T3 cells. Repair of mismatches in G_1 cells was almost always correct (see Table 4), compared with rates as low as 35% for the G:**A** mismatch at codon 12 in non-synchronized cells (53). These results indicate that DNA mismatch repair mechanisms are active and highly accurate during the G_1 stage of the mammalian cell cycle. It is important to note that our G_1 synchronized cells had significant amounts of time to repair the mismatched DNA before entering S-phase, while in non-synchronized cells, the amount of time available for repair is quite variable. These results show that given enough time before replication, NIH 3T3 cells have a significantly increased capacity to correctly repair all mismatches tested at the codon 12 H-*ras* oncogenic hotspot.

Table 4: Mismatch repair at codon 12 of H-*ras* in G_1synchronized NIH 3T3 cells[a]

NIH 3T3 G_1 MISMATCH	Ccrrectly repaired mismatch ⇒ G:C (Total Assayed)	Incorrectly Repaired Mismatch to T:A or A:T (Total Assayed)	Unrepaired Mismatch ⇒ G:C / T:A or G:C / A:T (Total Assayed)
G:T	92% (12/13)	8% (1/13)	0% (0/13)
G:A	100% (27/27)	0% (0/27)	0% (0/27)
A:C	100% (18/18)	0% (0/18)	0% (0/18)
T:C	100% (21/21)	0% (0/21)	0% (0/21)

[a] Greater than 96% of cells were in G_1, as determined by FACS analysis, see results and Table 3. Published in Matton et al 1999 (54).

Table 5: Mismatch repair at codon 12 of H-*ras* in DH5α *E.coli*[a]

DH5α *E.coli* MISMATCH	Correctly repaired mismatch ⇒ G:C (Total Assayed)	Incorrectly Repaired Mismatch to T:A or A:T (Total Assayed	Unrepaired Mismatch ⇒ G:C / T:A or G:C / A:T (Total Assayed)
G:T	95% (42/44)	5% (2/44)	0% (0/44)
G:A	89% (65/73)	3% (2/73)	8% (6/73)
A:C	97% (38/39)	0% (0/39)	3% (1/39)
T:C	100% (35/35)	0% (0/35)	0% (0/35)

[a] A portion of each mismatch preparation used in the NIH 3T3 studies was used to transform mismatch proficient *E.coli* (DH5α) as a control.

Published in Matton et al 1999 (54).

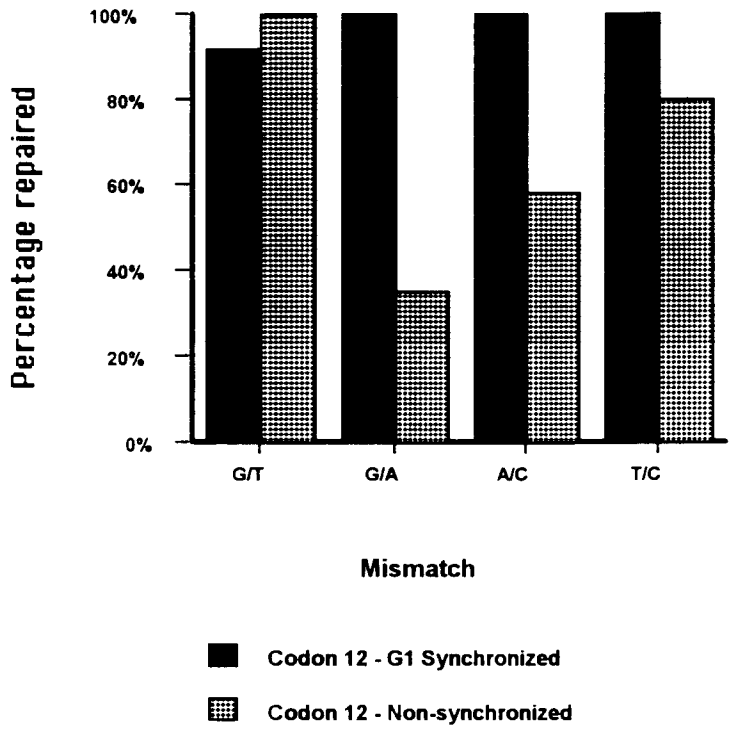

Figure 10: Comparison of mismatch rates in G_1 synchronized and non-synchronized NIH 3T3 cells

Repair rates for codon 12 of H-ras in non-synchronized cells were reported by Arcangeli and Williams (234) and are shown here for comparison, (correct repair: G:T = 100%, G:A = 35%, A:C = 58%, T:C = 80%). Repair rates include only those mismatches repaired correctly to G:C but not mismatches which were replicated before repair and thus were found as mixtures in the resulting colony. Published in Matton et al 1999 (54).

PART II: Effects of p,p'-DDE on cell toxicity and mismatch repair ability at an oncogenic hotspot

Section I: Preliminary experiments to investigate the toxic effects of environmentally relevant concentrations of DDE on two immature mammalian cell types.

A. Short-term assays of chemical toxicity

(i) Assay for changes in cell number

Figure 11 illustrates the effects over time of both 1X and 10X cord blood concentration on the cell quantity of the two embryonic mammalian cell types. NIH 3T3 cells exhibit a small decrease in cell number in both 1X and 10X DDE treated samples by 2-4 hours exposure as compared to acetone alone samples (hereafter controls) (Figure 11A). In addition, there is a second decrease in cell number in comparison to controls by 12 hours exposure to 10X DDE. However, the results of subsequent assays (discussed below), consistently showed no significant differences between treated and control samples at 12 hours exposure. We therefore conclude that this conflicting result from the DABA assay was due to either to sampling error or more subtle effects not detected by subsequent assays. At the next time-point tested, 24 hours, the number of cells on all plates is similar indicating that confluence has been reached and the cell population is at a maximum in all samples.

Unlike the NIH 3T3 controls, the WS1 control samples exhibit a decrease in cell number by 2 hours exposure to the treatment media (Figure 11B). We believe that this

effect may simply be due to the mechanical effects of media removal as these normal human cells are easily dislodged from the plate.

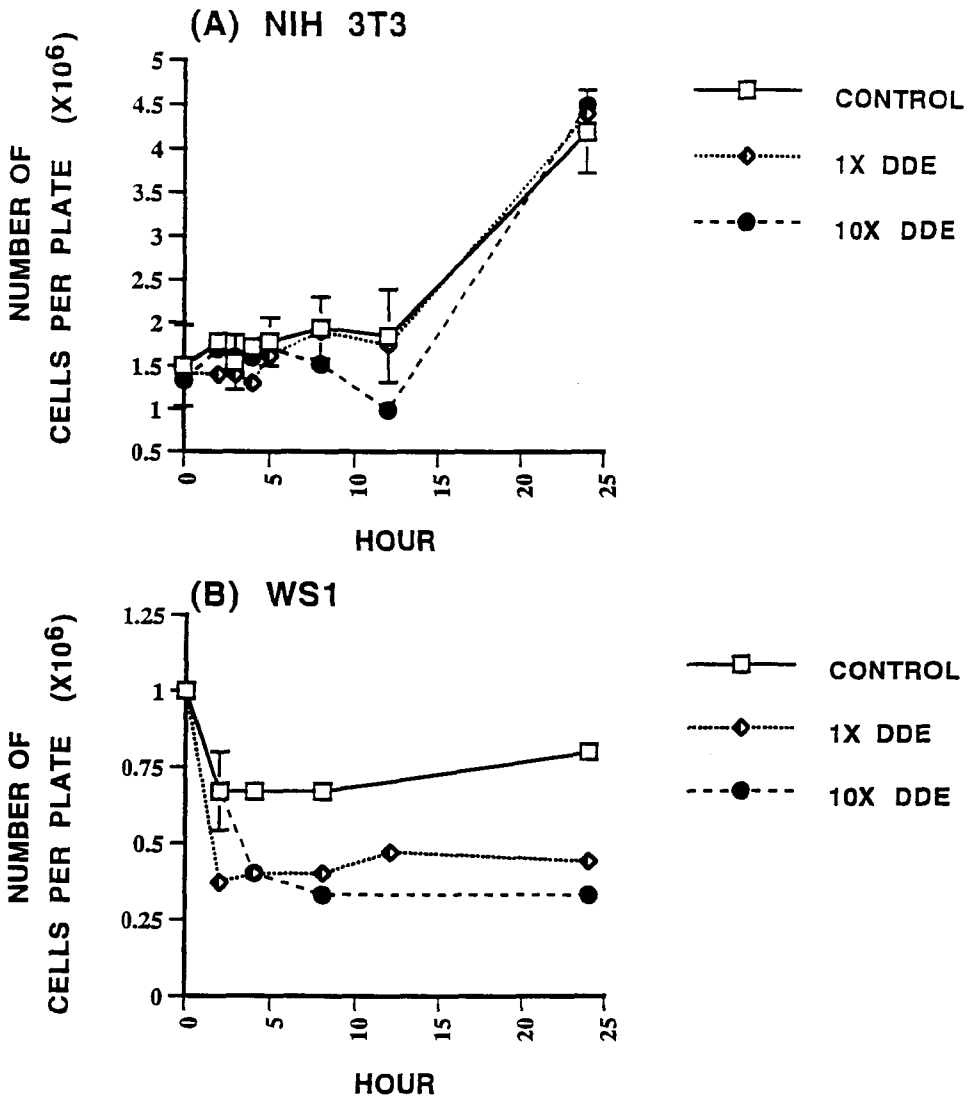

Figure 11: Assay for changes in cell number

Effect of acetone alone (control), 1X or 10X DDE and duration of exposure on the cell number of two cell types. NIH 3T3 (A) and WS1 (B) cell cultures were harvested in duplicate at the indicated time-points after the addition of media containing acetone alone (control), 1X or 10X DDE. The total DNA from each plate was determined using the diaminobenzoic acid assay (see materials and methods). Cell numbers were calculated by comparison to the DNA quantities of known numbers of cells. The graphs represent the average number of cells per duplicate sample per time-point of harvest ± SD. Data points without error bars represent those duplicate samples in which the SD was too small to be represented on the graph. Published in Simonetti et al 2001 (213).

Nonetheless, WS1 cells exposed to 1X or 10X DDE for 2-4 hours exhibit an even greater decrease in cell number in comparison to controls. In contrast to the NIH 3T3 cells, we find neither a recovery to control levels or an additional depletion in WS1 cell number up to 24 hours exposure. At the next time-point tested, 72 hours, (not shown on graph), there is no significant difference between the number of cells on control, 1X or 10X treated plates (mean = 8.3 x 10^6 cells per plate). This indicates that the cells in each treatment group have grown to confluence and are no longer dividing due to contact inhibition.

(ii) Cell viability (Trypan Blue) assay

The percentages of non-viable NIH 3T3 and WS1 cells that result from exposure to 1X or 10X DDE at 2, 4 or 6 hours are shown in Table 6. As compared to controls, there is a significant increase in the percentage of non-viable NIH 3T3 cells after 2 and 4 hours exposure to both 1X and 10X DDE ($p < 0.05$). However, at both 6 (Table 6) and 12 hours (data not shown) there is no significant difference between the amount of cell death found on control NIH 3T3 plates or those treated with 1X or 10X DDE. WS1 cells treated with 1X or 10X DDE for 2, 4 or 6 hours exhibit no increase in cell death as compared to controls.

(iii) Assays for total glutathione (GSH & GSSG) and reduced glutathione (GSH)

(a) Assay for total glutathione (GSH + GSSG)

The effects of 1X and 10X DDE on the total glutathione levels of NIH 3T3 and WS1 cells are shown in Figure 12 [A and B].

Table 6: Assay of cell viability (Trypan Blue) [a]

CELL TYPE	TREATMENT	PERCENTAGE NON-VIABLE CELLS n ≥ 1000		
		2h	**4h**	**6h**
NIH 3T3	Control	2.4%	9.3%	6.0%
	1X DDE	**6.4%[b]**	**13.9%[c]**	4.4%
	10X DDE	**8.1%[b]**	**17.4%[c]**	5.8%
WS1	Control	5.6%	6.7%	5.8%
	1X DDE	3.9%	6.3%	4.6%
	10X DDE	3.5%	6.7%	4.6%

[a] Non-viable cells were identified by their permeability to 0.4% trypan blue, as compared to viable cells which are impermeable to the dye (240).
The number of non-viable cells (blue) is expressed as a percentage (%) of the total number of cells counted (unstained and blue).
Total number of cells counted was ≥ 1000 for all time-points and treatments.
[b] Significant increase ($p < 0.05$) in cell death, by 2 hours of 1X or 10X DDE treatment, as compared to NIH 3T3 control cells.
[c] Significant increase ($p < 0.05$) in cell death, by 4 hours of 1X or 10X DDE treatment, as compared to NIH 3T3 control cells.
Published in Simonetti et al 2001 (213).

There are no significant differences, as compared to controls, in the total glutathione levels of NIH 3T3 cells exposed to 1X or 10X DDE for 2,4 or 6 hours (Figure 12A). In contrast, WS1 cells similarly treated exhibit significant differences in their total glutathione levels (Figure 12B). At 2 hours exposure, although 1X DDE WS1 cells were not significantly different from controls, 10X DDE WS1 cells exhibit a large reduction in total glutathione levels as compared to controls ($p > 0.05$). By 4 hours exposure WS1 total glutathione levels have increased significantly above controls in 1X DDE samples and have attained approximate control levels in samples exposed to 10X DDE. WS1 cells exposed to 1X DDE for 6 hours have returned to total glutathione levels similar to controls. In contrast, the total glutathione levels of WS1 cells exposed to 10X DDE for 6 hours have increased slightly but not significantly above control levels.

(b) Assay for reduced glutathione (GSH)

The effects of 1X and 10X DDE on the reduced glutathione levels of NIH 3T3 and WS1 cells are shown in Figure 12 (C and D). NIH 3T3 cells exhibit a significant *increase* in reduced glutathione at 4 hours exposure to 1X DDE, however, by 6 hours exposure there is no significant difference between the reduced glutathione levels of the 1X DDE treated and control samples (Figure 12C). In contrast, NIH 3T3 cells exposed to 10X DDE for 2 hours show a significant *decrease* in reduced glutathione level as compared to controls. However, at both 4 and 6 hours (Figure 12C) exposure to 10X DDE there is no significant difference in glutathione levels as compared to controls

Figure 12D illustrates the results of the reduced glutathione assay for WS1 cells exposed to 1X or 10X DDE for 2, 4 or 6 hours. The reduced glutathione content of WS1 cells treated for 2 hours with 1X DDE is significantly *increased* above that of control cells. By 4 hours exposure to 1X DDE the reduced glutathione content is only 50% of the control level, but by 6 hours exposure to 1X DDE reduced glutathione levels have rebounded back to control levels. WS1 cells exposed to 10X DDE for 2 hours exhibit a slight but not significant increase in reduced glutathione level as compared to controls. By 4 hours the 10X DDE exposed WS1 cells exhibit a significant *decrease* in reduced glutathione levels as compared to controls. By 6 hours the reduced glutathione level of 10X DDE treated WS1 cells have rebounded and are significantly *increased* above control levels.

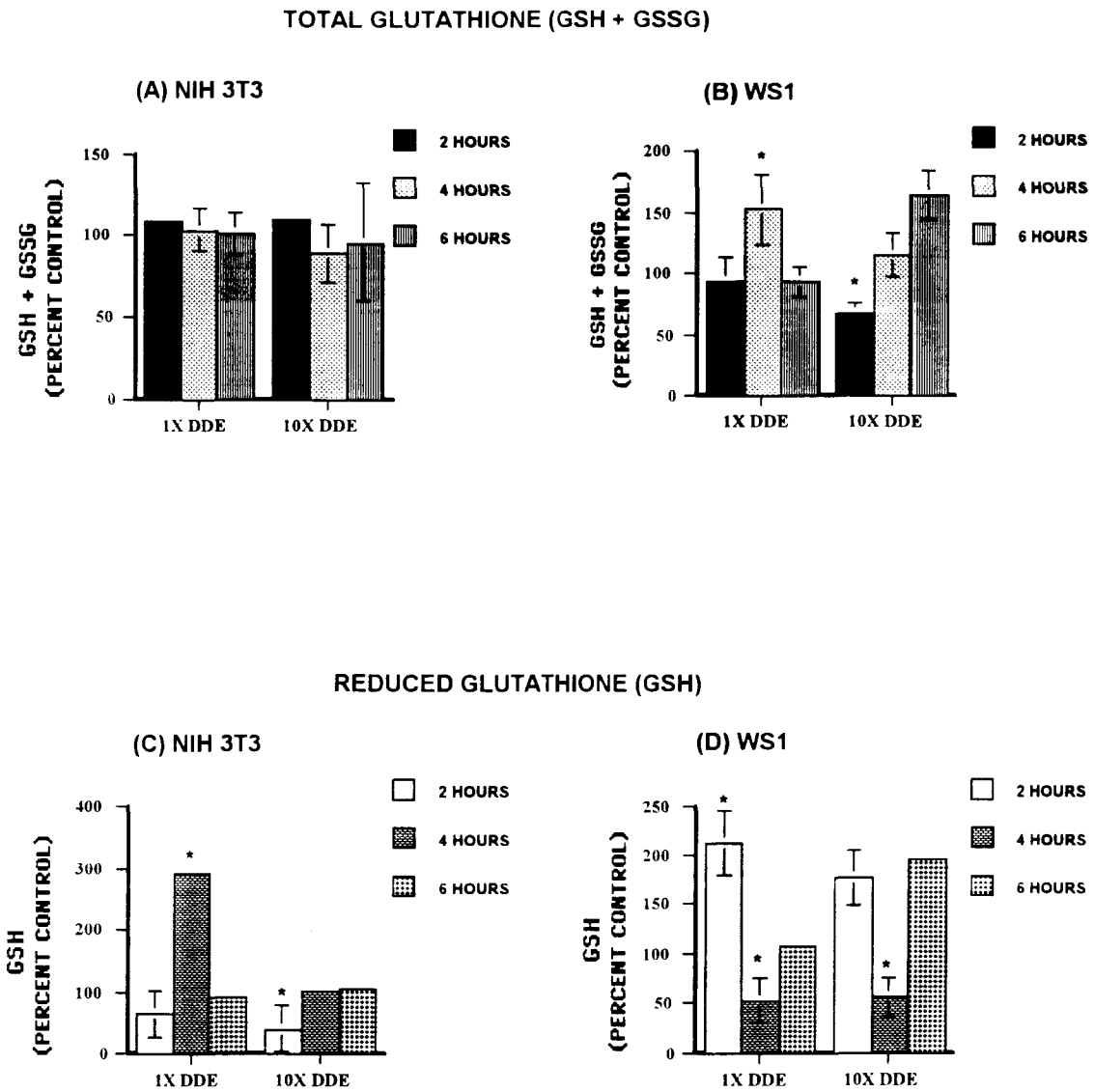

Figure 12: Assays for total glutathione {GSSG + GSH} and reduced glutathione {GSH}

See following page for legend.

Figure 12: Legend

Effect of 1X and 10X DDE on the total cellular glutathione levels within (A) NIH 3T3 and (B) WS1 and reduced glutathione levels within (C) NIH 3T3 and (D) WS1. NIH 3T3 and WS1 cells were plated in duplicate and treated with acetone alone (control), 1X or 10X DDE for the times indicated. Cells were subsequently harvested by trypsinization and pelleted. Total glutathione concentration per mg protein was measured using the Tietze method (241, 242). Reduced glutathione concentration per mg protein was determined using the Bioxytech GSH 400 kit as per the manufacturer's instructions. The data points represent the average total or reduced glutathione levels expressed as a percentage of the total or reduced glutathione concentration per mg protein in control samples measured at the same time-points. Asterisk * indicates a significant difference from acetone alone (control) by one-way ANOVA ($p > 0.05$). Published in Simonetti et al 2001 (213).

(iv) DNA damage assay

The Comet assay (244) was performed to determine if exposure to 1X or 10X DDE resulted in DNA damage. When assayed by alkaline electrophoresis, DNA damage, specifically single-strand breaks, results in an increased displacement between the leading edge of the nucleus and the end of the tail (comet) and is expressed as an increase in total DNA length, (see Figure 13 for example). Table 7 contains the average measurements of the total DNA lengths of WS1 and NIH 3T3 cells exposed to acetone alone (control), 1X or 10X DDE for 4 hours.

When compared to controls, there was a significant increase in NIH 3T3 total DNA length after 4 hours exposure to both 1X and 10X DDE ($p < 0.05$) although the 1X and 10X lengths are not significantly different from each other. In contrast the total DNA lengths of WS1 cells treated with acetone alone (control), 1X or 10X DDE for 4 hours are not significantly different from each other.

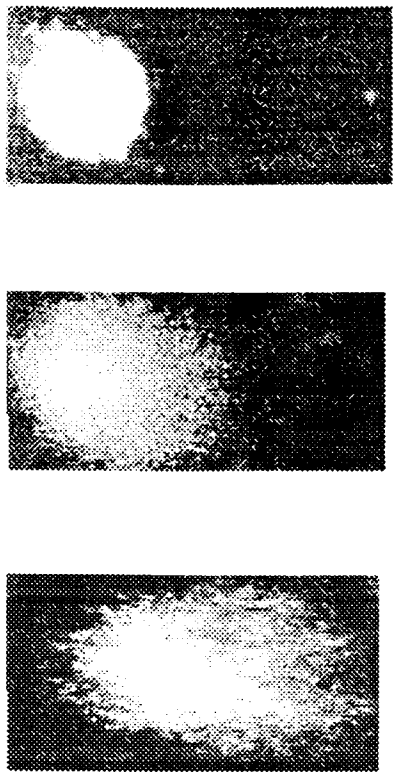

Figure 13: Comet assay

The Comet assay was performed to determine if exposure to DDE resulted in DNA damage. Within individual cells, damage to nuclear DNA results in the increased migration of DNA through agarose. Shown here are typical examples of the "Comet tails" formed by the DNA of NIH 3T3 cells exposed to Control (A), 1X DDE (B) and 10X DDE (C) for 4 hours. See Table 7 for actual measurements.

Table 7: DNA damage assay (Comet assay) [a]

CELL TYPE	TREATMENT 4h	TOTAL DNA LENGTH AVERAGE
NIH 3T3	Control	15.9 ± 1.4 mm
	1X DDE	**18.7 ± 1.76 mm** [b]
	10X DDE	**19.7 ± 2.7 mm** [b]
WS 1	Control	14.7 ± 3.5 mm
	1X DDE	14.6 ± 4.2 mm
	10X DDE	14.2 ± 3.3 mm

[a] The Comet assay (243) was performed to determine if 4 hours exposure to 1X or 10X DDE resulted in DNA damage. Damage to nuclear DNA within individual cells, results in an increased ability of the DNA to migrate through agarose during electophoresis and is expressed as an increase in total DNA length. The total DNA length (the displacement between the leading edge of the nucleus and the end of the tail) of a minimum of 50 cells per treatment was measured and the average length calculated ± SD.

[b] Significant increase ($p < 0.05$) in DNA migration, indicating increased strand breakage, as compared to NIH 3T3 control cells. Published in Simonetti et al 2001 (213).

(v) Cell cycle kinetics assay

The effects of 1X and 10X DDE on the progression of WS1 and NIH 3T3 cells through the cell cycle are shown in Figure 11. FACS results reveal no significant difference between the number of cells entering S phase in the control, 1X and 10X DDE treated NIH 3T3 cells at the time-points tested between 0 h and 30 h (Figure 14A).

Similar to NIH 3T3 cells, WS1 acetone alone (control) cells began to incorporate BrdU within 4 hours after it was added to the media (Figure 14B). In contrast, 1X DDE treated WS1 cells did not begin to incorporate BrdU until approximately 6 hours after the initiation of DDE exposure. Furthermore, the 1X DDE treated cells maintain the 2-hour lag in the number of cells entering S phase up to 30 hours after the chemical has been added. No data is available for WS1 cells treated with 10X DDE, as despite repeated attempts to obtain this information, this treatment group of cells could not survive the combined flow cytometric protocol and exposure to 10X DDE.

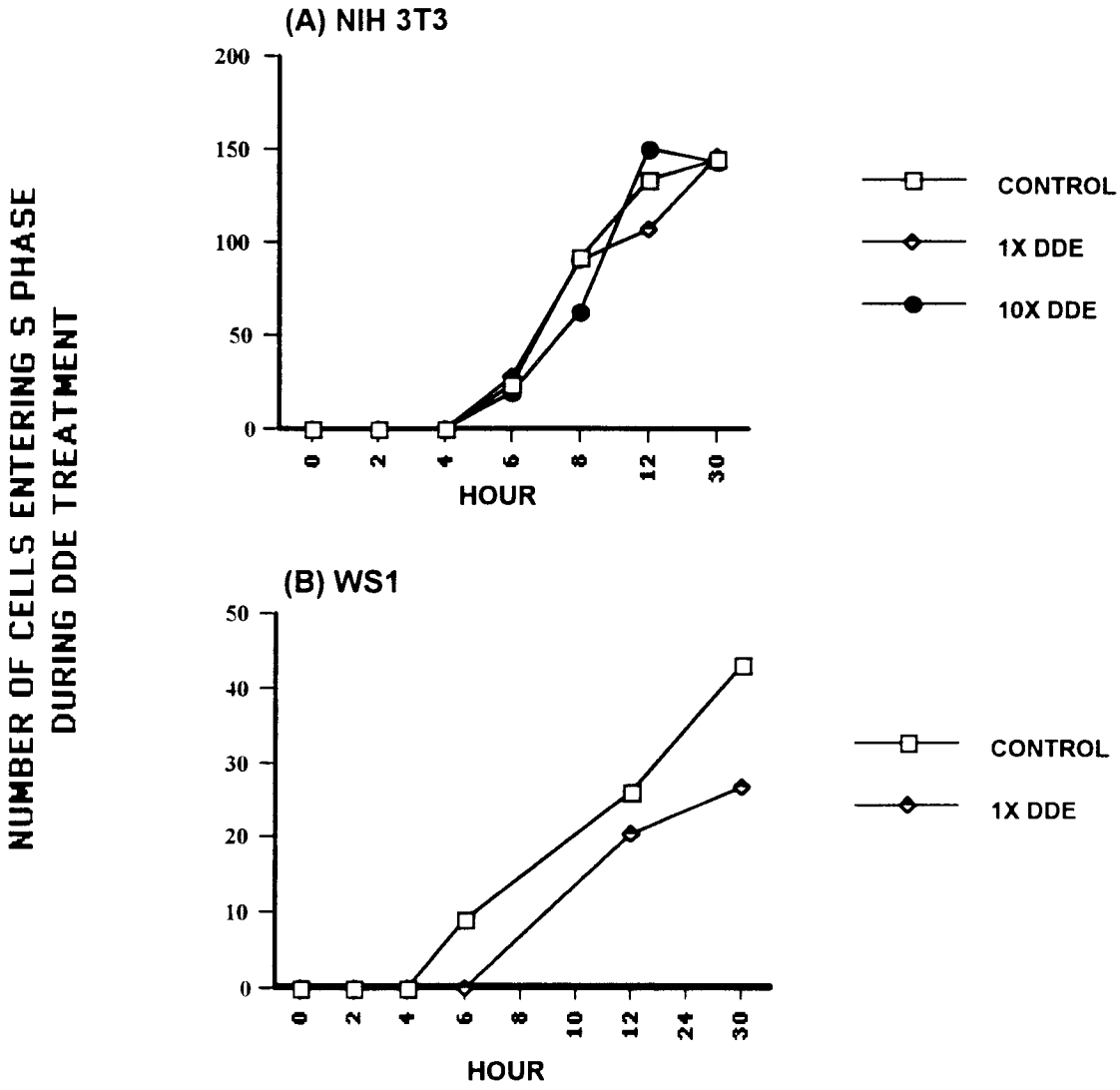

Figure 14: Cell cycle kinetics assay

Cell cycle kinetics of NIH 3T3 and WS1 cells exposed to acetone alone (control), 1X or 10X DDE. NIH 3T3 (A) and WS1 (B) cells were exposed to media containing BrdU, deoxycytidine and either acetone alone (control), 1X or 10X DDE. Samples were harvested by trypsinization at the indicated time-points and underwent BrdU–Hoescht flow cytometric analysis. Data points representing WS1 cells exposed to 10X DDE are absent, as despite repeated trials, these cells could not survive both the cytometric protocol and DDE exposure. Published in Simonetti et al 2001 (213).

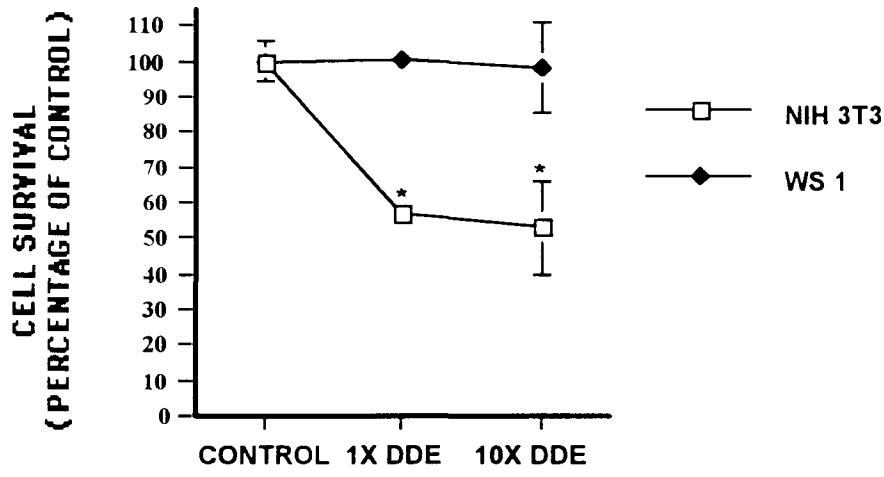

Figure 15: Colony forming ability

Comparison of the effect of DDE on the long-term survival of NIH 3T3 and WS1 cells exposed to acetone alone (control), 1X or 10X DDE. Cells were plated in duplicate per treatment and grown in the presence of DDE for 12-14 days. The cells were then fixed, stained and the number of colonies counted per plate. Cell survival per treatment is expressed as a percentage of the number of surviving colonies on the control plates. The graph represents the average percent survival from three independent experiments. Asterisk (*) indicates a significant difference from acetone alone (control) cells by one-way Anova ($p<0.05$). Published in Simonetti et al 2001 (213).

B. Long-term assays of chemical toxicity

(i) Colony-forming ability

Neither 1X nor 10X DDE had an effect on the number of WS1 cells surviving to form colonies. There was no significant difference between the number of colonies formed by WS1 cells treated with acetone alone (control), 1X or 10X DDE, (control = 100% ± 3.8%, 1X = 100.5% ± 2.5%, 10X = 98% ± 12.7%) (Figure 15). In contrast, both 1X and 10X DDE had a significant effect on the number of NIH 3T3 cells surviving to form colonies ($p < 0.05$). Treatment with both 1X and 10X DDE resulted in a decrease in the number of colonies formed by NIH 3T3 cells, specifically, control = 100%± 5.8%, 1X = 57%± 3.8% and 10X = 53% ± 13.4% with no significant difference in cell survival between the two DDE treatments (Figure 15).

(ii) Transformation assay

No significant difference was found between the number of foci formed by control (n = 39 ± 8.2) or DDE exposed NIH 3T3 cells treated with 1X (n = 39 ± 4.6), 10X (n = 39 ± 9.1) or 100X DDE (n = 38 ± 5.6) (Published in 213).

Section II: Effects of environmentally relevant concentration of p,p'-DDE on mismatch repair rates at an oncogenic hotspot

A. Mismatch repair rates at codon 12 of H-ras in the presence of p,p'-DDE

Mismatches at the middle base position of codon 12 H-*ras* (G:**T** and G:**A**) were introduced into WS1 and NIH 3T3 cells in the presence and absence of DDE. These particular mismatches were chosen because they represent the best and worst repaired codon 12 mismatches in mammalian cells respectively (53). Extraction of the plasmid DNA from NIH 3T3 cells and subsequent transformation of the mismatch deficient NR9374 bacteria with the extracted plasmid eliminated the problem of contaminating human genomic H-*ras* sequences from the WS1 cells. As well, cells were exposed to 10X DDE only, as this quantity represents the highest concentration found in Inupiat umbilical cord blood and in a sense the "worst case" scenario. It must be stressed that the results presented here are preliminary, due to small numbers, and it is difficult to draw firm conclusions from them. Further work is necessary for a more in-depth investigation of the effect of DDE exposure on mismatch repair in human and murine cells in culture.

WS1 cells: Shown in Table 8 are the results of this preliminary investigation into the effects of DDE on mismatch repair in WS1 human cells. DDE does not appear to have a discernable effect on the ability of WS1 cells to correctly repair G:**T** mismatches (G:T + DDE = 87%, G:T - DDE = 85%). However there appears to be a slight decrease in the

Table 8: Mismatch repair at codon 12 of H-*ras* in p,p'-DDE treated and untreated WS1 cells

WS1 cells Mismatch and Treatment	Correctly repaired mismatch ⇒ G:C (Total Assayed)	Incorrectly Repaired Mismatch to T:A or A:T (Total Assayed	Unrepaired Mismatch ⇒ G:C / T:A or G:C / A:T (Total Assayed)
G:T + p,p'-DDE	87% (20/23)	4% (1/23)	9% (2/23)
G:T – p,p'-DDE	85% (17/20)	10% (2/20)	5% (1/20)
G:A + p,p'-DDE	93% (14/15)	0% (0/15)	7% (1/15)
G:A – p,p'-DDE	67% (6/9)	0% (0/9)	33% (3/9)

amount of G:T mismatch that is incorrectly repaired (resulting in activating mutation) in DDE exposed cells as compared to unexposed WS1 cells (G:T + DDE = 4%, G:T – DDE = 10%).

In contrast, WS1 cells treated with DDE exhibit a much *improved* repair of the G:A mismatch as compared to untreated cells (G:A + DDE = 93%, G:A – DDE = 67%) (Table 8). There is also a concomitant decrease in the amount of G:A mismatch left un-repaired in DDE treated cells as compared to unexposed WS1 cells (G:A + DDE 7%, G:A – DDE = 33%).

NIH 3T3 cells: Mismatch repair rates for NIH 3T3 cells treated with and without 10X DDE are shown in Table 9. DDE treatment has no apparent effect on the ability of NIH 3T3 cells to repair G:T mismatches, as both treated and un-treated cells repair G:T with 100% efficiency.

In contrast, DDE treated cells show a slight *increase* in the amount of G:A mismatch that is correctly repaired (G:A + DDE = 89%, G:A – DDE = 80%) (Table 9). NIH 3T3 cells also exhibit a slight decrease in the amount of G:A mismatch that remains un-repaired while the cells are exposed to DDE (G:A + DDE = 0%, G:A - DDE = 10%) with no substantial difference between treated and un-treated cells in the amount of mismatch that is repaired incorrectly and results in an activating mutation.

Table 9: Mismatch repair at codon 12 of H-*ras* in p,p'-DDE treated and untreated NIH 3T3 cells

NIH 3T3 cells Mismatch and Treatment	Correctly repaired mismatch ⇒ G:C (Total Assayed)	Incorrectly Repaired Mismatch to T:A or A:T (Total Assayed	Unrepaired Mismatch ⇒ G:C / T:A or G:C / A:T (Total Assayed)
G:T + p,p'-DDE	100% (10/10)	0% (0/10)	0% (0/10)
G:T – p,p'-DDE	100% (8/8)	0% (0/8)	0% (0/8)
G:A + p,p'-DDE	89% (16/18)	11% (2/18)	0% (0/18)
G:A – p,p'-DDE	80% (8/10)	10% (1/10)	10% (1/10)

IV. DISCUSSION

PART I: Mismatch repair at an oncogenic hotspot in G_1 synchronized NIH 3T3 cells

Since the discovery of the mismatch repair system in *E.coli* it has been considered primarily if not exclusively a post-replication DNA repair mechanism and, due to their similarities, the prokaryotic and eukaryotic mismatch repair systems were assumed to function within a similar timeframe. Therefore, with respect to the mammalian cell cycle, this would mean that the mismatch repair system would be most active in the G_2 phase of the cell cycle immediately following DNA replication (107, 247, 248). However, as discussed in the introduction, mismatches can occur throughout the cell cycle by a variety of processes, with failure to repair these lesions before DNA replication resulting in mutation fixation. As we know, faithful replication of DNA is of paramount importance for the maintenance of genomic integrity, therefore, we postulated that mismatch repair would be active during the G_1 phase of the mammalian cell cycle in order to ensure that DNA damage is repaired before DNA replication takes place. Indeed, results presented here show that repair of base:base mismatches at the codon 12 H-*ras* oncogenic hotspot is active and accurate during the G_1 phase of the mammalian cell cycle (Table 4). We have also shown that the Epstein-Barr virus derived p220.pbc plasmid replicates synchronously with the cell cycle in murine cells (Figure 8). In addition, the mismatch repair protein MSH2 was found in both cytoplasmic and nuclear extracts from G_1 synchronized cells and in relatively equal amounts as compared to extracts from non-synchronized cell cultures (Figure 9).

As discussed above a main goal of this study has been to determine whether the DNA mismatch repair system is active during the G_1 phase of the mammalian cell cycle. Using methods previously tested, single base:base mismatches were constructed at the H-*ras* codon 12 oncogenic hotspot and subsequently introduced into G_1 synchronized mammalian cells in culture. However, in order to study mismatch repair in synchronized cell populations several challenges had first to be overcome.

Firstly, a method had to be found that would synchronize large populations of NIH 3T3 cells in the G_1 phase of the cell cycle. Several synchronization methods exist for mammalian cells in culture (250). For example, drug treatments such as hydroxyurea, aphidicolin, thymidine and most recently, lovastatin, have been used to produce large populations of synchronous cells. However, treatment with these drugs can result in DNA damage or impaired cell function (251, 252, 253, 254, 255). As well, serum starvation has been used successfully as a means for achieving cell cycle synchronization in many cell types including NIH 3T3 fibroblasts (211, 235, 236, 256).

For exponential growth NIH 3T3 fibroblasts require exogenously added growth factors, usually supplied by supplementation of the growth medium with 10% serum. On serum withdrawal, these cells undergo growth arrest and remain in a quiescent state termed G_1. However, when stimulated with fresh serum the cells synchronously re-enter the cell cycle and engage in exponential growth with no apparent detrimental effects on cell function (257). Consequently we employed the method of serum starvation to achieve G_1 synchronous populations of cells. Indeed, our results show that over 96% of cells were arrested in G_1 by the third day of serum starvation (Table 3). Furthermore

greater than 96% of these cells remained in G_1 for up to 12 hours after media replacement after which time the cells began to re-enter the cell cycle (Table 3). The 12-hour delay in cell cycle progression provided sufficient time for transfection of the mismatched plasmid (4 hours, see materials and methods) and provided an additional 7-hour period for repair to occur before the cells entered the DNA synthesis phase of the cell cycle.

The second challenge of this study concerned replication kinetics of the mismatched plasmid vector. In order to ensure accurate results, it was important to document that the plasmid replicated synchronously with the cell cycle. Plasmid vectors based on the Epstein-Barr virus (EBV) origin of replication are maintained as extrachromosomal plasmids and replicate once per cycle at high efficiency in human and simian cells (258), however, no similar information exists as to how these plasmids behave in murine cells. Therefore we examined the replication kinetics of the wild-type p220.pbc EBV derived plasmid in G_1 synchronized NIH 3T3 cells. We have successfully shown that replication of the p220.pbc plasmid is substantially delayed in G_1 synchronized NIH 3T3 murine cells when compared to non-synchronized control cells (Figure 8) indicating that the p220.pbc plasmid replicates synchronously with the murine cell cycle.

Lastly, as discussed in the introduction, mismatch repair is not the only DNA repair mechanism capable of repairing mismatches. For example, the BER enzyme thymine DNA glycosylase can remove thymine from G:T mispairs (73, 74, 75, 76). Therefore, for additional evidence of mismatch repair activity we examined G_1 nuclear and cytoplasmic extracts for the presence of the MSH2 mismatch repair protein

(reviewed in introduction, part I). Our results clearly show that the MSH2 protein is found in both NIH 3T3 cytoplasmic and nuclear G_1 extracts and that it is present in relatively equal amounts in extracts from both synchronized and non-synchronized cells (Figure 9). These results agree with those of Meyers et al 1997 who found that, in human fibroblasts, the levels of hMSH2 mRNA and protein did not change throughout the cell cycle (211). Our data indicates that in NIH 3T3 cells at least one of the mismatch repair proteins responsible for the detection and repair of mismatched DNA is present in the G_1 phase of the cell cycle.

As a result of the experiments described above, we have successfully demonstrated; (1) serum starvation is a successful and non-toxic method to achieve G_1 synchrony in large populations of NIH 3T3 cells; (2) the p220.pbc plasmid replicates synchronously with the murine cell cycle; and (3) the MSH2 mismatch repair protein is present in G_1 cells indicating potential mismatch repair activity in G_1. Based on this information we then proceeded to examine mismatch repair activity in the G_1 phase of the mammalian cell cycle.

Our results for mismatch repair at the middle nucleotide hotspot of codon 12 in G_1-synchronized cells demonstrate that repair of mismatched DNA is active in the G_1 phase of the mammalian cell cycle (Table 4). Furthermore, we have observed correct repair of virtually all codon 12 mismatches transfected into G_1-synchronized cells, with the single exception of one incorrectly repaired G:T mismatch resulting in an activating mutation. Interestingly, this was the first time that we observed a mutated sequence at

codon 12 that did not result from replication before repair, which would have been indicated by a mixed sequence at this site (53, 54, 234).

Previously, we and other researchers have found that, when compared to other base:base mismatches, the G:T mismatch is repaired with highest efficiency in *E.coli*, murine and simian cells (53, 54, 234, 258). We believe that the reason for this is because several systems exist to repair G:T mismatches and the combined action of these systems results in extremely efficient repair. For example, in addition to the mismatch repair system, the BER thymine DNA glycosylase enzyme can repair G:T mismatches resulting either from misincorporation during DNA synthesis or deamination of 5-methylcytosine (73, 74, 75, 76). Several investigators have found that expression of the glycosylase enzymes is regulated during the cell cycle with the highest protein levels measured prior to DNA synthesis which corresponds to late G_1 phase (260, 261, 262, 263, 264, 265). Therefore, we spectulate that the G:T incorrect repair we observed was due to the down regulation of the BER enzyme during earlyG_1 phase of the cell cycle in NIH 3T3 cells. However, we must remember that the mutation observed represents one sample whose incorrect repair could be due to a number of, as yet, unexplained reasons.

In contrast, we found a much improved repair rate for the three remaining mismatches as compared to repair rates in non-synchronized cells (Figure 10). We previously found high rates of unrepaired mixtures at codon 12 in non-synchronized cells, which, we believe, resulted from plasmid replication before repair could take place (53, 234). Although it is theoretically possible that the increased correct mismatch repair rate observed in G_1 synchronized cells is due to *increased fidelity of repair* during the G_1

phase of the cell cycle, this seems unlikely. At best we would expect that the repair rate in G_1 would be similar to that for non-synchronized cells. Our FACS analysis results have shown that >96% of cells are in G_1 for as long as 7 hours after completion of transfection. Therefore, the increased correct mismatch repair rate during G_1 probably indicates a function of ***increased time*** for repair activity. Nevertheless, these results demonstrate that the mismatch repair system is active during the G_1 phase of the cell cycle and in addition, these results also provide some insight into mechanisms of repair at mutagenic hotspots throughout the cell cycle.

The reasons for the occurrence of mutagenic hospots, such as codon 12 of H-*ras*, remain unclear and the hypotheses put forward to explain them have been previously discussed (see introduction part I). One of these hypotheses states that there is decreased fidelity of repair or inefficient repair at particular sequences. For example, primer extension studies have demonstrated that both DNA polymerases α and β have a strong pause site at the nonmutated codon 12 location, suggesting stearic hindrance, a difficulty in the gap filling stage of the DNA repair process or a general difficulty in enzymatic reactions at this site (266). In addition, previous studies from this laboratory have found that mismatches at the middle nucleotide position of codon 10 H-*ras* in non-synchronized cells are repaired significantly more efficiently than when located at the codon 12 hotspot (54). Furthermore, gel-shift experiments have found mismatch specific binding to oligonucleotides containing mismatches at codon 10 but not to the same oligonucleotides containing mismatches at codon 12 (54).

These results suggest cellular deficiencies in the recognition of specific mismatches that in proliferating cells result in low levels of repair. However, the G_1 mismatch repair results presented here demonstrate that, given sufficient time before DNA replication, a mammalian cell can repair mismatches at an oncogenic hotspot with high efficiency. Therefore these results lend weight to the argument that mismatch repair is inefficient rather than inaccurate. Furthermore, repair is inefficient due to a rate-limiting step in the repair process that results in replication of the DNA before repair can take place.

PART II: Effects of p,p'-DDE on cell toxicity and mismatch repair ability at an oncogenic hotspot

This study demonstrates that DDE, at levels measured in the umbilical cord blood of Alaskan Inupiat newborns, does have significant effects on embryonic human and murine fibroblast cells in culture. The specific effects, discussed below, occur when cell cultures are exposed to concentrations of DDE that are environmentally relevant and are significantly lower than the concentrations used in all other published DDE toxicology studies. Results of the DABA assay for changes in cell number (Figure 11) suggest that these low concentrations of DDE caused NIH 3T3 and WS1 cell numbers to decrease within a few hours of exposure. Subsequent assays revealed that 1X and 10X DDE were cytotoxic to the NIH 3T3 embryonic mouse fibroblast cell line and consequently decreased overall long-term survival. However, DDE treatment had an entirely different effect on the WS1 human embryonic cell, in that exposure caused a pause in the cell cycle, which subsequently resulted in an *increase* in the correct rate of mismatch repair at the codon 12 H-*ras* oncogenic hotspot. This result, although surprising, is in agreement with our previous results from G_1 synchronized cells, in which we have found that increased time for repair results in a much improved repair rate. In addition, exposure to DDE had no apparent long-term effects on WS1 cell survival (Figures 14B and 15).

A modification of the DABA assay (240) was used to determine cell number at specific intervals after the initiation of chemical exposure. We have used this assay extensively and have found it to be an extremely reliable and sensitive method for detecting small changes in cell numbers over relatively short periods of time. Initial

experiments, performed to elucidate if short-term DDE exposure resulted in detectable changes in cell number, revealed that both NIH 3T3 and WS1 cells were affected within a similar time period by DDE (Figure 11). Furthermore, both cell types eventually recovered from the initial decrease in cell number and all treated samples attained cell numbers similar to controls when confluence had been reached and the cells had ceased to grow.

A decreased number of cells in the DDE treated plates could be the result of cell death, since dead cells detach from the plate and are washed away in the initial steps of the harvesting procedure. Another possible explanation for fewer cells per plate is an arrest in the cell cycle. In this scenario, although cells are not physically lost from the plate, a pause in the initial stages of the cell cycle, before DNA replication, would result in a lower cell number when compared to controls assayed at the same time-point. These initial experiments, in addition to demonstrating a toxic effect of DDE, also provided an indication of the time period within which the measured effects occurred for each cell type.

NIH 3T3 cells: Cell viability, as determined by the trypan blue assay, revealed that exposure to both 1X and 10X DDE resulted in significant NIH 3T3 cell death within 2-4 hours of treatment, as compared to control cells (Table 6). Cell death in NIH 3T3 cells occurred within the same time period at which the DABA assay demonstrated an initial decrease in cell number for both 1X and 10X DDE treatments (Figure 11A).

Comet assay results presented in Table 7 indicate that 1X and 10X DDE caused a significant amount of strand breaks in the DNA of NIH 3T3 cells. The DNA strand

breaks could be the result of a direct interaction between the chemical and nuclear DNA. As well, an increase in intracellular reactive oxygen species and the release of clastogenic elements (both possible consequences of DDE's action) and/or attempts to repair the damage caused by these agents could cause DNA strand breaks. Alternatively, it is also possible that the strand breaks found in NIH 3T3 cells were due to the DNA degradation that occurs during cell death. Results of the focus-forming assay revealed that up to 100X DDE (35µg/l) (see results) had no apparent mutagenic effect on the transforming potential of NIH 3T3 cells. Previous use of this assay by our laboratory has resulted in a several fold increase in the number of transformed foci formed by NIH 3T3 cells transfected with mutated H-*ras* (234). This information, along with the results of the trypan blue assay (Table 6), suggest that the DNA strand breaks observed in the comet assay are either the result of cell death or occur by some other mechanism.

As part of this investigation we determined if DDE treatment had any detectable effect on total glutathione concentration (GSH + GSSG) and/or the amount of glutathione in the reduced state (GSH). DDE is a lipophilic compound and as such, primarily targets the lipid rich plasma and organellar membranes (267). DDE has been found to modify basic membrane mechanisms, such as permeability to non-electrolytes and cation transport, through a physical interaction with the lipid bilayer (268). Glutathione has been implicated in a variety of cellular processes including detoxification of numerous electrophilic substances and peroxides, control of enzyme activity, regulation of the cell cycle and apoptosis (269, 270, 271, 272, 273).

Within the normal limits of cellular redox activity glutathione levels are maintained by a complex mechanism involving control of synthesis, transport and utilization (271, 272). However, glutathione levels have been found to fluctuate in response to a variety of cellular insults. For example, oxidative stress, which can originate from a variety of exogenous and endogenous sources, can produce a decrease in glutathione levels (274, 275, 276). Conversely, similar types of oxidative stress have been found to up-regulate the transcription of at least one of the enzymes involved in glutathione synthesis resulting in an increase in cellular glutathione levels (276, 277). As well, oxidation of reduced glutathione has been shown to occur during apoptosis resulting in decreased reduced glutathione levels (269).

It is possible that the increased membrane fluidity, induced by DDE, could result in the leakage of oxygen radicals out of the mitochondria and the increased movement of potentially damaging agents across the plasma membrane into the cell. Both of these processes would increase oxidative stress, initially depleting glutathione but in the process initiating the up-regulation of glutathione production, cumulating in an increase in total glutathione levels.

In NIH 3T3 cells DDE treatment does not alter total glutathione levels but does cause alterations in reduced glutathione levels (Figure 12A and 12C). The large increase in reduced glutathione in NIH 3T3 cells treated with the 1X concentration for 4 hours suggests an inductive response to DDE exposure (Figure 12C). We were unable to determine GSSG concentrations in these samples, therefore the increase in GSH may reflect a concomitant decrease in GSSG (which would not affect total glutathione levels)

or may simply reflect differences in the sensitivity of the two assays. The significant decrease of reduced glutathione at 2 hours of 10X DDE exposure may have been caused by the immediate and uncompensated oxidation of GSH to GSSG in response to the chemical insult.

The cell cycle kinetic analysis results demonstrate that NIH 3T3 progression through the cell cycle is unaffected by either 1X or 10X DDE treatments (Figure 14A). Chemical toxicity, as determined by NIH 3T3 colony-forming ability, did occur as exposure to both 1X and 10X DDE resulted in similarly decreased long-term survival of NIH 3T3 cells (Figure 15).

In addition, preliminary experiments to investigate the effect of DDE on DNA mismatch repair at an oncogenic hotspot were performed. No difference was observed in the repair rate of G:T mismatches regardless of the cellular exposure to DDE (Table 9). This is in agreement with previous studies from our laboratory in which we found that G:T mismatches were also repaired with 100% efficiency in NIH 3T3 cells (53, 234). In contrast, there was a slight *increase* in the amount of G:A mismatch that was correctly repaired in DDE treated cells, perhaps reflecting a cell cycle pause too short to be detected by FACS analysis (Table 9).

Our previous results have shown that the G:A mismatch is repaired with the poorest efficiency in proliferating NIH 3T3 cells (35%) with the majority of the mismatch being left unrepaired (53). The p220.pbc plasmid used in previous studies is capable of replication in mammalian cells with the result that unrepaired mismatch is represented by mixtures of mutated and wildtype sequences in the final analysis.

However, the pbc-N1 plasmid used in the DDE experiments cannot replicate in mammalian cells and therefore unrepaired mismatch remains in the cell. Perhaps it is due to the lack of plasmid replication and thus increased time of exposure to the DNA repair machinery that we see a much improved repair rate of G:A mismatches in both DDE treated and untreated NIH 3T3 cells. Interestingly, for the first time we found G:A mismatch which was incorrectly repaired to an activating mutation, in both DDE, treated, and untreated cells (Table 9).

The reasons for the incorrect repair of the G:A mismatch remain unclear but may possibly be due to its location at the H-*ras* codon 12 oncogenic hotspot, the mismatch itself or a combination of these factors. Other investigators have found the G:A mismatch to be particularly difficult to repair in both *in vivo* and *in vitro* repair studies regardless of its location (259, 278, 279). Perhaps the G:A mismatch coupled with its codon 12 location presents a particularly difficult repair scenario. Lack of repair of G:A mismatches may be biologically relevant as the resulting T:A transversion is a common activating mutation found at this codon 12 H-*ras* location in naturally occurring tumors (36, 37, 38, 39). Obviously further studies are needed to examine and compare repair rates at non-oncogenic hotspots such as codon 10 H-*ras* with the non-replicating plasmid. Such studies, at the very least, might help determine whether the G:A mismatch or its codon 12 location are primarily responsible for the incorrect repair found in this study.

Together, the results of these assays indicate that DDE, at both 1X (0.35μg/l) and 10X (3.5μg/l) concentrations, caused sufficient cell death of NIH 3T3 cells within the first hours of exposure to decrease overall long-term survival. Cell death may be due to

excessive DNA damage, the presence of which is indicated by the Comet assay, or some other mechanism of cell toxicity. Despite the use of several commercially available assays to determine whether cell death occurred by apoptosis or necrosis, it has not yet been possible to definitively identify which death process occurs in NIH 3T3 cells exposed to DDE. We suspect that the ambiguous results obtained with these assays are due, in part, to the membrane effects of DDE. We are currently investigating other methods of apoptosis /necrosis detection, which do not require the use of membrane, bound dyes. In addition, the classical DNA laddering effect, observed by agarose electrophoresis, caused by apoptosis cannot be used with NIH 3T3 cells because of their aneuploid nuclear DNA.

WS1 cells: In contrast, results from the above assays indicate that exposure to these low concentrations of DDE has an entirely different effect on WS1 cells. The findings of the trypan blue and Comet assays (Tables 6 and 7) indicate that neither 1X or 10X DDE caused cell death or significant DNA damage in WS1 cells. Therefore, the decrease in cell number observed in the DABA assay does not appear to be the result of cell death but must occur by another mechanism discussed below (Figure 11B).

Both 1X and 10X DDE caused significant alterations in the total glutathione levels of WS1 cells (Figure 12B). The significant increase in WS1 total glutathione level at 4 hours exposure to 1X DDE is most likely the result of up-regulation of glutathione synthesis. In addition, it has been reported that increased glutathione levels are associated with release from cell cycle arrest (273, 280, 281). Since the cell cycle kinetic results (discussed below) indicate a cell cycle arrest, this could account for the fluctuating total

glutathione levels. The initial significant decrease in total glutathione levels at 2 hours exposure to 10X DDE likely indicates that both GSH and GSSG are leaking out of the cells through damaged membranes. The initial loss of total glutathione could then trigger increased synthesis as is evident by the 4 hour and 6 hour stepwise increase of total glutathione (Figure 12B).

GSH levels exhibit a similar fluctuating pattern in both 1X and 10X DDE treated cells. The initial increase after 2 hours of exposure for both DDE treatments may indicate a cellular response that includes up-regulation of GSH production. The subsequent decrease in reduced glutathione levels by 4 hours for both treatments, suggests that GSH is undergoing oxidation to GSSG in direct response to the oxidative stress caused by the interaction of DDE with cellular membranes. As well, increased amounts of GSH, by 6 hours exposure to both DDE concentrations corresponds with the increased 4 and 6 hour total glutathione levels (Figure 12B).

Cell cycle kinetic analysis revealed that WS1 cells treated with 1X DDE experience a delay or arrest of at least two hours, in the initiation of BrdU incorporation, as compared to controls (Figure 14B). This delay/arrest occurs at approximately the same time as a decrease in cell number is observed and is indicative of a pause or arrest in the cell cycle (Figure 11B). As well, the observed increase in WS1 total glutathione level occurs at approximately the same time that these cells begin to re-enter the cell cycle (Figure 12B).

The results of the colony-forming assay indicate that WS1 cell survival is not affected by long-term exposure to either 1X or 10X DDE (Figure 15). Together with the

findings presented above it appears that the decrease in WS1 cell number observed for both DDE concentrations is not due to cell death, but to a delay or a short recoverable arrest in the cell cycle. It is possible that this cell cycle delay/arrest provides the time necessary to counteract the effects of these low environmental concentrations of DDE without compromising the long-term survival of the cell.

Mismatch repair rates at an oncogenic hotspot in WS1 cells in the presence and absence of DDE were also examined (Table 8). As was the case with the NIH 3T3 cells, DDE exposure did not appreciably change the correct repair rates of the G:T mismatch. In contrast, dramatic results were found when the repair rate of the G:A mismatch was examined. Exposure of WS1 cells to DDE resulted in a 26% increase in the correct repair of G:A mismatches back to the wildtype G:C sequence. We suspect that this increased repair rate was facilitated by the cell cycle arrest induced by DDE in these cells (Figure 14B). As described earlier, the plasmid used in these mismatch studies does not replicate in mammalian cells, therefore, the improved repair rate of the G:A mismatch can not be due to repair before replication as was the case in the study of mismatch repair in the G_1 phase of the cell cycle described in Part I. However, in addition to providing time for repair, cell cycle arrests can also result in the induction of DNA damage repair enzymes (206, 207). Therefore, we postulate that the improved repair rate seen in the WS1 cells exposed to DDE occurs as a direct consequence of the induction of repair enzymes by the cell cycle arrest machinery.

It is unclear why we find so much unrepaired G:A mismatch in the DDE untreated WS1 cells (33%). However, as was the case with the NIH 3T3 cells, this may be due to

the repair difficulties presented by this particular mismatch in combination with its location at the codon 12 hotspot. Further studies that examine repair rates at a non-oncogenic hotspot with this non-replicating plasmid would help determine the roles played by both the codon 12 location and the mismatch combination in the incorrect repair found in these studies.

Interestingly, in all but the glutathione assay, we found no significant difference between the effects of 1X and 10X DDE. Also, the effects of DDE on both cell types, although different, occurred soon after the initiation of DDE treatment and did not increase in severity with long-term exposure. It has been reported that artificial vesicles can absorb up to several hundred times the equivalent of the 10X DDE concentration used in these studies without affecting the integrity of the membrane (267). Therefore, lack of a difference in effect between 1X and 10X DDE may be due to the ability of the cellular membrane to absorb and sequester these relatively small amounts of DDE.

This study has also demonstrated that two immature mammalian cell types can have significantly different cellular responses to the same exposure levels of a single chemical. DDE exposure at both 1X and 10X concentrations resulted in significantly increased NIH 3T3 cell death, DNA damage either prior to or due to cell death, altered reduced glutathione levels and decreased long-term cell survival, but had no effect on cell cycle kinetics or DNA mismatch repair abilities. Conversely, DDE treatment of WS1 cells at identical concentrations and times of exposure did not cause cell death, DNA damage, decrease cell viability, or affect long-term cell survival, but did alter the levels

of both total and reduced glutathione, affected progression through the cell cycle and, most significantly actually *improved* mismatch repair rates at an oncogenic hotspot.

The most striking difference between the responses of the two cell types is that WS1 cells respond to DDE exposure with a delay or an arrest in their cell cycle, whereas the cell cycle of NIH 3T3 cells is unaffected by DDE treatment. We therefore conclude that the NIH 3T3 cell death that occurred during exposure to DDE, was not due to the direct effects of the chemical, but rather occurred due to this cell type's inability to arrest its cell cycle and thus respond appropriately to the damage caused by DDE. In contrast, because WS1 cells have the ability to delay/arrest the cell cycle they did not suffer the same cytotoxic consequences when exposed to DDE. However, the cell cycle arrest may have serious consequences for a developing embryo, as normal development requires precisely timed cellular proliferation and differentiation events (282, 283).

The results of this study demonstrate that DDE, at concentrations relevant to the Alaskan environment, has detectable effects on embryonic mammalian cells in culture. Furthermore, DDE has specific effects on human and mouse embryonic fibroblasts, which lack a mature hepatic cell's capacity to significantly metabolize the chemical to a more or less toxic compound. Finally, the results of this study emphasize the importance of further investigations to determine the effects of DDE on the sensitive systems of the developing embryo, such as the immune, endocrine, hepatic and central nervous system.

V. REFERENCES

1. Lindahl, T. (1993) Instability and decay of the primary structure of DNA. *Nature*, **362**, 709-715.

2. Friedberg, E.C., Walker, G.C. and Siede, W. (1995) *DNA repair and Mutagenesis*. Washington D.C.: ASM Press.

3. Franken-Schwager, M. (1990) Induction, repair and biological relevance of radiation-induced DNA lesions in eukaryotic cells. *Radiat. Environ. Biophys.*, **29**, 273-292.

4. Hsieh, D.P.H., Wong, J.J., Wong, Z.A., Michas, C. and Ruebner, B.H. (1977) Hepatic Transformation of Aflatoxin and Its Carcinogenicity. P. 697-707. In H.H. Hiatt, J.D. Watson and J.A. Winston (ed.), *Origins of human cancer,Book B*. Cold spring Harbor Laboratory, Cold Spring Harbor, N.Y.

5. Roberts, J.J. and Pascoe, J.M. (1972) Cross-linking of Complementary Strands of DNA in Mammalian Cells by Antitumour Platinum Compounds. *Nature*, **235**, 282-284.

6. Tomatis, L. (2000) The identification of human carcinogens and primary prevention of cancer. *Mutat. Res.*, **462**, 407-421.

7. Lindahl, T. and Nyberg, B. (1972) Rate of Depurination of Native Deoxyribonucleic Acid. *Biochemistry*, **11**, 3610-3618

8. Matsumoto, Y., Kim, K., Hurvitz, J., Gary, R., Levin, D.S., Tomkinson, A.E. and Park, M.S. (1999) Reconstitution of Proliferating Cell Nuclear Antigen-dependent Repair of Apurinic/Apyrimidinic Sites with Purified Human Proteins. *J. Biol. Chem.*, **274**, 33703-33708.

9. Wagner, J.R., Hu, C.C. and Ames, B.N. (1992) Endogenous oxidative damage of deoxycytidine in DNA. *Proc. Natl. Acad. Sci. USA*, **89**, 3380-3384.

10. Richter, C., Park, J.W. and Ames, B.N. (1988) Normal oxidative damage to mitochondrial and nuclear DNA is extensive. *Proc. Natl. Acad. Sci. USA*, **85**, 6465-6467.

11. Helbrock, H.J., Beckman, K.B., Shigenaga, M.K., Walter, P.B., Woodall, A.A., Yeo, H.C. and Ames, B.N. (1998) DNA oxidation matters: The HPLC-electrohemical detection assay of 8-oxo-deoxyguanosine and 8-oxo-guanine. *Proc. Natl. Acad. Sci. USA*, **95**, 288-293.

12. Rajeski, S., Jackson, B.A. and Barton, J.K. (2000) DNA repair: models for damage and mismatch recognition. *Mutat. Res.*, **447**, 49-72.

13. Steitz, T.A. (1999) DNA polymerases: Structural Diversity and Common Mechanisms. *J. Biol. Chem.*, **274**, 17395-17398.

14. Ochs, K., Sobol, R.W., Wilson, S.H. and Kaina, B. (1999) Cells Deficient in DNA Polymerase β are Hypersensitive to Alkylating Agent-induced Apoptosis and Chromosomal Breakage. *Cancer Res.*, **59**, 1544-1551.

15. Umar, A. and Kunkel, T.A. (1996) DNA-replication fidelity, mismatch repair and genome instability in cancer cells. *Eur. J. Biochem.*, **238**, 297-307.

16. Loeb, K.R. and Loeb, L.A. (2000) Significance of multiple mutations in cancer. *Carcinogenesis,* **21**, 379-385.

17. Jirincy, J. (1998) Replication errors: cha(lle)nging the genome. *EMBO. J.*, **17**, 6427-6436.

18. Lindahl, T. and Wood, R.D. (1999) Quality Control by DNA Repair. *Science*, **286**, 1897-1905.

19. Loeb, L. (1991) Mutator Phenotype may be Required for Multistage Carcinogenesis. *Cancer Res.*, **51**, 3075-3079.

20. Meyn, M.S. (1997) Chromosome Instability Syndromes: Lessons for Carcinogenesis. *In. Genetic instability and tumorigenesis; Current topics in Microbiology and Immunology,* **221**, 72-148.

21. Loeb, L.A. (1998) Cancer Cells Exhibit a Mutator Phenotype. *Adv. Cancer Res.*, 25-36.

22. Marra, G. and Boland, C.R. (1995) Hereditary Nonpolyposis Colorectal Cancer: the Syndrome, the Genes, and Historical Perspectives. *J. Nat. Cancer Inst.*, **87**, 1114-1125.

23. Fearon, E.R. and Vogelstein, B. (1990) A Genetic Model for Colorectal Tumorigenesis. *Cell*, **61**, 759-767.

24. Peltomaki, P., Lothe, R.A., Aaltonen, L.A., Pylkkanen, L., Nystrom-Lahti, M., Seruca, R., David, L., Holm, R., Ryberg, D., Haugen, A., Brogger, A., Borresen,

A-L. and de la Chapelle, A. (1993) Microsatellite Instability is Associated with Tumors that Characterize the Hereditary Non-Polyposis Colorectal Carcinoma Syndrome. *Cancer Res.*, **53**, 5853-5855.

25. Peltomaki, P. and Vasen, H.F.A. (1997) Mutations predisposing to Hereditary Nonpolyposis Colorectal Cancer: database and Results of a Collaborative Study. *Gastroenterology*, **113**, 1146-1158.

26. Peltomaki, P. (1997) DNA Mismatch repair Gene Mutations in Human cancer. *Environ. Health Persp.*, **105**, 775-780.

27. Loeb, L.A. (1994) Microsatellite Instability: Marker of a Mutator Phenotype in Cancer. *Cancer Res.*, **54**, 5059-5063.

28. Bhattacharyya, N.P., Skandalis, A., Groden, J. and Meuth, M. (1994) Mutator phenotype in human colorectal carcinoma cell lines. *Pro. Natl. Acad. Sci. USA*, **91**, 6319-6323.

29. Boyer, J.C., Umar, A., Risinger, J.L., Lipford, J.R., Kane, M., Yin s., Barrett, J.C., Kolodner, R.D. and Kunkel, T.A. (1995) Microsatelltie Instability, Mismatch Repair Deficiency and Genetic Defects in Human Cancer Cell Lines. *Cancer Res.* **55**, 6063-6070.

30. Benzer, S. (1961) Genetic fine structure, *Harvey lecture* **56**, 1-21.

31. Tomita-Mitchell, A., Kat, A.G., Marcelino, L.A., Li-Sucholeiki, X-C., Goodluck-Griffith, J. and Thilly, W.G. (2000) Mismatch repair deficient human cells: spontaneous and MNNG-induced mutational spectra in the HPRT gene. *Mutat. Res.*, **450**, 125-138.

32. Drake, J.W., Charlesworth, B., Charlesworth, D. and Crow, J.F. (1998) Rates of Spontaneous Mutation. *Genetics*, **148**, 1667-1686.

33. Maronpot, R.R., Fox, T., Malarkey, D.E. and Goldsworthy, T.L. (1995) Mutations in the *ras* proto-oncogene: clues to etiology and molecular pathogenesis of mouse liver tumors. *Toxicology*, **101**, 125-156.

34. Anderson, M.W., Reynolds, S.H., Ming, Y. and Maronpot, R.M. (1992) Role of Proto-oncogene Activation in Carcinogenesis. *Env. Health Persp.*, **98**, 13-24.

35. Balmain, A. and Brown, K. (1988) Oncogene Activation in Chemical Carcinogenesis. *Adv. Cancer Res.*, **51**, 147-182.

36. Barbacid, M. (1987) *ras* GENES. *Ann. Rev. Biochem.*, **56**, 779-827.

37. *Barbacid, M. (1990) ras oncogenes: their role in neoplasis.* Eur. J. Clin. Invest., ***20**, 225-235.*

38. Bos, J.L. (1988) The *ras* gene family and human carcinogenesis. *Mutat. Res.*, **195**, 255-271.

39. Kiaris, H. and Spandidos, D.A. (1995) Mutations of ras genes in human tumors. *Inl. J. Oncol.*, 7, 413-421.

40. Khosravi-Far, R. and Der, C.J. (1994) The Ras signal transduction pathway. *Cancer and Metatasis Rev.*, **13**, 67-89.

41. Engelbergs, J., Thomale, J. and Rajewsky, M.F. (2000) Role of DNA repair in carcinogen-induced *ras* mutation. *Mutat. Res.*, **450**, 139-153.

42. Pfeifer, G.P. (2000) Involvement of DNA damage and repair in mutational spectra. *Mutat. Res.*, **450**, 1-3.

43. Dogliotti, E., Hainout, P., Hernandez, T., D'Errico, M. and DeMarini, D.M. (1998) Mutation Spectra resulting from Carcinogenic Exposure: from model Systems to Cancer-related Genes. *Rec. Res. Cancer Res.*, **51**, 147-182.

44. Denissenko, M. F., Pao, A., Tang, M-S. and Pfeifer, G.P. (1996) Preferential Formation of Benzo[a]pyrene Adducts at Lung cancer Mutational Hotspots in P53. *Science*, **274**, 430-432.

45. Chen, J.X., Zheng, Y., West, M. and Tang, M-S. (1999) Carcinogens Preferentially Bind at methylated CpG in the p53 Mutational Hot Spots. *Cancer Res.*, **58**, 2070-2075.

46. Denissenko, M.F., Pao, A., Pfeifer, G.P. and Tang, M-S. (1998) Slow repair of bulky DNA adducts along the nontranscribed strand of the human *p53* gene may explain the strand bias of transversion mutations in cancers. *Oncogene*, **16**, 1241-1247.

47. Wei, D., Maher, V.M. and Mc.Cormick, J.J (1995) Site-specific rates of excision repair of benzo[a]pyrene diol epoxide adducts in the hypoxanthine phosphoribosyltransferase gene of human fibroblasts: Correlation with mutation spectra. *Proc. Natl. Acad. Sci. USA*, **92**, 2204-2208.

48. Tornaletti, S. and Pfeifer, G.P. (1994) Slow repair of Pyrimidine Dimers at p53 mutation Hotspots in Skin Cancer. *Science*, **263**, 1436-1440.

49. Mitra, G., Pauly, G.T., Kumar, R., Pei, G.K., Hughes, S.H., Moschel, R.C. and Barbacid, M. (1989) Molecular analysis of O^6-substituted guanine-induced mutagenesis of *ras* oncogenes. *Proc. Natl. Acad. Sci. USA*, **86**, 8650-8654.

50. Pillaire, M.J., Margot, A., Villani, G., Sarasin, A., Defais, M. and Gentil, A. (1994) Mutagenesis in monkey cells of a vector containing a single d(GPG) *cis*-diamminedichloroplatinum(II) adduct placed on codon 13 of the human H-*ras* proto-oncogene. *Nucleic Acids Res.*, **22**, 2519-2524.

51. Tan, X., Grollman, A.P. and Shibutani, S. (1999) Comparison of the mutagenic properties of 8-oxo-7,8-dihydro-2'-deoxyguanosine DNA lesions in mammalian cells. *Carcinogenesis*, **20**, 2287-2292.

52. Carty, M.P., El-Saleh, S., Zernik-Kobak, M. and Dixon, K. (1995) Analysis of Mutations Induced by Replication of UV-Damaged Plasmid DNA in Hela Cell extracts. *Environ. Mol. Mutagen.*, **26**, 139-146.

53. Arcangeli, L., Simonetti, J., Pongratz, C. and Williams, K.J. (1997) Site- and strand-specific mismatch repair of human H-*ras* genomic DNA in a mammalian cell line. *Carcinogenesis*, **18**, 1311-1318.

54. Matton, N., Simonetti, J. and Williams, K. (1999) Inefficient *in vivo* repair of mismatches at an oncogenic hotspot correlated with lack of binding by mismatch repair proteins and with phase of the cell cycle. *Carcinogenesis*, **20**, 1417-1424.

55. Jacobs, A., Bopp, A. and Hagen, U. (1972) *In vitro* repair of single-strand breaks in γ-irradiated DNA by polynucleotide ligase. *Int. J. Radiat. Biol.*, **22**, 431-435.

56. Sancar, A. (1996) DNA EXCISION REPAIR. *Ann. Rev. Biochem.*, **65**, 43-81.

57. Kato Jr, T., Todo, T., Ayaki, H., Ishizaki, K., Morita, T., Mitra, S. and Ikenaga, M. (1994) Cloning of a marsupial DNA photolyase gene and the lack of related nucleotide sequences in placental mammals. *Nucleic Acids Res.*, **22**, 4119-4124.

58. Sutherland, B.M. and Bennett, P.V. (1995) Human white blood cells contain cyclobutyl pyrimidine dimmer photolyase. *Proc. Natl. Acad. Sci. USA*, **92**, 9732-9736.

59. Sutherland, B.M. (1996) Mutagenic Lesions in carcinogenesis: Induction and Repair of Pyrimidine Dimers. *Photochem. Photobiol.*, **63**, 375-376.

60. Todo, T., Tsuji, H., Otoshi, E., Hitomi, K., Kim, S-T. and Ikenaga, M. (1997) Characterization of a human homolog of (6-4) photolyase. *Mutat. Res.*, **384**, 195-204.

61. Van der Spek, P.J., Kobayshi, K., Bootsma, D., Takao, M., Eker, A.P.M. and Yasui, A. (1996) Cloning, Tissue Expression, and mapping of a Human Photolyase Homolog with Similarity to Plant Blue-Light Receptors. *Genomics*, **37**, 177-182.

62. Li, Y.F., Kim, S-T. and Sancar, A. (1993) Evidence for lack of DNA photoreactivating enzyme in humans. *Proc. Natl. Acad. Sci. USA*, **90**, 4389-4393.

63. Yu, Z., Chen, J., Ford, B.N., Bracklry, M.E. and Glickman, B.W. (1999) Human DNA Repair Systems: An Overview. *Environ. Mol. Mutagen.*, **33**, 3-20.

64. Sedgwick, B. (1997) Nitrosated peptides and polyamines as endogenous mutagens in O^6-alkylguanine-DNA alkyltransferase deficient cells. *Carcinogenesis*, **18**, 1561-1567.

65. Vaughan, P., Lindahl, T. and Sedgwick, B. (1993) Induction of the adaptive response of *Escherichia coli* to alkylation damage by the environmental mutagen, methyl chloride. *Mutat. Res.*, **293**, 249-257.

66. Moore, M.H., Gulbis, J.M., Dodson, E.J., Demple, B. and Moddy, P.C.E. (1994) Crystal structure of a suicidal DNA repair protein: the Ada O^6-methylguanine-DNA methyltransferase from E.coli. *Embo. J.*, **13**, 1495-1501.

67. Srivenugopal, K.S., Yuan, X-H., Friedman, H.S. and Ali-Osman, F. (1996) Ubiquitination-Dependent Proteolysis of O^6-Methylguanine-DNA Methyltransferase in Human and Murine Tumor Cells following Inactivation with O^6-Benzylguanine or 1,3-Bis(2-chloroethyl)-1-nitrourea. *Biochemistry*, **35**, 1328-1334.

68. Mol, C.D., Parikh, S.S., Putnam, C.D., Lo, T.P. and Tainer, J.A. (1999) DNA Repair Mechanisms For The Recognition And Removal Of Damaged DNA Bases. *Annu. Rev. Biomol. Struct.*, **28**, 101-128.

69. Waters, T.R. and Swann, P.F. (1998) Kinetics of the Action of Thymine DNA Glycosylase. *J. Biol. Chem.*, **273**, 20007-20014.

70. Sanderson, R.J. and Mosbaugh, D.W. (1998) Fidelity and Mutational Specificity of Uracil-initiated Base Excision DNA repair Synthesis in human Glioblastoma Cell Extracts. *J. Biol. Chem.*, **273**, 24822-24831.

71. Krokan, H.E., Standal, R. and Slupphaug, G. (1997) DNA glycosylases in the base excision repair of DNA. *Biochem. J.*, **325**, 1-16.

72. Savva, R., McAuley-Hecht, Brown, T. and Pearl, L. (1995) The structural basis of specific base-excision repair by uracil-DNA glycosylase. *Nature*, **373**, 487-493.

73. Neddermann, P. and Jirincy, J. (1994) Efficient removal of uracil from G.U mispairs by the mismatch-specific thymine DNA glycosylase from Hela cells. *Proc. Natl. Acad. Sci. USA*, **91**, 1642-1646.

74. Wiebauer, K. and Jirincy, J. (1989) In vitro correction of G.T mispairs to G.C pairs in nuclear extracts from human cells. *Nature*, **339**, 234-236.

75. Wiebauer, K. and Jirincy, J. (1990) Mismatch-specific thymine DNA glycosylase and DNA polymerase β mediate the correction of G.T mispairs in nuclear extracts from human cells. *Proc. Natl. Acad. Sci. USA*, **87**, 5842-5845.

76. Hang, B., Medina, M., Fraenkel-Conrat, H. and Singer, B. (1998) A 55-kDa protein isolated from human cells shows DNA glycosylase activity toward 3,N^4-ethenocytosine and the G/T mismatch. *Proc. Natl. Acad. Sci. USA*, **95**, 13561-13566.

77. Mc.Golderick, J.P., Yeh, Y-C., Solomon, M., Essigmann, J.M. and Lu, A-L. (1995) Characterization of a Mammalian Homolog of the *Escherichia coli* MutY Mismatch Repair Protein. *Mol. Cell. Biol.*, **15**, 989-996.

78. Porello, S.L., Leyes, A.E. and David, S.S. (1998) Single-Turnover and pre-Steady-State Kinetics of the Reaction of the Adenine glycosylase MutY with Mismatch-Containing DNA Substrates. *Biochemistry*, **37**, 14756-14764.

79. Parker, A., Gu, Y., Mahoney, W., Lee, S-H., Singh, K.K. and Lu, A-L. (2000) Human homolog of the MutY repair protein (hMYH) physically interacts with proteins involved in long-patch DNA base excision repair. *J. Biol. Chem.*,

80. Dantzer, F., de la Rubia, G., Menissier-de Muricia, J., Hostomsky, Z., de Murcia, G. and Schreiber, V. (2000) Base excision Repair Is Impaired in Mammalian Cells Lacking Poly(ADP-ribose) Polymerase-1. *Biochemistry*, **39**, 7559-7569.

81. Krokan, H.E., Nilsen, H., Skorpen, F., Otterlei, M. and Slupphaug, G. (2000) Base excsion repair of DNA in mammalian cells. *FEBS Letters*, **476**, 73-77.

82. Frosina, G., Fortini, P., Rossi, O., Carrozzino, F., Raspaglio, G., Cox, L.S., Lane, D.P., Abbondandolo, A. and Dogliotti, E. (1996) Two Pathways for Base Excision Repair in Mammalian Cells. *J. Biol. Chem.* **271**, 9573-9578.

83. Wilson III, D.M. and Thompson, L.H. (1997) Life without DNA repair. *Proc. Natl. Acad. Sci. USA*, **94**, 12754-12757.

84. Fortini, P., Pascucci, B., Parlanti, E., Sobol, R.W., Wilson, S.H. and Dogliotti, E. (1998) Different DNA Polymerases Are Involved in Short- and Long-Patch Base Excision Repair in Mammalian Cells. *Biochemistry*, **37**, 3575-3580.

85. Barnes, D.E., Tomkinson, A.E., Lehmann, A.R., Webster, D.B. and Lindahl, T. (1992) Mutations in the DNA Ligase I Gene of an Individual with Immunodeficiencies and Cellular Hypersensitivity to DNA-Damaging Agents. *Cell*, **69**, 495-503.

86. Kubota, Y., Nash, R.A., Klungland, A., Schar, P., Barnes, D.E. and Lindahl, T. (1996) Reconstitution of DNA base excision-repair with purified human proteins: interaction between DNA polymerase β and the XRCC1 protein. *EMBO, J.* **15**, 6662-6670.

87. Srivastava, D.K., Vande Beerg, B. J., Prasad, R., Molina, J.T., Beard, W.A., Tomkinson, A.E. and Wilson, S.H. (1998) Mammalian Abasic Site Base Excision Repair. *J. Biol. Chem.*, **273,** 21203-21209.

88. Pascucci, B., Stucki, M., Jonsson, Z.O., Dogliotti, E. and Hubscher, U. (1999) Long Patch Base excision Repair with purified Human Proteins. *J. Biol. Chem.*, **274**, 33696-33702.

89. Horton, J.K., Prasad, R., Hou, E. and Wilson, S.H. (2000) Protection against Methylation-induced Cytotoxicity by DNA Polymerase β-Dependent Long Patch Base Excision Repair. *J. Biol. Chem.*, **275**, 2211-2218.

90. Cleaver, J.E. (1968) Defective Repair Replication of DNA in Xeroderma Pigmentosum. *Nature*, **218**, 652-656.

91. Ma, L., Hoeijmakers, J.H.J. and van der Eb, A.J. (1995) Mammalian nucleotide excision repair. *Biochimica et Biophysica Acta*, **1242**, 137-164.

92. De Boer, J. and Hoeijmakers, J.H.J. (2000) Nucleotide excision repair and human syndromes. *Carcinogenesis*, **21**, 453-460.

93. Batty, D.P. and Wood, R.D. (2000) Damage recognition in nucleotide excision repair of DNA. *Gene*, **241**, 193-204.

94. Cleaver, J.E. and Kraemer, K.H. (1995) Xeroderma Pigmentosum and Cockayne Syndrome. In: *The Metabolic Basis of Inherited Disease*. New York: McGraw-Hill.

95. Sugasawa, K., Ng, J.M., Masutani, C., Iwai, S., van der Spek, P.J., Eker, A.P., Hanaoka, F., Bootsma, D. and Hoeijmakers, J.H. (1998) Xeroderma pigmentosum group C protein complex is the initiator of global genome nucleotide excision repair. *Mol. Cell*, **2**, 223-232.

96. Aboussekhra, A., Biggerstaff, M., Shivji, M.K.K., Vilpo, J.A., Moncollin, V., Podust, V.N., Protic, M., Hubscher, U., Egly, J-M. and Wood, R.D. (1995) Mammalian DNA Nucleotide excision Repair reconstituted with Purified Protein Components. *Cell*, **80**, 859-868.

97. Buschta-Hedayat, N., Buterin, T., Hess, M.T., Missura, M. and Naeeli, H. (1999) Recognition of nonhybrdizing base pairs during nucleotide excision repair of DNA. *Proc. Natl. Acad. Sci. USA*, **96**, 6090-6095.

98. Friedberg, E.C. (1996) RELATIONSHIPS BETWEEN DNA REPAIR AND TRANSCRIPTION. *Ann. Rev. Biochem.*, **65**,15-42.

99. Leadon, S.A. (1999) Transcription-Coupled repair of DNA Damage: Unanticipated Players, Unexpected Complexities. *Am. J. Hum. Genet.*, **64**, 1259-1263.

100. Mullenders, L.H.F. (1998) Transcription response and nucleotide excision repair. *Mutat. Res.*, **409**, 59-64.

101. Tung, B.S., McGregor, W.G., Wang, Y-C., Maher, V.M. and McCormick, J.J. (1996) Comparison of the rate of excision of major UV photoproducts in the strands of the human *HPRT* gene of normal and xeroderma pigmentosum variant cells. *Mutat., Res.*, **362**, 65-74.

102. Hanawalt, P.C (1994) Transcription-Coupled Repair and Human Disease. *Science*, **266**, 1957-1958.

103. De Laat, W.L., Appeldorn, E., Sugasawa, K., Weterings, E., Jaspers, N.G.J. and Hoeijmakers, J.H.J. (1998) DNA-binding polarity of human replication protein A positions nucleases in nucleotide excision repair. *Genes Dev.*, **12**, 2598-2609.

104. Marra, G. and Schar, P. (1999) Recognition of DNA alterations by the mismatch repair system. *Biochem. J.*, **338**, 1-13.

105. Modrich, P. (1994) Mismatch Repair, Genetic Stability, and Cancer. *Science*, **266**, 1959-1960.

106. Dao, V. and Modrich, P. (1998) Mismatch-, MutS-, MutL-, and helicase II-dependent Unwinding from the Single-strand Break of an Incised Heteroduplex. *J. Biol. Chem.*, **273**, 9202-9207.

107. Modrich, P. and Lahue, R. (1996) MISMATCH REPAIR IN REPLICATION FIDELITY, GENETIC RECOMBINATION, AND CANCER BIOLOGY. *Annu. Rev. Biochem.*, **63**, 101-133.

108. Jirincy, J. (1998) Eukaryotic mismatch repair: an update. *Mutat. Res.*, **409**, 107-121.

109. Yang, W. (2000) Structure and function of mismatch repair proteins. *Mutat. Res.*, **460**, 245-256.

110. Haber, L.T. and Walker, G.C. (1991) Altering the conserved nucleotide binding motif in the *Salmonella typhimurium* MutS mismatch repair protein affects both its ATPase and mismatch binding activities. *EMBO J.*, **10**, 2707-2715.

111. Allen, D.J., Makhov, A., Grilley, M., Taylor, J., Thresher, R., Modrich, P. and Griffith, J.D. (1997) MutS mediates heteroduplex loop formation by a translocation mechanism. *EMBO J.*, **16**, 4467-4476.

112. Yamaguchi, M., Dao, V. and Modrich, P. (1998) MutS and MutL Activate DNA Helicase II in a Mismatch-dependent Manner. *J. Biol. Chem.*, **273**, 9197-9201.

113. Spampinato, C. and Modrich, P. (2000) The MutL ATPase Is Required for Mismatch Repair. *J. Biol. Chem.*, **275**, 9863-9869.

114. Hall, M.C., Jordan, J.R. and Matson, S.W. (1998) Evidence for a physical interaction between the *Escherichia coli* methyl-directed mismatch repair proteins MutL and UvrD. *EMBO J.*, **17**, 1535-1541.

115. Mechainc, L.E., Frankel, B.A. and Matson, S.W. (2000) *Eschericha coli* MutL Loads DNA Helicase II onto DNA. *J. Biol. Chem.*, **275**, 38337-38346.

116. Viswanathan, M. and Lovett, S.T. (1998) Single-Strand DNA-Specific Exonucleases in *Escherichia coli*: Roles in Repair and Mutation Avoidance. *Genetics*, **149**, 7-16.

117. Chi, N-W. and Kolodner, R.D. (1994) The Effect of DNA Mismatches on the ATPase Activity of MSH1, a Protein in Yeast Mitochondria That Recognizes DNA Mismatches. *J. Biol. Chem.*, **269**, 29993-29997.

118. Buermeyer, A.B., Deschenes, S.M., Baker, S.M. and Liskay, R.M. (1999) Mammalian DNA Mismatch Repair. *Annu. Rev. Genet.* **33**, 533-567.

119. Bocker, T., Barusevicius, A., Snowden, T., Rasio, D., Gurrette, S., Robbins, D., Schmidt, C., Burczak, J., Croce, C.M., Copeland, T., Kovatich, A.J. and Fishel, R. (1999) hMSH5: A Human MutS Homologue That Forms a Novel heterodimer with hMSH4 and Is Expressed during Spermatogenesis. *Cancer Res.*, **59**, 816-822.

120. Kolodner, R.D. and Marsischky, G.T. (1999) Eukaryotic DNA mismatch repair. *Curr. Opin. Genet. Dev.*, **9**, 89-96.

121. Haber, L.T., Patty, P.P., Sobell, D.I., Mankovich, J.A. and Walker, G.C. (1988) Nucleotide Sequence of the *Salmonella typhimurium mutS* Gene Required for

Mismatch Repair: Homology of MutS and HexA of *Streptococcus pneumoniae*. *J. Bacteriology*, **170**, 197-202.

122. Drummond, J.T., Li, G-M., Longley, M.J. and Modrich, P. (1995) Isolation of an hMSH2-p160 Heterodimer That Restores DNA Mismatch Repair to Tumor cells. *Science*, **268**, 1909-1914.

123. Marsischty, G.T. and Kolodner, R.D. (1999) Biochemical Characterization of the Interaction between the Saccharomyces cerevisiae MSH2-MSH6 Complex and Mispaired Bases in DNA. *J. Biol. Chem.*, **274**, 26668-26682.

124. Macpherson, P., Humbert, O. and Karran, P. (1998) Frameshift mismatch recognition by the human MutSα complex. *Mutat. Res.*, **408**, 55-66.

125. Iaccarino, I., Marra, G., Palombo, F. and Jirincy, J. (1998) hMSH2 and hMSH6 play distinct roles in mismatch binding and contribute differently to the ATPase activity of hMutSα. *EMBO, J.*, **17**, 2677-2686.

126 Gradia, S., Acharya, S. and Fishel, R. (1997) The Human Mismatch Recognition Complex hMSH2-hMSH6 Functions as a Novel Molecular Switch. *Cell*, **91**, 995-1005.

127. Blackwell, L.J., Bjornson, K.P. and Modrich, P. (1998) DNA-dependent Activation of the hMutSα ATPase. *J. Biol. Chem.*, **273**, 32049-32054.

128. Gradia, S., Subramanian, D., Wilson, T., Acharya, S., Makhov, A., Griffith, J. and Fishel, R. (1999) hMSH2-hMSH6 forms a hydrolysis-independent sliding clamp on mismatched DNA. *Mol. Cell.*, **3**, 255-261.

129. Fishel, R. (1998) Mismatch repair, molecular switches, and signal transduction. *Genes Dev.*, **12**, 2096-2101.

130. Blackwell, L.J., Martik, D., Bjornson, K.P. and Modrich, P. (1998) Nucleotide-promoted Release of hMutSα from Heteroduplex DNA is Consistent with an ATP-dependent Translocation Mechanism. *J. Biol. Chem.*, **273**, 32055-32062.

131. Gradia, S., Acharya, S. and Fishel, R. (2000) The Role of Mismatched Nucleotides in Activating the hMSH2-hMSH6 Molecular Switch. *J. Biol. Chem.*, **275**, 3922-3930.

132. Wilson, T., Gurrette, S. and Fishel, R. (1999) Dissociation of Mismatch Recognition and ATPase Activity by hMSH2-hMSH3. *J. Biol. Chem.*, **274**, 21659-21664.

133. Iaccarino, I., Marra, G., Dufner, P. and Jirincy, J. (2000) Mutation in the Magnesium Binding site of hMSH6 Disables the hMutSα Sliding Clamp from Translocating along DNA. *J. Biol. Chem.*, **275**, 2080-2086.

134. Dufner, P., Marra, G., Raschle, M. and Jirincy, J. (2000) Mismatch Recognition and DNA-dependent Stimulation of the ATPase Activity of hMutSα Is abolished by a Single Mutation in the hMSH6 Subunit. *J. Biol. Chem.*, **275**, 36550-36555.

135. Papadopoulos, N., Nicolaides, N.C., Liu, B., Parsons, R., Lengauer, C., Palombo, F., D'Arrigo, A., Markowitz, S., Willson, J.K.V., Kinzler, K.W., Jirincy, J. and Vogelstein, B. (1995) Mutations of GTBP in Genetically Unstable Cells. *Science*, **268**, 1915-1916.

136. Genschel, J., Littman, S.J., Drummond, J.T. and Modrich, P. (1998) Isolation of MutSβ from Human Cells and Comparison of the Mismatch Repair Specificities of MutSβ and MutSα. *J. Biol. Chem.*, **273**, 19895-19901.

137. Leung, W.K., Kim, J.J., Wu, L., Sepulveda, J.L. and Sepulveda, A.R. (2000) Identification of a Second MutL DNA Mismatch Repair Complex (hPMS1 and hMLH1) in Human Epithelial Cells. *J. Biol. Chem.*, **275**, 15728-125732.

138. Raschle, M., Marra, G., Nystrom-Lahti, M., Schar, P. and Jirincy, J. (1999) Identification of hMutLβ, a Heterodimer of hMLH1 and hPMS1. *J. Biol. Chem.*, **274**, 32368-32375.

139. Matton, N., Simonetti, J. and Williams, K. (2000) Identification of Mismatch Reapir Protein complexes in Hela Nuclear Extracts and their Interaction with Heteroduplex DNA. *J. Biol. Chem.*, **275**, 17808-17813.

140. Lipkin, S.M., Wang, V., Jacoby, R., Banerjee-Basu, S., Baxevanis, A.D., Lynch, H.T., Elliott, R.M. and Collins, F.S. (2000) *MLH3*: a DNA mismatch repair gene associated with mammalian microsatellite instability. *Nat. Genetics*, **24**, 27-35.

141. Jirincy, J. (2000) Mediating mismatch repair. *Nat. Genetics*, **24**, 6-8.

142. Umar, A., Buermeyer, A.B., Simon, J.A., Thomas, D.C., Clark, A.B., Liskay, R.M. and Kunkel, T.A. (1996) Requirement for PCNA in DNA Mismatch repair at a Step Preceding DNA Resynthesis. *Cell*, **87**, 65-73.

143. Gu, L., Hong, Y., Mc. Culloch, S., Watanabe, H. and Li, G-M. (1998) ATP-dependent interaction of human mismatch repair proteins and dual role of PCNA in mismatch repair. *Nucleic Acids Res.*, **26**, 1173-1178.

144. Hughes, P., Tratner, I., Ducoux, M., Piard, K. and Baldacci, G. (1999) Isolation and identification of the third subunit of mammalian DNA polymerase delta by PCNA-affinity chromatography of mouse FM3A cell extracts. *Nucleic Acids Res.*, **27**, 2108-2114.

145. Clark, A.B., Valle, F., Drotschmann, K., Gary, R.K. and Kunkel, T.A. (2000) Functional interaction of PCNA with MSH2-MSH6 and MSH2-MSH3 complexes. *J. Biol. Chem.*, 275, 36498-36501.

146. Holmes, J., Clark, S. and Modrich, P. (1990) Strand-specific mismatch correction in nuclear extracts of human and *Drosphila melanogaster* cell lines. *Proc. Natl. Acad. Sci. USA*, **87**, 5837-5841.

147. Thomas, D.C., Roberts, J.D. and Kunkel, T.A. (1991) Heteroduplex Repair in Extracts of Human Hela Cells, *J. Biol. Chem.*, **266**, 3744-3751.

148. Tran, H.T., Gordenin, D.A. and Resnick, M.A. (1999) The 3'→5' Exonucleases of DNA Polymerases δ and ε and the 5'→3' Exonuclease Exo1 Have Major Roles in Postreplication Mutation avoidance in *Saccharomyces cerevisiae*. *Mol. Cell. Biol.*, **19**, 2000-2007.

149. Fiorentini, P., Huang, K.N., Tishkoff, D.X., Kolodner, R.D. and Symington, L.S. (1997) Exonuclease I of Saccharomyces cerevisiae Functions in Mitotic recombination In Vivo and In Vitro. *Mol. Cell. Biol.*, **17**, 2764-2773.

150. Tishkoff, D.X., Boerger, A.L., Bertrand, P., Filosi, N., Gaida, G.M., Kane, I. and Kolodner, R.D. (1997) Identification and characterization of *Saccharomyces cerevisiae EXO1*, a gene encoding an exonuclease that interacts with MSH2. *Proc. Natl. Acad. Sci. USA*, **97**, 7487-7492.

151. Schmutte, C., Marinescu, R.C., Sadoff, M.M., Gurrette, S., Overhauser, J. and Fishel, R. (1998) Human Exonuclease I Interacts with the Mismatch Repair protein hMSH2. *Cancer Res.*, **58**, 4537-4542.

152. Rasmussen, L.J., Rasmussen, M., Lee, B-I., Rasmussen, AK., Wilson III, D.M., Nielson, F.C. and Bisgaard, H.C. (2000) Identification of factors interacting with hMSH2 in the fetal liver utilizing the yeast two-hybrid system. In vivo interaction through the C-terminal domains of hEXO1 and hMSH2 and comparative expression analysis. *Mutat. Res.*, **460**, 41-52.

153. Tishkoff, D.X., Filosi, N., Gaida, G,M. and Kolodner, R.D. (1997) A Novel Mutation Avoidance Mechanism Dependent on S. cerevisiae *RAD27* Is Distinct from DNA Mismatch Repair. *Cell*, **88**, 253-263.

154. Li, G-M. and Modrich, P. (1995) Restoration of mismatch repair to nuclear extracts of H6 colorectal tumor cells by a heterodimer of human MutL homologs. *Proc. Natl. Acad. Sci. USA*, **92**, 1950-1954.

155. Reitmair, A.H., Risley, R., Bristow, R.G., Wilson, T., Ganesh, A., Jang, A., Peacock, J., Benchimol, S., Hill, R.P., Mak, T.W., Fishel, R. and Meuth, M. (1997) Mutator Phenotype in *Msh2*-deficient Murine Embryonic Fibroblasts. *Cancer Res.*, **57**, 3765-3771.

156. Thibodeau, S.N., French, A.J., Cunningham, J.M., Tester, D., Burgart, L.J., Roche, P.C., McDonnell, S.K., Schaid, D.J., Walsh Vockely, C., Michels, V.V., Farr, G.H. and O'Connell, M.J. (1998) Microsatellite Instability in Colorectal Cancer: Different Mutator Phenotypes and the Principal Involvement of *hMLH1*. *Cancer Res.*, **58**, 1713-1718.

157. Shcherbakova, P.V. and Kunkel, T.A. (1999) Mutator Phenotypes Conferred by *MLH1* Overexpression and by Heterozygosity for *mlh1* mutations. *Mol. Cell. Biol.*, **19**, 3177-3183.

158. Longley, M.J., Pierce, A.J. and Modrich, P. (1997) DNA Polymerase δ Is Required for Human Mismatch Repair in Vitro. *J. Biol. Chem.*, **272**, 10917-10921.

159. Lin, Y-L, Shiviji, M.K.K., Chen, C., Kolodner, R., Wood, R.D. and Dutta, A. (1998) The Evolutionarily Conserved Zinc Finger Motif in the Largest Subunit of Human Replication Protein A Is required for DNA Replication and Mismatch Repair but Not for Nucleotide excision Repair. *J. Biol. Chem.*, **273**, 1453-1461.

160. Fishel, R.A., Lescoe, M.K., Rao, M.R.S., Copland, N., Jenkins, N., Garber, J., Kane, M. and Kolodner, R. (1993) The human mutator gene homolog MSH2 and its association with hereditary nonpolyposis colon cancer. *Cell*, **75**, 1027-1038.

161. Palombo, F., Hughes, M., Jirincy, J., Truong, O. and Hsuan, J. (1994) Mismatch repair and cancer. *Nature*, **367**, 417-419.

162. Arnheim, A. and Shibata, D. (1997) DNA mismatch repair in mammals: role in disease and meiosis. *Curr. Opin.Genet. Dev.*, 7, 364-370.

163. Kolodner, R.D., Tytell, J.D., Schmeits, J.L., Kane, M.F., Das Gupta, R., Weger, J., Wahlberg, S., Fox, E.A., Peel, D., Ziogas, A., Garber, J.E., Syngal, S., Anton-Culver, H. and Li, F.P. (1999) Germ-line *msh6* Mutations in Colorectal Cancer Families. *Cancer Res.*, **59**, 5068-5074.

164. Gurrette, S., Acharya, S. and Fishel, R. (1999) The Interaction of the Human MutL Homologues in Hereditary Nonpolyposis Colon Cancer. *J. Biol. Chem.*, **274**, 6336-6341.

165. Wheeler, J.M., Loukola, A., Aaltonen, L.A., Mortensen, N.J. and Bodmer, W.F. (2000) The role of hypermethylation of the hMLH1 promoter region in HNPCC versus MSI+ sporadic colorectal cancers. *J. Med. Genet.*, **37**, 588-92.

166. Fleischer, A.S., Esteller, M., Harpaz, N., Leytin, A., Rashid, A., Xu, Y., Liang, J., Stine, O.C., Yin, J., Zou, T-T., Abraham, J.M., Kong, D., Wilson, K.T., James, S.P., Herman, J.G. and Meltzer, S.J. (2000) Microsatellite Instability in Inflammatory Bowel Disease-associated Neoplastic Lesions Is Associated with Hypermethylation and Diminished Expression of the DNA Mismatch Repair Gene, hMLH1. Cancer Res., **60**, 4864-4868.

167. Esteller, M. (2000) Epigeneic lesions causing genetic lesions in human cancer. Promoter hypermethylation of DNA repair genes. Eur. J. Cancer, **36**, 2294-2300.

168. Duckett, D.R., Drummond, J.T., Murchie, A.I.H., Reardon, J.T., Sancar, A., Lilley, D.M.J. and Modrich, P. (1996) Human MutSα recognizes damaged DNA base pairs containing O^6-methylguanine, O^4-methylthymine, or the cisplatin-d(GpG) adduct. Proc. Natl. Acad. Sci. USA, **93**, 6443-6447.

169. Yamada, M., O'Regan, E., Brown, R. and Karran, P. (1997) Selective recognition of a cisplatin-DNA adduct by human mismatch repair proteins. *Nucleic Acids Res.*, **25**, 491-495.

170. Mu, D., Bessho, T., Nechev, L.V., Chen, D.J., Harris, T.M., Hearst, J.E. and Sancar, A. (2000) DNA Interstrand Cross-Links Induce Futile repair Synthesis in Mammalian Cell Extracts. *Mol. Cell. Biol.*, **20**, 2446-2454.

171. Wang, H., Lawrence, C.W., Li, G-M. and Hays, J.B. (1999) Specific Binding of Human MSH2-MSH6 Mismatch-Repair Protein Heterodimers to DNA incorporating Thymine- or Uracil-containing UV Light Photoproducts Opposite Mismatched Bases. *J. Biol. Chem.*, **274**, 16894-16900.

172. Dosch, J., Christmann, M. and Kaina, B. (1998) Mismatch G-T binding activity and MSH2 expression is quantitatively related to sensitivity of cells to methylating agents. *Carcinogenesis*, **19**, 567-573.

173. Mello, J.A., Trimmer, E.E., Kartalou, M. and Essigmann, J.M. (1998) Conflicting Roles of Mismatch and Nucleotide Excision repair in Cellular susceptibility to Anticancer Drugs. *Nucleic Acids and Molecular Biology*, **12**, 249-274.

174. Berardini, M., Mazurek, A. and Fishel, R. (2000) The Effect of O^6-Methylguanine DNA Adducts on the Adenosine Nucleotide Switch functions of hMSH2-hMSH6 and hMSH2-hMSH3. *J. Biol. Chem.*, **275**, 27851-27857.

175. Christmann, M. and Kaina, B. (2000) Nuclear Translocation of Mismatch repair Proteins MSH2 and MSH6 as a response of Cells to Alkylating Agents. *J. Biol. Chem.*, **275**, 36256-36262.

176. Li, G.M. (1999) The role of mismatch repair in DNA damage-induced apoptosis. *Oncol. Res.*, **11**, 393-400.

177. Wu, J., Gu, L., Wang, H., Geacintov, N.E. and Li, G.M. (1999) Mismatch repair processing of carcinogen-DNA adducts triggers apoptosis. *Mol. Cell. Biol.*, **19**, 8292-8301.

178. Zeng, M., Narayanan, L., Xu, X.S., Liskay, R.M. and Glazer, P.M. (2000) Ionizing radiation-induced apotosis via separate Pms2- and p53-dependent pathways. *Cancer Res.*, **60**, 4889-4893.

179. Hickman, M.J. and Samson, L.D. (1999) Role of DNA mismatch repair and p53 in signaling induction of apoptosis by alkylating agents. *Proc. Natl. Acad. Sci. USA*, **96**, 10764-10769.

180. Duckett, D.R., Bronstein, S.M., Taya, Y. and Modrich, P. (1999) hMutSα- and hMutLα-dependent phosphorylation of p53 in response to DNA methylator damage. *Proc. Natl. Acad. Sci. USA*, **96**, 12384-12388.

181. Toft, N.J., Winton, D.J., Kelly, J., Howard, L.A., Dekker, M., Riele, H.T., Arends, M.J., Wyllie, A.H., Margison, G.P. and Clarke, A.R. (1999) *Msh2* status modulates both apoptosis and mutation frequency in the murine small intestine. *Proc. Natl. Acad. Sci. USA*, **96**, 3911-3915.

182. Zhang, H., Richards, B., Wilson, T., Lioyd, M., Cranston, A., Thorburn, A., Fishel, R. and Meuth, M. (1999) Apoptosis Induced by Overexpression of *hMSH2* or *hMLH1*. *Cancer Res.*, **59**, 3021-3027.

183. Singer, B., Chavez, F., Goodman, M.F., Essigmann, J.M. and Dosanjh, M.K. (1989) Effect of 3' flanking neighbours on kinetics of pairing of dCTP or dTTP opposite O^6-methylguanine in a defined primed oligonucleotide when *Escherichia coli* DNA polymerase I is used. *Proc. Natl. Acad. Sci. USA*, **86**, 8271-8274.

184. Singh, J., Su, L. and Snow, E.T. (1996) Replication across O^6-methylguanine by Human DNA Polymerase β *in Vitro*. *J. Biol. Chem.*, **271**, 28391-28398.

185. Vaisman, A., Varchenko, M., Umar, A., Kunkel. T.A., Risinger, J.L., Barrett, J.C., Hamilton, T.C. and Chaney, S.G. (1998) The Role of hMLH1, hMSH3, and hMSH6 defects in Cisplatin and Oxaliplatin Resistance: Correlation with Replicative bypass of Platinum-DNA Adducts. *Cancer Res.*, **58**, 3579-3585.

186. Goldmacher, V.S., Cuzick Jr, R.A. and Thilly, W.G. (1986) Isolation and Partial Characterization of Human Cell Mutants Differing in Sensitivity to Killing and Mutation by Methylnitrosourea and *N*-Methyl-*N'*-nitro-*N*-nitrosoguanidine. *J. Biol. Chem.*, **261**, 12462-12471.

187. Karran, P. and Bignami, M. (1992) Self-destruction and tolerance in resistance of mammalian cells to alkylation damage. *Nucleic Acids Res.*, **20**, 2933-2940.

188. Fishel, R. (1999) Signaling mismatch repair in cancer. *Nat. Med.*, **5**, 1239-1241.

189. Mellon, I. and Champe, G.N. (1996) Products of DNA mismatch repair genes *mutS* and *mutL* are required for transcription-coupled nucleotide-excision repair of the lactose operon in *Escherichia coli*. *Proc. Natl. Acad. Sci. USA*, **93**, 1292-1297.

190. Mellon, I., Rajpal, D.P., Koi, M., Boland, C.B. and Champe, G.N. (1996) Transcription-coupled Repair Deficiency and Mutations in Human Mismatch Repair Genes. *Science*, **272**, 557-560.

191. Leadon, S.A. and Avrutskaya, A.V. (1997) Differential Involvement of the human Mismatch Repair Proteins, hMLH1 and hMSH2, in Transcription-coupled Repair. *Cancer Res.*, **57**, 3784-3791.

192. Bertrand, P., Tishkoff, D.X., Filosi, N., Dasgupta, R. and Kolodner, R.D. (1998) Physical interaction between components of DNA mismatch repair and nucleotide excision repair. *Proc. Natl. Acad. Sci. USA*, **95**, 14278-14283.

193. Wang, Y., Cortez, D., Yazdi, P., Neff, N., Elledge, S.J. and Qin, J. (2000) BASC, a super complex of BRCA1-associated proteins involved in the recognition and repair of aberrant DNA structures. *Genes Dev.*, **14**, 927-939.

194. Chambers, S.R., Hunter, N., Louis, E.J. and Borts, R.H. (1996) The Mismatch Repair System Reduces Meiotic Homeologous Recombination and Stimulates Recombination-Dependent Chromosome Loss. *Mol. Cell. Biol.*, **16**, 6110-6120.

195. Datta, A., Hendrix, M., Lipstitch, M. and Jinks-Robertson, S. (1997) Dual roles for DNA sequence identity and the mismatch repair system in the regulation of mitotic crossing-over in yeast. *Proc. Natl. Acad. Sci. USA*, **94**, 9757-9762.

196. De Wind, N., Dekker, M., Berns, A., Radman, M. and Riele, H.T. (1995) Inactivation of the Mouse *Msh2* Gene Results in Mismatch repair Deficiency, Methylation Tolerance, Hyperrecombination, and Predisposition to Cancer. *Cell*, **82**, 321-330.

197. Saparhaev, M., Prakash, L. and Prakash, S. (1996) Requirement of Mismatch Repair Genes MSH2 and MSH3 in the RAD1-RAD10 Pathway of Mitotic Recombination in *Saccharomyces cerevisiae*. *Genetics*, **142**, 727-736.

198. Evans, E. and Alani, E. (2000) Roles for Mismatch Repair Factors in Regulating Genetic Recombination. *Mol. Cell. Biol.*, **20**, 7839-7844.

199. Zhang, H., Marra, G., Jirincy, J., Maher, V.M. and McCormick, J.J. (2000) Mismatch repair is required for O^6-methylguanine-induced homologous recombination in human fibroblasts. *Carcinogenesis*, **21**, 1639-1646.

200. Sengstag, C. (1994) The role of mitotic recombination in carcinogenesis. *Crit. Rev. Toxicol.*, **24**, 323-353.

201. Kaufmann, W.K. and Paules, R.S. (1996) DNA damage and cell cycle checkpoints. *FASEB J.*, **10**, 238-247.

202. Nojima, H. (1997) Cell Cycle Checkpoints, Chromosome Stability and the Progression of Cancer. *Human Cell*, **10**, 221-230.

203. Weinart, T. (1998) DNA Damage and Checkpoint pathways: Molecular Anatomy and Interactions with Repair. *Cell*, **94**, 555-558.

204. Agami, R. and Bernards, R. (2000) Distinct Initiation and Maintenance Mechanisms Cooperate to Induce G1 Cell Cycle Arrest in Response to DNA Damage. *Cell*, **102**, 55-66.

205. Hawn, M.T., Umar, A., Carethers, J.M., Marra, G., Kunkel, T.A., Boland, C.R. and Koi, M. (1995) Evidence for a Connection between the Mismatch Repair System and the G_2 Cell Cycle Checkpoint. *Cancer Res.*, **55**, 3721-3725.

206. Zhou, B-B, S. and Elledge, S.J. (2000) The DNA damage response: putting checkpoints in perspective. *Nature*, **408**, 433-439.

207. Aquillina, G., Crescenzi, M. and Bignami, M. (1999) Mismatch repair, G_2/M cell cycle arrest and lethality after DNA damage. *Carcinogenesis*, **20**, 2317-2325.

208. Davis, T.W., Wilson-Van Patten, C., Meyers, M., Kunugi, K.A., Cuthill, S., Reznikoff, C., Garces, C., Boland, C.R., Kinsella, T.J., Fishel, R. and Boothman, D.A. (1998) Defective Expression of the DNA Mismatch Repair Protein, MLH1,

Alters G2-M Cell Cycle Checkpoint Arrest following Ionizing Radiation. *Cancer Res.*, **58**, 767-778.

209. Bronstein, S.M., Skopek, T.R. and Swnberg, J.A. (1992) Efficient repair of O6-ethylguanine but not O4-ethylthymine or O2-ethylthymine is dependent upon O6-alkylguanine-DNA alkyltransferase and nucleotide excision repair activities in human cells. *Cancer Res.*, **52**, 2008-2011.

210. Marra, G., Chang, C.L., Laghi, L.A., Chauhan, D.P., Young, D. and Boland, C.R. (1996) Expression of human MutS homolog 2 (hMSH2) protein in resting and proliferating cells. *Oncogene*, **13**, 2189-2196.

211. Meyers, M., Theodosiou, M., Acharya, S., Odegaard, E., Wilsom, T., Lewis, J.E., Davis, T.W., Wilson Van Patten, C., Fishel, R. and Boothman, D.A. (1997) Cell Cycle Regulation of the Human DNA Mismatch Repair Genes *hMSH2, hMLH1*, and *hPMS2*. *Cancer Res.*, **57**, 206-208.

212. Marietta, C., Palombo, F., Gallinari, P., Jirincy, J. and Brooks, P.J. (1998) Expression of long-patch and short-patch DNA mismatch repair proteins in the embryonic and adult mammalian brain. *Molecular Brain Res.*, **53**, 317-320.

213. Simonetti, J., Berner, J. and Williams, K. (2001) Effects of *p,p'*-DDE on immature cells in culture by concentrations relative to the Alaskan environment. *Toxicol. in Vitro*, In Press.

214. Hansen, J.C. (1998) The human health programme under AMAP. *Int. J. Circumpolar Health*, **57**, 280-291.

215. Ecobichon, D.J. (1996). In: *Toxicology: The basic Science of poisons, 5th ed.* Cassarett and Doull's (C.D. Klaassen, ED.), pp. 648-654. Mc-Graw Hill, New York.

216. Bradley, M. (1999) Arctic contaminants-a cast of characters. In: *Alaska Pollution Issues*, pp 1-4. Alaska native Epidemiology center, Anchorage, AK.

217. Pinto, J.D., Camien, M.N. and Dunn, M.S. (1965) Metabolic fate of p,p'-DDT (1,1,1-trichloro-2,2-bis (p-chlorophenyl)ethane) in rats. *J. Biol. Chem.*, **240**, 2149-2154

218. Nims, R.W., Lubet, R.A., Fox, S.D., Jones, C.R., Thomas, P.E., Reddy, A.B. and Kocarek, T.A. (1998) Comparative pharmacodynamics of CYP2B induction by DDT, DDE and DDD in male rat liver and cultured rat hepatocytes. *J. Toxicol. Environ. Health*, **53**, 455-477.

219. Metcalf, R.L., Kapoor, I.P., Lu, P.-Y., Schuth, C.K. and Sherman, P. (1973) Model ecosystems studies of the environmental fate of six organochlorine pesticides. *Environ. Health Perspect.*, **4**, 35-44.

220. Toppari, J, and Larsen, J.C. (1996) Male reproductive health and environmental xenoestrogens. *Environ. Health Perspect.*, **104**, 741-805

221. Morgan, D.P. and Roan, C.C. (1974) The metabolism of DDT in man. *Essays in Toxicology* (W. Hayes, Jr., Ed.) vol. 5, pp. 39-97. Academic Press, New York.

222. ATSDR Public Health Statement: DDT, DDE, and DDD (1989). Agency for Toxic substances and disease registry, Division of toxicology, Atlanta, GA.

223. Tomatis, L., Turusov, V. and Charles, R.T. (1974) Effect of long-term exposure to 1,1-dichloro-2,2-bis(p-chlorophenyl)ethylene, to 1,1-dichloro-2,2-bis(p-chlorophenyl)ethane and to the two chemicals combined on CF-1 mice. *J. Natl. Cancer Inst.* **52**, 883-891.

224. Mahr, U. and Miltenburger, H.G. (1976) The effect of insecticides on Chinese Hamster cell cultures. *Mutat. Res.*, **40**, 107-118.

225. Lundholm, C.E. and Bartonek, M. (1991) A study of the effects of p,p'-DDE and other related chlorinated hydrocarbons on inhibition of platelet aggregation. *Arch. Toxicol.*, **65**, 570-574.

226. You, L., Casanova, M., Archibeque-Engle, S., Sar, M., Fan, L. and Heck. H.d'A. (1998) Impaired male sexual development in perinatal spraque-Dawlwy and Long-Evans hooded rats exposed in utero and lactationally to p,p'-DDE. *Toxicol. Sci.*, **45**. 162-173.

227. Kelce, W.R., Stone, C.R., Laws, S.C., Gray, E.L., Kemppainen, J.A. and Wilson, E.M. (1995) Persistent DDT metabolite p,p'-DDE is a potent androgen receptor antagonist. *Nature* **375**, 581-584.

228. Kelce, W.R., Lambright, C.R., Gray Jr., E. and Roberts, K.P. (1997). Vinclozolin and p,p'-DDE alter androgen-dependent gene expression: *in vivo* confirmation of an androgen receptor-mediated mechanism. *Toxicol. Appl. Pharmacol.* **142**, 192-200.

229. Nims, R.W. (1995) Induction of cytochrome P-450 in the norway rat, *Rattus Norvegicus*, following exposure to potential environmental pollutants. *J. Toxic. Env. Health* **46**, 271-292.

230. You, L., Chan, S.K., Bruce, J.M., Archibeque-Engle, S., Casanova, M., Corton, J.C. and Heck, H.d'A. (1999) Modulation of Testosterone-metabolizing Hepatic Cytochrome P-450 Enzymes in Developing Spraque-Dawley rats following *in utero* exposure to p,p'-DDE. *Toxicol. Appl. Pharmacol.* **158**, 197-205.

231. Perera, F.P., Jedrychowski, W., Rauh, V. and Whyatt, R.M. (1999) Molecular epidemiologic research on the effects of environmental pollutants on the fetus. *Env. Health Perspect,* **107**, 451-460.

232. Elledge, S.J. (1996) Cell Cycle Checkpoints: Preventing an Identity Crisis. *Science*, **274**, 1664-1671.

233. Dasika, G.K., Lin, S-C, J., Zhao, S., Sung, P., Tomkinson, A. and Lee, E, Y-H,P. (1999) DNA damage-inducd cell cycle checkpoints and DNA strand break repair in development and tumorigenesis. *Oncogene*, **18**, 7883-7899.

234. Arcangeli, L. and Williams, K.J. (1995) Mammalian assay for site-specific DNA damage processing using the human H-*ras* proto-oncogene. *Nucleic Acids Res.*, **23**, 2269-2276.

235. Chen, Y. and Rabinovitch, P.S. (1990) Mitogen Response and Cell cycle Kinetics of Swiss 3T3 Cells in Defined Medium: Differences from Human Fibroblasts and Effects of Cell Density. *Exp. Cell Res.*, **190**, 145-150.

236. Rabinovitch, P.S., Kubbies, M., Chen, Y.C., Schindler, D. and Hoehn, H. (1988) BrdU-Hoescht flow cytometry: a unique tool for quantitative cell cycle analysis. *Exp. Cell. Res.* **174**, 309-318.

237. Dignam, J.D., Lebovitz, R.M. and Roeder, R.G. (1983) Accurate transcription initation by RNA polymerase II in a soluble extract from isolated mammalian nuclei. *Nucleic Acids Res.*, **11**, 1475-1489.

238. Bradford, M.M. (1976). A rapid and sensitive method for the quantitation of microgram quantities of protein utilizing the principle of protein dye binding. *Anal. Biochem.* **72**: 248-254.

239. Higuchi, R. (1989) In Erlich, H.A. (ed.), *PCR Technology*. Stockton Press, USA. Pp. 31-38.

240. Erwin, B.G., Stoscheck, C.M. and Florini, J.R. (1981) A rapid flurometric method for the estimation of DNA in cultured cells. *Anal. Biochem.*, **110**, 291-294.

241 Kaltenbach, J.P., Kaltenbach, M.H., and Lyons, W.B. (1958). Nigrosin as a dye for differentiating live and dead ascites cells. *Exp. Cell Res.* **15**, 112-117.

242. Tietze, F. (1969) Enzymic Method for Quantitative determination of nanogram Amounts of Total and Oxidized Glutathione: Applications to Mammalian Blood and Other Tissues. *Anal. Biochem.*, **27**, 502-522.

243. Griffith, O.G. (1980) Determination of Glutathione and Glutathione Disulfide Using Glutathione Reductase and 2-Vinylpyridine. *Anal. Biochem.*, **106**, 207-212.

244. Singh, N.P., Mc.Coy, M.T., Tice, R.R. and Schneider, E.L. (1988) A simple technique for quantitation of low levels of DNA damage in individual cells. *Exp. Cell Res.* **175**, 184-191.

245. Todaro, G.J. and Green, H. (1963) Quantitative studies of the growth of mouse embryo cells in culture and their development into established cell lines. *J. Cell Biol.* **17**, 299-313.

246. Pulciani, S., Santos, E., Lauver, A., Long, L.K. and Barbacid, M. (1982) Transforming genes in human tumors. *J. Cell. Biochem.*, **20**, 51-61.

247. Yates, J.L., Warren, N. and Sugden, B. (19850 Stable replication of plasmids derived from Epstein-Barr virus in various mammalian cells. *Nature*, **313**, 812-815.

248. Modrich, P.(1991) MECHANISMS AND BIOLOGICAL EFFECTS OF MISMATCH REPAIR. *Ann. Rev. Genetics*, **25**, 229-253.

249. Kolodner, R. (1996) Biochemistry and genetics of eukaryotic mismatch repair. *Genes and Development*, **10**, 1433-1442.

250. Pagano, M (ed.). (1996) Cell Cycle- Materials and Methods. *Springer Lab Manual*, Springer-Verlag Publications.

251. Yan, Z-A, Li, X. and Zhou, X. (1987) The effect of hydroxyurea on the expression of the common fragile site at 3p14. *J. Med. Genetics*, **24**, 593-596.

252. Yang, S.J., Hahn, G.M. and Bagshaw, M.A. Chromosome aberrations induced by thymidine. *Exp. Cell. Res.*, **42**, 130-135.

253. Moore, R.C. and Randall, C. (1987) Different effects of 1-β-D-arabinofuranosylcytosine and aphidicolin in S-phase cells; chromosome aberrations, cell cycle delay and cytotoxicity. *Mutat. Res.*, **178**, 73-80.

254. Keyomarsi, K., Sandoval, L , Band, V. and Pardee, A.B. (1991) Synchronization of Tumor and Normal Cells from G_1 to Multiple Cell Cycles by Lovastatin. *Cancer Res.*, **51**, 3602-3609.

255. Keyomarsi, K. (1996) Synchronization of mammalian cells by Lovastatin. *Methods in Cell Science*, **18**, 109-114.

256. Orren, D.K., Petersen, L.N. and Bohr, V.A. (1995) A UV-Responsive G_2 Checkpoint in Rodent Cells. *Mol. Cell. Biol.*, **15**, 3722-3730.

257. Vaziri, C. and Faller, D.V. (1997) A Benzo[a]pyrene-induced Cell Cycle Checkpoint Resulting in p53-independent G_1 Arrest in 3T3 Fibroblasts. *J. Biol. Chem.*, **272**, 2762-2769.

258. Krysan, P.J. and Calos, M.P. (1993) Epstein-Barr virus-based vectors that replicate in rodent cells. *Gene*, **136**, 137-143.

259. Brown, T.C. and Jirincy, J. (1988) Different Base/Base Mispairs are Corrected with Different Efficiencies and Specificities in Monkey Kidney Cells. *Cell*, **54**, 705-711.

260. Luna, L., Bjoras, M., Hoff, E., Rognes, T. and Seeberg, E. (2000) Cell-cycle regulation, intracellular sorting and induced overexpression of the human NTH1 DNA glycosylase involved in removal of formamidopyrimidine residues from DNA. *Mutat. Res.*, **460**, 95-104.

261. Ganguly, T. and Duker, N.J. (1990) Differential cell cycle modulation of human DNA glycosylases against oxidized pyrimidines. *Mutat. Res.*, **235**, 137-146.

262. Gupta, P.K. and Sirover, M.A. (1981) Cell cycle regulation of DNA repair in normal and repair deficient human cells. *Chem. Biol. Interact.*, **36**, 19-31.

263. Cool, B.L. and Sirover, M.A. (1990) Proliferation-dependent regulation of DNA glycosylases in progeroid cells. *Mutat. Res.*, **237**, 211-220.

264. Schrader, T.J. (1992) Differences in nucleotide and base DNA excision repair observed during mitogenic stimulation of bovine lymphocytes. *Mutat. Res.*, **273**, 29-42.

265. Muller, S.J. and Caradonna, S. (1993) Cell cycle regulation of a human cyclin-like gene encoding uracil-DNA glycosylase. *J.Biol. Chem.*, **268**, 1310-1390.

266. Hoffman, J.-S., Fry, M., Ji, J., Williams, K.J. and Loeb, L.A. (1993) Codons 12 and 13 of H-ras Protooncogene Interrupt the Progression of DNA Synthesis Catalyzed by DNA Polymerase α. *Cancer Res.*, **53**, 2895-2900.

267. Buff, K., and Berndt, J. (1981). Interaction of DDT (1,1,1-trichloro-2,2-bis(p-chlorophenyl)ethane with liposomal phospholipids. *Biochim. Biophys. Acta,*, **663**, 205-212.

268. Antunes-Madeira, M.C., and Madeira, V.M.C. (1979).Interaction of insecticides with lipid membranes. *Biochim. Biophys. Acta,* **550**, 384-392.

269. Esteve, J.M., Mompo, J., De La Asunicion, J.G., Sastre, J., Aseni, M., Boix, J., Vina, J.R. and Pallardo, F.V. (1999) Oxidative damage to mitichondrial DNA and glutathione oxidation in apoptosis: studies in vivo and in vitro. *FASEB J.*, **13**, 1055-1064.